

---

Theses and Dissertations

---

Spring 2018

# Urban and rural flood forecasting: a case study of a small town in Iowa

Lauren Elise Grimley  
*University of Iowa*

Copyright © 2018 Lauren Elise Grimley

This thesis is available at Iowa Research Online: <https://ir.uiowa.edu/etd/6118>

---

## Recommended Citation

Grimley, Lauren Elise. "Urban and rural flood forecasting: a case study of a small town in Iowa." MS (Master of Science) thesis, University of Iowa, 2018.  
<https://doi.org/10.17077/etd.50dadj9x>.

---

Follow this and additional works at: <https://ir.uiowa.edu/etd>



Part of the [Civil and Environmental Engineering Commons](#)

URBAN AND RURAL FLOOD FORECASTING:  
A CASE STUDY OF A SMALL TOWN IN IOWA

by

Lauren Elise Grimley

A thesis submitted in partial fulfillment  
of the requirements for the Master of Science  
degree in Civil and Environmental Engineering in the  
Graduate College of  
The University of Iowa

May 2018

Thesis Supervisor: Professor Witold F. Krajewski

Copyright by  
LAUREN ELISE GRIMLEY  
2018  
All Rights Reserved

Graduate College  
The University of Iowa  
Iowa City, Iowa

CERTIFICATE OF APPROVAL

---

MASTER'S THESIS

---

This is to certify that the Master's thesis of

Lauren Elise Grimley

has been approved by the Examining Committee for  
the thesis requirement for the Master of Science degree  
in Civil and Environmental Engineering at the May 2018 graduation.

Thesis Committee:

---

Witold F. Krajewski, Thesis Supervisor

---

Allen A. Bradley

---

Ricardo Mantilla



To my IHR friends and the Grimley family and pets:  
Will, Donna, Oma, Everett, Carolyn, Julianne, Martin,  
Uber, Floofy, and Zoe

## ACKNOWLEDGEMENTS

Thanks to Witold Krajewski for giving me the opportunity to work with him and others at the Iowa Flood Center. Thank you for advising me in my research and for showing me the value (and necessity) of clear communication whether to scientists or the public. I appreciate your patience and sincerity. What a privilege to work with such a leading scientist in the field of hydrology who was approachable and generous in his guidance of my work.

I would like to acknowledge Felipe Quintero who was a great mentor and friend constantly giving research guidance, a practical outlook to solving problems, and most importantly a good sense of humor. To all my colleagues and friends at IIHR, thanks to everyone who shared their passions with me and enlightened me on the many exciting areas within hydrology. The community at IIHR made my graduate experience formative and enriching, and I am honored to have had the chance to work with the students, staff, and faculty.

This project was possible thanks to Ryan Wicks and others at Fehr and Graham for making data available and hosting me at Manchester. The project's momentum was continually fueled by the participation of Shirley Johnson (USACE) and members of other local agencies. Thank you to all other local agencies who provided data and models for this project.

## ABSTRACT

Floods are the most common natural disaster in the U.S. as reported by the Federal Emergency Management Administration (FEMA), and there is a need to provide advance warning to vulnerable communities on the potential risks of flooding after intense storms. The key drivers of urban hydrological research include climate change impacts and adaption, city resilience to hydrological extremes, and integration with emergency management and city planning disciplines. Significant advances in modeling techniques and computational resources have made real-time flood forecasting tools in urban and rural areas an achievable goal, but there is no universal method for flood modeling. Urban landscapes pose a challenge because of fine-scale features and heterogeneities in the landscape including streets, buildings, pipes, and impervious land cover.

A nested regional-local modeling approach was used to evaluate its capabilities to provide useful and accurate flood related information to a small community in Iowa. The advantage of a nested approach is the ability to harness the computational efficiency of the regional model while providing reasonably accurate streamflow boundary conditions to the local model. The nested model incorporates the tools and products maintained at the Iowa Flood Center (IFC) including the streamflow bridge sensors, rain gauges, radar rainfall product, and statewide model. A one-way connection was made between the regional model of the upper Maquoketa Watershed (275 mi<sup>2</sup>) and the local model of the City of Manchester (5 mi<sup>2</sup>). The uncalibrated, nested model was validated using photos and streamflow records for flood events that occurred in July 2010 and September 2016. Multiple radar rainfall estimates were used as input to the model to better understand the

impacts of the spatial and temporal resolution and variations of rainfall on streamflow predictions. A local storm event analysis was completed to determine the vulnerable areas of the stormwater network in eastern Manchester.

The two main sources of flooding in Manchester are from the river and from local runoff. During extreme flood events caused by the river, the hydrologic impacts of the urban catchment are masked and the stormwater network system is overwhelmed. The coarse, regional model is limited in producing streamflow results for the small tributaries draining the eastern areas of Manchester. In the case of localized rainfall, a fine resolution model that takes into account the stormwater network and rainfall-runoff dynamics are crucial to capturing the hydrologic response of the urban area. Overall, the nested model showed skill in reproducing the hydrographs and the flood extents. Using an ensemble of rainfall input, the multiple model realizations envelope the observed streamflow indicating that the uncertainty of the rainfall is implicitly captured in the model results. The simulated streamflow at the outlet varies significantly depending on the spatial resolution of the rainfall but shows small sensitivity to the temporal resolution of the rainfall input. However, the local rainfall-runoff volumes vary significantly depending on the spatial and temporal resolution of the rainfall input. Recommendations are given to Manchester to highlight areas at risk to flooding. Recommendations are given to the IFC on the capabilities of the nested regional-local modeling approach along with suggestions for future work to incorporate urban areas into the statewide flood forecasting system.

## **PUBLIC ABSTRACT**

Many cities in Iowa have experienced extreme flooding caused by heavy rainfall and high flows through neighboring rivers. After the disastrous floods of 2008, the Iowa Flood Center (IFC) was established to provide the state with real-time flood data. Residents need up-to-date information before, during, and after flooding occurs. City terrains use concrete extensively which means that rainfall onto these impervious surfaces quickly drains into the stormwater network (pipes, channels, ditches). Cities pose a challenge for engineers and scientists because the stormwater movement is channeled by the buildings, streets, underground pipes, and other man-made obstructions. Understanding the way flood waters behave in urban areas is important to provide accurate, real-time flood information for citizens.

The objective of this work was to create an urban flood model and test its capabilities to provide accurate streamflow predictions. This project focused on the hydrologic and hydraulic impacts of the City of Manchester, Iowa in the largely, rural Maquoketa River watershed. The sources of error that influence the accuracy of the model were investigated. The model can inform decision-makers and local emergency managers on the areas vulnerable to flood-related hazards. This report discusses the advantages to the modeling approach selected and provides recommendations for future work to apply similar models to all urban areas in Iowa.

# TABLE OF CONTENTS

LIST OF TABLES .....	ix
LIST OF FIGURES .....	xi
CHAPTER 1: INTRODUCTION .....	1
1.1 Motivation .....	3
1.2 Objective .....	7
1.3 Overall Approach .....	8
CHAPTER 2: LITERATURE REVIEW .....	10
2.1 Modeling Approaches .....	10
2.2 Urban Key Features .....	13
2.3 Uncertainty .....	17
CHAPTER 3: FLOOD EVENTS, DATA AND MODELS .....	21
3.1 Case Study .....	21
3.2 Models .....	25
3.2.1 Regional Model .....	27
3.2.2 Local Model .....	28
3.2.3 Model Comparison .....	29
3.3 Streamflow Data .....	31
3.4 Precipitation Data .....	32
3.5 Flood Events Summary .....	33
CHAPTER 4: METHODOLOGY .....	37
4.1 Local Model .....	37
4.1.1 1D Domain .....	37
4.1.2 2D Domain .....	45
4.1.3 Model Settings .....	49
4.2 Model Combinations .....	50
CHAPTER 5: MODEL EVALUATION .....	54
5.1 Model Validation .....	54
5.1.1 July 2010 .....	57
5.1.2 September 2016 .....	62
5.2 Model Performance .....	65
5.2.1 July 2010 .....	67
5.2.2 September 2016 .....	73
5.3 Uncertainty .....	78
5.3.1 Model Structure .....	78
5.3.2 Rating Curve .....	79
5.3.3 Rainfall .....	80
5.4 Discussion .....	82

CHAPTER 6: MODEL APPLICATION .....	83
6.1 Design Storms .....	83
6.2 Local Flooding .....	89
6.3 Hazard and Flood Maps .....	95
CHAPTER 7: RECOMMENDATIONS AND CONCLUSIONS .....	100
7.1 Recommendations for Manchester .....	100
7.2 Recommendations for IFC .....	105
7.3 Conclusions .....	108
REFERENCES .....	111

## LIST OF TABLES

Table 1. Annual average climate normals for Delaware County .....	24
Table 2. Peak streamflow and stage records on the Maquoketa River at Manchester (USGS) compared to the NWS Flood Categories .....	33
Table 3. The Manchester stormwater network components included in local XPSWMM model .....	40
Table 4. XPSWMM subcatchment infiltration types.....	44
Table 5. XPSWMM runoff subcatchment information .....	45
Table 6. XPSWMM 2D landuse types and parameters used in the Manchester model.....	48
Table 7. XPSWMM 2D soil types and parameters used in the Manchester model.....	48
Table 8. XPSWMM model components for configurations XP-C1 and XP-C2 .....	53
Table 9. Comparison of the NWS COOP rain gauge accumulated precipitation measurements to the radar rainfall estimates for July 2010 and September 2016.....	55
Table 10. Statistical analysis to evaluate model performance in predicting the discharge at the outlet for the flood of July 2010.....	70
Table 11. Statistical analysis to evaluate model performance in predicting the stage at the outlet for the flood of July 2010.....	71
Table 12. Statistical analysis to evaluate model performance in predicting the Major Flood Stage at the outlet for the flood of July 2010.....	72
Table 13. Statistical analysis to evaluate model performance in predicting the discharge at the outlet for the flood of September 2016 .....	75
Table 14. Statistical analysis to evaluate model performance in predicting the stage at the outlet for the flood of September 2016 .....	76
Table 15. Statistical analysis to evaluate model performance in predicting the majort flood stage at the outlet for the flood of September 2016 .....	77
Table 16. Summary of Statewide Urban Design and Specifications (SUDAS) for Stormwater .....	85
Table 17. Change in 2D landuse percent impervious for saturated ground during October 2007 flood .....	90



Table 18. Uniform loss method of infiltration used for saturated ground during October 2007 flood .....	90
Table 19. Statistical analysis of the simulated discharge and the USGS observed streamflow for October 7, 2007 .....	92
Table 20. HLM stage output compared to measurements across the upper Maquoketa River basin for September 2016.....	103
Table 21. Travel times for observed and measured peaks throughout the upper Maquoketa River basin for September 2016.....	104
Table 22. Useful stormwater network data for building a 1D/2D hydrodynamic model for an urban area.....	105
Table 23. Computational requirements for individual XPSWMM model simulations .....	106

## LIST OF FIGURES

Figure 1. The majority of the land in Iowa is rural (gray) compared to the urban areas (red).....	2
Figure 2. Photo of local flooding on Main Street in downtown Manchester on July 24, 2010 .....	5
Figure 3. Drone photo of flooding in downtown Manchester during September 2016.....	6
Figure 4. The Maquoketa River watershed (red) and the upper Maquoketa River watershed (green) drain into the Mississippi River at the northeastern border of Iowa. ....	22
Figure 5. The Maquoketa River drains directly through downtown Manchester where a whitewater park was installed in 2016. ....	23
Figure 6. Historical crests that exceeded the NWS Flood Stage on the Maquoketa River at the Manchester USGS gauge from 2000-2018.....	24
Figure 7. Maximized precipitation calculated using the method described in HMR-51 for the upper Maquoketa River watershed. ....	25
Figure 8. Areas of interest for the regional and local models are the upper Maquoketa River watershed and the city limits of Manchester, respectively. ....	26
Figure 9. The land surface representation as hillslopes and links by the HLM.....	27
Figure 10. The HLM representation of eastern Manchester as hillslopes and links (white) compared to the actual stormwater network (black and blue).....	30
Figure 11. The spatial resolution of the radar rainfall products over Manchester including (a) StageIV-4km, (b) MRMS-1km and (c) IFC-500m.....	33
Figure 12. A comparison of the accumulated precipitation over the upper Maquoketa watershed for the July 2010 flood event with (a) StageIV and (b) IFC radar rainfall estimates .....	34
Figure 13. StageIV rainfall intensity, the NWS Flood Categories, and USGS discharge records on the Maquoketa River at Manchester for July 2010.....	35
Figure 14. A comparison of the Accumulated precipitation over the upper Maquoketa watershed for the September 2016 flood event with (a) StageIV and (b) MRMS radar rainfall estimates.....	36

Figure 15. StageIV rainfall intensity, the NWS Flood Categories, and USGS discharge records on the Maquoketa River at Manchester for September 2016.....	36
Figure 16. The density and layout of the Maquoketa River cross-sections used in XPSWMM before and after the whitewater park addition in 2016 .....	38
Figure 17. Manchester’s stormwater network system modeled in the local XPSWMM model .....	41
Figure 18. The location of XPSWMM runoff subcatchments, their connection to 2D Domain, and a visualization of the natural drainage for the landsurface. ....	42
Figure 19. The topography of downtown Manchester and the Maquoketa River as represented by a 1m DEM .....	45
Figure 20. The XPSWMM 2D landuse types used in the Manchester model .....	47
Figure 21. A flow diagram of the overall approach to the nested regional-local model.....	51
Figure 22. Nested regional-local model configuration XP-C1 .....	52
Figure 23. Nested regional-local model configuration XP-C2 .....	52
Figure 24. Areas of interest for model validation including the Sports Complex, River St., Main St., and north of Hwy 20 .....	56
Figure 25. The output max flood extent for stages 16, 20, and 24 ft from a 1D HEC-RAS river model compared to the output of XP-C2 IFC for July 2010.....	58
Figure 26. Model results for XP-C2 IFC including flood depths at the time of peak flow (7/23/10 22:15) for July 2010 .....	59
Figure 27. July 2010 flood event photos used for validation against model outputs at (a) the Sports Complex, (b) River St., (c) Main St., and (d) Hwy 20 .....	61
Figure 28. Model result of XP-C2 MRMS including flood depths at the time of peak flow (9/23/16 14:30) for September 2016 .....	63
Figure 29. September 2016 flood event photos used for validation at .....	65
Figure 30. Comparison of the observed USGS hydrograph and the model results for the July 2010 flood .....	68

Figure 31. Comparison of the USGS stage records and the model results for the July 2010 flood.....	69
Figure 32. Comparison of the observed USGS hydrograph and the model results for the September 2016 flood.....	74
Figure 33. Comparison of the USGS stage records and the model results for the September 2016 flood .....	74
Figure 34. The effect of the rainfall temporal and spatial resolution on the hydrologic response of eastern Manchester up to the railroad crossing for the July 2010 flood .....	81
Figure 35. The effect of the rainfall temporal and spatial resolution on the hydrologic response of eastern Manchester up to the railroad crossing for the September 2016 flood.....	82
Figure 36. Design storms for 5, 10, 50, 100, and 500yr return periods with a 6hr duration for northeast Iowa .....	86
Figure 37. Model results for the 100yr-6hr design storm scenario shows (a) ditch capacity is exceeded, (b) culvert is overtopped into streets, and (c) detention pond is able to store excess flows .....	87
Figure 38. Flow in Eastern Tributary at Railroad Crossing for the 6hr design storms with a return interval of 5, 10, 50, 100, 500yr.....	88
Figure 39. Stage IV rainfall and USGS streamflow records for October 2007 compared with HLM and XP simulations.....	91
Figure 40. Streamflow for the October 2007 flood event at the confluence of Tributary A and Tributary 2 at the railroad tracks in the east .....	92
Figure 42. XPSWMM output for Oct 2007: saturated conditions with (a) the stormwater system active and (b) overland flow only .....	93
Figure 41. High water levels in the Maquoketa River nearly touching the low-chord of the railroad crossing during the July 2010 flood .....	94
Figure 43. XP-C2 IFC max depth and velocity map output for July 2010 compared to photos .....	96
Figure 44. XP-C2 IFC max hazard (VxD) map for the July 2010 event compared to photos.....	97
Figure 45. XP-C2 IFC max road safety risk for the July 2010 event compared to photos .....	98

Figure 46. XP-C2 IFC max property safety risk for the July 2010 event compared to photos .....	98
Figure 47. XP-C2 IFC time to peak water surface elevation (hr) for the July 2010 event compared to photo .....	99
Figure 48. Locations of crest measurement across the upper Maquoketa River Watershed.....	101
Figure 49. HLM forced with StageIV output compared to stage measurements across the upper Maquoketa River basin during September 2016.....	102

## **CHAPTER 1: INTRODUCTION**

In a world where social dynamics have evolved during the last century to concentrate 81 percent of the population into urban areas (e.g. US Census 2016), urban hydrologic and hydraulic engineering play an important role when discussing the potential hazards of water in an urban environment. Urban hydrology describes the design, analysis, and management of urban stormwater drainage systems, as well as hydrological modeling and prediction. Hydraulic engineering describes the dynamics of fluid flows in pipes, channels, rivers, and around or through other features. There is a growing interest in learning how hydrologic extremes of interest, such as flash floods and droughts, would impact urban areas. This implies global relevance of the field of hydrology because of the ubiquitous reaches of water. More recent attention has been brought to natural hazards that impact urban areas because of the safety risks and destruction of infrastructure.

The state of Iowa is approximately 56,300 mi<sup>2</sup> of mostly agricultural land as shown in Figure 1. Even though Iowa is primarily rural, the urban areas are vulnerable to hazardous flooding. The urban areas in Iowa range from small towns (1 mi<sup>2</sup>) to larger cities (90 mi<sup>2</sup>). At the Iowa Flood Center (IFC), researchers are working to improve forecasting methods and tools so that decision-makers have accurate information before and during a potential flood. Urban landscapes pose a challenge because of the fine-scale features and terrain modifications made by engineered structures including the streets, buildings, stormsewers, and impervious surfaces. This project focuses on integrating hydrologic and hydraulic tools to evaluate the impacts of an urban area in a largely, rural

watershed. In this study, the term “local” refers to the smaller, urban area of interest that is within a “regional” watershed that is characterized by rural or more natural terrain.

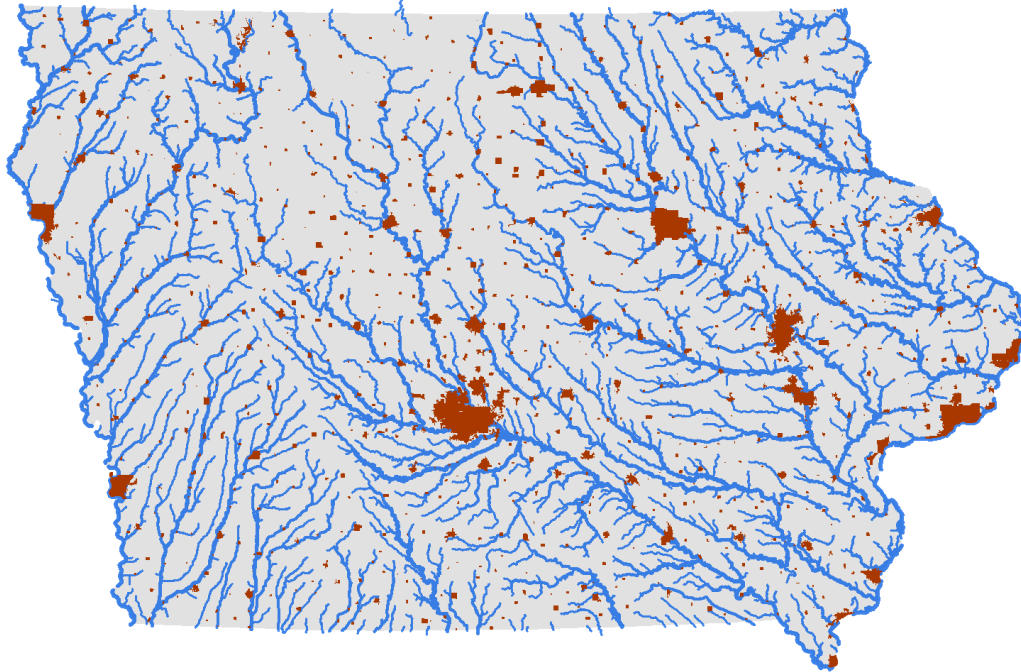


Figure 1. The majority of the land in Iowa is rural (gray) compared to the urban areas (red).

Different considerations must be given to the type of hydrologic and hydraulic model that should be used in an urban versus rural area. There is a drastic shift in spatial and temporal scales between a regional model and a local model. To explain the concept of spatiotemporal scales, create a hydrological model for the state of Iowa that can be used to model the annual water fluxes in that region. This model likely uses a coarse-spatial resolution ( $50\text{ m} >$ ) and a large temporal resolution (weeks or months). Another hydrologist might be using a model with a fine-spatial resolution ( $< 5\text{ m}$ ) and small temporal resolution ( $< 24\text{ hr}$ ) to simulate the runoff generation of a single rainfall event over a city. For real-time applications, these rural and urban models need to operate at a temporal resolution of minutes to hours. Careful attention must be given to understanding

the dominant physical processes at both scales and how they interact. Researchers in the field of urban hydrology are driven by the question: Why is it necessary to distinguish the local and regional areas in hydrological models for accurate flood predictions?

## **1.1 Motivation**

Understanding the hydrologic and hydraulic processes in urban areas is important for improved accuracy in real-time flood information at the local scale. Given an impending extreme storm, people need to be continuously informed on the potential impacts before, during, and after the flooding occurs. Answers to the following sample questions would be invaluable:

- How much time do I have to evacuate my home?
- What roads do I use to evacuate safely?
- How much water will there be and how quickly will it be moving?

The aim of this research is to provide insight into how to use existing modeling tools to answer these questions. The hydrologic and hydraulic results presented in this report are intended to (1) enlighten the public on the different risks of flooding and (2) contribute to the IFC's overall goal to incorporate all urban areas in Iowa (Figure 1) into the operational real-time flood information system.

The IFC was established at the University of Iowa in 2009 after the devastating floods of 2008 revealed that there was a critical lack of flood information available to the public (Witold F. Krajewski et al. 2017). The center is an academic research unit under the College of Engineering and is hosted at IIHR-Hydroscience and Engineering (IIHR). The IFC was charged by the legislature to improve the availability of flood-relevant information to Iowans. Some of the IFC's projects include the deployment of over 250 bridge-mounted stream-stage sensors, the creation of a community flood inundation map



library, the development of a statewide, real-time streamflow forecasting system, and the Iowa Watershed Approach (IWA) Project. A priority of the IFC staff is to provide flood-relevant information to the public, emergency management, and state and local authorities through an interactive portal called Iowa Flood Information System (IFIS).

The IFC developed an operational real-time flood forecasting system that forces evapotranspiration and radar rainfall inputs into a rainfall-runoff distributed model with streamflow routing. The model is called the Hillslope Link Model (HLM), based on its decomposition of the landscape into hillslopes connected to link channels (Krajewski et al., 2017). This model is not calibrated and provides streamflow predictions for over 2,000 points on the river network across Iowa including 1,000 communities (Krajewski et al., 2017). The IFC forecasting system uses radar-based, statewide rainfall data that can provide rainfall accumulation products at 5-min, hourly, daily, and two-week intervals. The IFC is continuously working to improve the HLM model by taking a closer look at specific hydrological processes and the way they are represented in the model. One area that requires further investigation is how to account for the hydrologic impacts of urban areas.

Many cities in Iowa experience extreme flooding because of overflow from the rivers. The northeastern counties of Iowa experienced a period of extreme flooding that was declared a Major Disaster by FEMA in 2010. Located in the upper Maquoketa River watershed, the City of Manchester was flooded by the overwhelming flows in the river during the summer of 2010 (Figure 2).



Figure 2. Photo of local flooding on Main Street in downtown Manchester on July 24, 2010

The National Flood Insurance Program Bureau and Statistical Agent Iowa reported 27 claims with over \$1.4 million dollars of damage payment in the Delaware County for July 23-26, 2010 (Eash, 2012). The city has experienced numerous extreme floods that were documented by the community including river crests measurements throughout the basin, photographs, and drone footage. More recently, in September of 2016, the upper Maquoketa River basin experienced torrential rainfall, flash flooding, and major riverine flooding that left the City of Manchester inundated as shown in Figure 3.



Figure 3. Drone photo of flooding in downtown Manchester during September 2016

The IFC seeks to work with and on behalf of smaller communities who might not have the resources required for an in-depth flood study. Manchester was an ideal option for a case study given the historical significance of flooding. Due to the medium size of the city and the availability of data, a significant amount of time was spent on constructing the details of the urban model. The momentum for this project was derived from the strong working relationship the IFC has with the City of Manchester and the local agencies. To date, web-meetings are held multiple times a year to discuss ongoing and potential projects with local citizens invested in the area including representatives from the US Army Corps of Engineers (USACE), the Iowa Department of Natural Resources (IDNR), the National Weather Service (NWS), the City of Manchester, Delaware County Emergency Management (EMA), and the IFC.

## 1.2 Objective

Hydrologic flows in urban landscapes are characterized by fast runoff and short response times due to the extensive amount of impervious surfaces (Miller et al., 2014). To reproduce these physical processes, models of urban areas typically require a numerical model that computes the water balance using smaller time and spatial scales than those used for rural hydrology. In areas where rain gauge data is not present, radar rainfall is an ideal candidate because it has the capabilities to be resolved to small scales that are suitable for application to urban models (Thorndahl et al., 2017). Further research is needed to understand the impacts of the spatiotemporal variability of rainfall impacts the results of flood models, and thus the accuracy of urban flood predictions (Bruni, Reinoso, Van De Giesen, Clemens, & Ten Veldhuis, 2015; Krajewski, Kruger, Singh, Seo, & Smith, 2013; Ochoa-Rodriguez et al., 2015; Peleg, Blumensaat, Molnar, Fatichi, & Burlando, 2016; B. K. Smith, Smith, Baeck, Villarini, & Wright, 2013; Thorndahl et al., 2017; Wang et al., 2015; Wright, Smith, Villarini, & Baeck, 2014). There remains a significant amount of uncertainty from rainfall inputs and most hydrologists use ensembles to make predictions. Essentially, the idea of an ensemble is to provide a range of possible model results (realizations) using multiple rainfall inputs. Capturing the non-linear, spatiotemporal patterns of rainfall is an ongoing battle for many researchers. In this study the impact of various radar rainfall inputs into a flood inundation model are compared.

Typically, urban models are developed on an “as needed” basis and for a specific purpose (Bisht et al., 2016), but more recently there is a need to develop a method that can more efficiently be applied to give accurate, flood information for all cities. The objective of this project is to test the abilities of a nested regional-local model to provide

accurate flood predictions in an urban area and to operate in real-time. The model should incorporate the tools and products maintained at the IFC including the streamflow bridge sensors, rain gauges, radar rainfall product, and statewide model. The results presented in this study are intended to provide a basis for future work at the IFC to incorporate all urban areas into the operational system. This work was guided by the following research questions:

- Is it feasible to model all urban areas in Iowa with a high-resolution, small scale model?
- What are the data requirements for creating a detailed model of a city?
- How do the key features in urban areas impact the hydrologic response?
- What is the spatial and temporal resolution of rainfall input required for accurate urban hydrologic modeling?
- What is the correct spatiotemporal scale to use when modeling the fluxes in an urban area? What simplifications are appropriate?
- What are the main sources of uncertainty and how do we account for them?
- What is the balance between model complexity and computational efficiency?
- Is the nested regional-local modeling approach suitable for real-time forecasting?
- What model outputs are most useful and how should it be presented?

### **1.3 Overall Approach**

A case study using a nested regional-local modeling approach was completed for Manchester, Iowa located within the upper Maquoketa River basin. The aim was to investigate how using various rainfall resolutions and urban rainfall-runoff dynamics impacts streamflow predictions. Two of the advantages of using a nested regional-local model is that the regional model operates at a computational efficiency needed for real-time simulation while providing reasonably good characterizations of runoff inflows into the local model (Bermúdez et al., 2017). Higher resolutions are required for urban models when street-level information is desired whereas a low-resolution model, with simplified physics, is typically sufficient for regional models (Chen et al., 2012). Hydrological

processes that are significant in an urban model are not necessarily of the same level of importance in a regional watershed model.

A nested regional-local model was developed to simulate two historical floods documented in Manchester. Various rainfall estimates from different radar products were used as input to the regional model and local model. The boundary conditions for the local model were the streamflow outputs of the regional model. It is hypothesized that for extreme rainfall events, the uncertainties of the model structure and rainfall input will mask the hydrologic impacts of the local model. The varying spatial and temporal resolution of rainfall inputs is expected to heavily influence the rainfall-runoff processes in both the regional and local models (Emmanuel, Andrieu, Leblois, Janey, & Payrastre, 2015; Ochoa-Rodriguez et al., 2015; Wright et al., 2014). To reproduce the rainfall-runoff processes and surface/subsurface routing unique to urban areas, a 1D/2D model with a fine resolution is preferred because of the detailed spatiotemporal output. For smaller, localized storms that occur more frequently, it is expected that a detailed, fine-resolution model of an urban area is necessary to accurately capture the hydrologic response.

An overview of the literature relevant to hydrologic and hydraulic modeling in urban areas will be discussed followed by an overview of the case study details. More information on the historic flood events of interest, the streamflow and precipitation data, and the models used will be discussed. After establishing the background of the project, the methodology and modeling approach will be presented. The model results for each flood event will be validated using photos, crest records, and 1D model flood extents. Statistical analysis is used to compare the performance of the models to predict the

observed streamflow. For different scenarios, the nested model was applied to improve the flood awareness and preparedness of the community and local officials. Finally, a summary of the main findings and recommendations will be provided to both the IFC and the town of Manchester.

## **CHAPTER 2: LITERATURE REVIEW**

Flood modeling is an inter-disciplinary challenge requiring knowledge on climate, river, and hydrological models. Flood inundation models are intended to improve our ability to understand, assess, and predict floods and the impacts. They have many uses including real-time predictions, water quality, risk assessment, mitigation strategies, urban planning, amongst many others (Czajkowski, Cunha, Michel-Kerjan, & Smith, 2016; Fletcher, Andrieu, & Hamel, 2013; Garcia et al., 2015; Ha, Stenstrom, & Asce, 2008; Henonin, Russo, Mark, & Gourbesville, 2013; Salas et al., 2017). The challenge at hand is finding a way to rapidly and accurately generate flood models for urban areas. Currently, there is no universal method or standard for simulating an urban stormwater system at the catchment scale.

### **2.1 Modeling Approaches**

The main models used for inundation modeling include empirical, hydrodynamic, and conceptual models. Empirical methods use data including, satellite imagery, aerial photographs, on-ground measurements, or surveys to represent reality. The results of these models are widely used in flood monitoring and also for validating hydrodynamics models (Teng et al., 2017; Yang, Smith, Baeck, & Zhang, 2016). Hydrodynamic models are mathematical models that solve equations that describe the physics of water movement, typically as one, two, and three-dimensional models (1D, 2D, and 3D) (Teng

et al., 2017). 2D models can provide predictions of flow pattern at the scale of the individual buildings which is useful for risk analysis (Ernst et al., 2010). 2D porous shallow water models have more recently been used to simulate flow in the overland surface because they do not have a computational demanding mesh (Dottori & Todini, 2013; Guinot et al., 2017; Schubert, Sanders, Smith, & Wright, 2008).

Semi-distributed models are conceptual models that use a hybrid approach to describe the catchment with effective parameters that represent a global hydrologic behavior, usually found through calibration (Barco, Wong, Stenstrom, & Asce, 2008; Gires et al., 2016; Simões et al., 2015). These parameters cannot be directly measured and their relationship to the physical processes being modeled are not fully explainable. Modelers run the risk over over-parameterization when increasing in model complexity which introduces additional uncertainty in parameter determination and doubts on the model's robustness and reliability (Fletcher et al., 2013; Teng et al., 2017). Conceptual models or non-physics based methods do not simulate the physical process of inundation but are based on simplified hydraulic concepts. These methods are commonly used in flood prediction because they have the advantage of having minimal computational costs compared to hydrodynamic models. Examples include the Rapid Flood Spreading Method (RFSM) or the Height Above the Nearest Drainage (HAND) of which both derive the flood extent by simplifying and normalizing the topography (Falter et al., 2013; Nobre et al., 2016).

Defining the model's purpose and intended application is necessary when choosing the appropriate model. A model is selected based on the desired output variables and level of accuracy while working within the constraints of the model's



computational and data requirements. Neelz and Pender (2013) groups the modeling packages into three categories. First, the “3-term models” solve the shallow water equations (SWE) but neglect the advective acceleration term. The “2-term models” use the Manning’s uniform flow law and solve the SWE without the acceleration term. Lastly, the “0-term models” are based on continuity and topographic connectivity, thus providing the final state of inundation. Modeling packages that are based on the 3-term approach (LISFLOOD-FP, RFSM-EDA) can predict water levels and velocities comparable to the SWE packages. The 2-term packages (such as ISIS Fast Dynamic, UIM) are suitable for predicting the final inundation extent but not velocities. The 0-term packages provide information on the final water levels but give no information on the flow dynamics.

Accuracy and efficiency are two major indicators of the performance of a flood inundation model. Typically, high accuracy in model results is attained by (1) considering more terms in the governing equation to explain the flow behavior, (2) by applying numerical methods that have a higher order precision and calculation that reduces machine error, and (3) finally by using a finer spatiotemporal resolution to capture the unique heterogeneities of the land surface (Chen et al., 2012). In contrast, to improve the efficiency of the model the user can neglect less significant terms in the governing equations, use numerical schemes that have increase the solving speed, reduce the dimensions of the model, and use better hardware (Chen et al., 2012).

With an increase in model resolution, the number of grid cells increased by square of the resolution ratio, thus decreasing the computational timestep to ensure model stability. With an increase in cell size, there might be an improvement in model

efficiency that comes at the loss of information about the surface features. Falter et al. (2013) completed a nationwide flood risk assessment in Germany to compare the results of a Raster-based inertia model, a Dynamic Rapid Flood Spreading Model (Dynamic RFSM) and the fully dynamic SWE model InfoWorks RS 2D at resolutions varying from 25 to 500 m. Both the RFSM and InfoWorks models could simulate the final inundation extent and depths. Coarsening the grid resolution for the Raster-based model improved computational efficiency but the accuracy gradually decreased. Some studies use a fully coupled model to simulate the interactions between surface runoff, forced infiltration and groundwater feedbacks in an urban area (Kidmose, Trolborg, Refsgaard, & Bischoff, 2015). Inflows and outflows through the many urban systems, such as infiltration or groundwater inflow into the sewer network, should be considered (Sto. Domingo, Refsgaard, Mark, & Paludan, 2010). Sto, et al. (2010) compared a 1D/2D model (Mike Flood) to a 3D hydrologic model coupled to a 1D model of the drainage network (MOUSE-SHE) and found that depending on the catchment, certain hydrologic processes contribute to flooding and a holistic view of the water cycle is necessary for accurate flood inundation modeling. The implementation of a 1D/2D hydrodynamic model in real-time forecasting is typically dependent on the computational resources and data availability of the area. However, Russo et al. (2015) created a calibrated and validated model for an urban area in Barcelona using the 1D/2D software InfoWorks that achieved computational performances suitable for real-time flood warning applications.

## **2.2 Urban Key Features**

Data availability, model construction time, and model computational expenses are a major challenge for developing comprehensive flood inundation models for each

individual urban area. Accurately representing the heterogeneous landscape and spatially-distributed hydrological processes across an urban landscape is difficult. The distribution of the impervious land cover, storm sewer network, and stormwater management structures are a few of the features that are known to impact the hydrologic response of the watershed (Meierdiercks, Smith, Baeck, & Miller, 2010). Modifications to the drainage network and conveyance characteristics have significant effects on flooding in urbanized catchments. The systems unique to urban landscapes can be classified as ‘major systems’ which include the streets, sidewalks, and other surface conveyance systems and ‘minor systems’ which include the subsurface sewer network (Russo et al., 2015). Modeling the flow interchanges between these systems is crucial for an accurate depiction of the complex water flows in urban morphologies (Mark, Weesakul, Apirumanekul, Aroonnet, & Djordjević, 2004; Russo et al., 2015; Sto. Domingo et al., 2010). Additional complications arise in urban areas because subsurface utilities often drain across the boundaries of surface catchments. Modelers must account for both major and minor flow pathways.

The methods that are suitable for delineating rural landscapes are not easily fitted for use in urban landscapes (Jankowfsky et al. 2013). A balance of model accuracy and computational efficiency is required because the quality of the topography and drainage network representation improves with the degree of segmentation but the computing-time grows as well. Hydrodynamic models can represent the terrain using cells of the same shape and size or as non-uniform meshes composed of polygons or triangles (Gironás, Niemann, Roesner, Rodriguez, & Andrieu, 2010; Sonja Jankowfsky, Branger, Braud, Gironás, & Rodriguez, 2013; Rodriguez, Bocher, & Chancibault, 2013). A more recent

tool developed called Geo-PUMMA generates vectorial meshes for distributed hydrological modeling and is capable of extracting drainage patterns in urban catchments while preserving features at scales of 80 -150m (Sanzana et al., 2017).

The grid resolution for hydraulic models of urban flooding is determined by the building dimensions, street widths, and separation distances. These unique features define the minimum grid cell size for urban applications to be roughly equal to the shortest length scale of the urban structures (Fewtrell, T.J., Bates, P.D., Horritt, M. and Hunter, Fewtrell, Bates, Horritt, & Hunter, 2008; Mignot, Paquier, & Haider, 2006). To model the hazards of flooding in urban areas, the representation of the terrain must be fine enough to resolve the urban features and the high-velocity, shallow flows around structures. A grid resolution of 1-5m is recommended (Fewtrell, T.J., Bates, P.D., Horritt, M. and Hunter et al., 2008; Mark et al., 2004) while resolutions up to 10 m are adequate for representing the peak flood levels (J. D. Brown, Spencer, & Moeller, 2007).

Accurately representing the deflection of flood waters caused by buildings in numerical models is important for reproducing the flood behavior. Flood inundation models should represent buildings to understand how they affect flows by (1) blocking the flow, (2) resistance to the floodwater, (3) inundation by floodwater, (4) potential loss of floodplain volume, (5) changes in infiltration rates and pathways, and (6) destruction of buildings during extreme events (Bellos & Tsakiris, 2015; J. D. Brown et al., 2007; Schubert & Sanders, 2012; G. P. Smith, Wasko, & Miller, 2012; Syme, 2008). There are a few experimental studies on the flow behavior in urban areas both focusing on a single street intersection and those that analyze the entire flow field in an urban area (Arrault et al., 2016; Dottori & Todini, 2013). Numerous methods have been devised to represent the

influence of buildings on flood flow behavior in either account for the effect of buildings by physically including them in the topography or by introducing additional head loss in the model computational grid points at the building footprints. Different techniques for modeling buildings include (1) increasing the model roughness for building footprints, (2) removing model elements from the active grid for building footprints, (3) modeling building exterior walls partially by increasing the elevation, (4) using external walls, and (5) modeling buildings as ‘porous’ elements by modifying the shallow water equations (Syme, 2008).

Deducing the drainage patterns and catchment areas in urbanized areas purely from a terrain analysis does not properly account for the complex surface and subsurface flow patterns. The use of LIDAR has been proven successful for detecting anthropogenic modifications (e.g. streets or ditches), however, they cannot detect the underground drainage system (Jankowfsky et al 2013). Attempts have been made to integrate artificial objects such as buildings, streets, or pipes into the digital elevation model (DEM) or force the flow direction grid to follow the street network (Gironás et al., 2010). Jankowfsky et al. (2013) developed a semi-automated approach to derive the drainage areas in suburban areas (up to 10km<sup>2</sup>) that combines DEM-based methods adapted for natural areas and object-oriented methods more suitable for urban landscapes. This method assumes that the flow direction of the subsurface utilities follows the surface topography, but this is not always the case. Other approaches are being explored to simulate the dynamic flow interactions between the overland surface and the stormsewers (Chang, Wang, & Chen, 2015; Liu et al., 2015; Obermayer et al., 2010). For peri-urban areas, where urban areas are scattered in a largely rural landscape, Jankowfsky et al. (2014) developed an

integrated distributed model (PUMMA) and tested it on a small catchment in France. The uncalibrated model results emphasize the importance of impervious areas for summer flows and rural contributions for winter events. They also concluded that the runoff created from the impervious areas is not directly connected to the drainage system (S. Jankowsky et al., 2014).

### **2.3 Uncertainty**

Two prominent problems in urban hydrology include (1) the spatiotemporal gap between the physical scale of the flow processes and the resolution of the model and (2) a lack of understanding of the interactions between urban and natural hydrological systems (Salvadore, Bronders, & Batelaan, 2015). Given the complex interaction between natural and artificial surface covers and the natural and modified drainage networks, significant uncertainties emerge because of the underlying variability of the stochastic processes (Di Lazzaro, Zarlenga, & Volpi, 2016). Thomas Steven Savage et al. (2016) tried to determine if it was more beneficial to spend computation resources running fewer models with a fine resolution or more models at a coarser resolution that are each exploring the effects of other uncertainty factors. Ultimately, the factors that are most influential vary depending on the chosen model output (Thomas Steven Savage et al., 2016). The combined impacts of input data uncertainties and calibration data uncertainty on the parameters and outputs of urban drainage models have not been extensively studied (Dotto, Kleidorfer, Deletic, Rauch, & McCarthy, 2014).

Resampling data to a finer resolution (spatial perturbations) can affect the simulated peak flow in urban hydrological models (Krebs, Kokkonen, Valtanen, Setälä, & Koivusalo, 2014). The average water depth and max flood extent are primarily

influenced by the inflow hydrographs and boundary conditions (Bermúdez et al., 2017; Thomas Steven Savage et al., 2016). The rising limb of the hydrograph is steep because during the wetting phase, the water levels are sufficient to overcome any potential blockages. Capturing the recession of the hydrograph continues to pose a challenge to modelers because the channel water level drops and the remaining water in the floodplain drains via small flow paths. The sampling resolution of the DEM influences the recession of the hydrograph because of how the smaller flow paths are represented (Thomas Steven Savage et al., 2016).

Changes in imperviousness have a significant effect on the flood peaks for moderately extreme and extreme storms, but are relatively unimportant in terms of runoff efficiency and volume (Ogden, Raj Pradhan, Downer, & Zahner, 2011). Most storms are short and the runoff is quick relative to the rate of water movement from the surface to the subsurface. Models have an inherent storage of water that is ponded because of depressions in the DEM (Leandro, Schumann, & Pfister, 2016). B. K. Smith et al. (2013) found that the differences in urban land cover does not fully account for the differences in hydrologic response in urban catchments, thus emphasizing the important role of runoff production and timing of hydrologic response in the overall urban stormwater system response. Urban features, such as roads and buildings, had medium to high impact on the estimated overland flood-depths while the cumulative effect of the features results in a higher impact (Leandro et al., 2016). The rainfall-runoff from buildings can often be disregarded because of the small percentage of direct runoff generated from buildings is small compared to the total rainfall (Leandro et al., 2016).

The hydrologic importance of the storm drains is heavily dependent on the rainfall event and intensity (Javier, Smith, Meierdiercks, Baeck, & Miller, 2007). Storm drains increase the flood peaks but are overwhelmed during extreme rainfall events and have a negligible effect (Ogden et al., 2011). The local hydrological input from the urban drainage infrastructure due to direct rainfall and small ungauged tributaries is generally assumed to have a minor impact on discharge in fluvial flood modeling, but may become important in a sparse gauge network area or in flooding events with significant local rainfalls (Bermúdez et al., 2017; Neal, Schumann, & Bates, 2012).

Urban areas are vulnerable to the adverse impacts of the increasing occurrences of heavy rainfalls and flooding accounts for most of the natural disasters across the nation (Czajkowski et al., 2016; Salas et al., 2017; Teng et al., 2017). Urban flood risk management is a highly relevant topic because of increased urbanization, climate change, and the magnitude and frequency of extreme rainfall events. Capturing the hydrologic response of an urban area is dependent on the spatiotemporal resolution of the inputs. At a local scale, the effects of rainfall-runoff dynamics and uncertainty in the boundary conditions are difficult to simulate and do not always improve the model performance (Bermúdez et al., 2017). The runoff response, catchment characteristics, and storm characteristics help define the spatiotemporal resolution of the input data needed. Given the nature of the heterogeneity of the land cover and stormwater management structures, there is a quick rainfall-runoff response that is most accurately modeled with smaller spatial and temporal scales (Thorndahl et al. 2017). Thorndahl et al. (2017) recommends that for accurate rainfall inputs into hydrological models include at least 20 years of records and a spatiotemporal resolution of 1 km<sup>2</sup> and 1 min.



The modeled runoff peaks are sensitive to the rainfall resolution compared to the maximum water depths because of the damping effect of flow routing on the water level variations. The hydrologic response of urbanized watersheds is heavily influenced by the temporal and spatial variability of rainfall, more specifically the rainfall rate (Meierdiercks et al., 2010; Ogden et al., 2011). Yang et al. (2016) found that the temporal rainfall variability is relatively more important than the spatial rainfall variability in representing the urban flood response, especially for extreme storm events. Ochoa-Rodriguez et al. (2015) also observed that the variations in temporal resolution of rainfall inputs affect hydrodynamic modeling results more than the spatial variations.

The timing and volume of rainfall turned into runoff has been shown to be a result of the spatial variability of rainfall for large catchments, but there is far less evidence of this for small urban catchments (Bruni et al., 2015). Bruni et al. (2015) says that urban models are less sensitive to variations in the temporal resolution of the rainfall inputs compared to the spatial resolution. This is because urban landscapes are characterized by impervious surfaces, the influence of the spatial variability of rainfall on the magnitude of the peak flow is significantly more prominent than in rural catchments. This is because in rural areas the rainfall is infiltrated into the impervious areas and delayed within the soil (Bruni et al., 2015). Peleg et al. (2016) found that the dominant contributor to the total variability of peak flows in an urban drainage system are attributed to the climate variability and that the spatial variability of rainfall becomes more prominent with longer return periods (10yrs or greater) or catchments of increased area.

The approaches and data used to create flood inundation models vary significantly as a result of the varying objectives. Hydrological models are increasingly complex and

are subject to even higher uncertainty that must be identified (Renard, Kavetski, Kuczera, Thyer, & Franks, 2010; Salvadore et al., 2015). Methods to characterize and quantify uncertainties in model structures and inputs is a significant issue (Gupta, Clark, Vrugt, Abramowitz, & Ye, 2012; Renard et al., 2010). Methods for evaluating model performance area also not consistent across modeling communities (Bennett et al., 2013; Gupta, Kling, Yilmaz, & Martinez, 2009; Legates & McCabe Jr., 2005).

### **CHAPTER 3: FLOOD EVENTS, DATA AND MODELS**

The purpose of this thesis is to evaluate the capabilities of a nested regional-local model for real-time streamflow predictions and to test the sensitivity of the model outputs to various rainfall inputs. In this chapter, an overview of the case study area, Manchester and the Maquoketa River watershed, is given. The models used for the local and regional areas are described followed by a brief explanation of the streamflow and precipitation inputs. Finally, background is provided on the historical floods, July 2010 and September 2016, simulated using the nested model.

#### **3.1 Case Study**

Founded in 1850, the City of Manchester is the largest community in the Delaware County with a population of approximately 5,053 and a square area of 4.7 square miles. Given the size of Manchester, it was an ideal area for the local model because of its moderate size and the availability of data documenting the stormwater infrastructure. Manchester is in the upper Maquoketa River basin in the northeastern region of Iowa as shown in Figure 4.

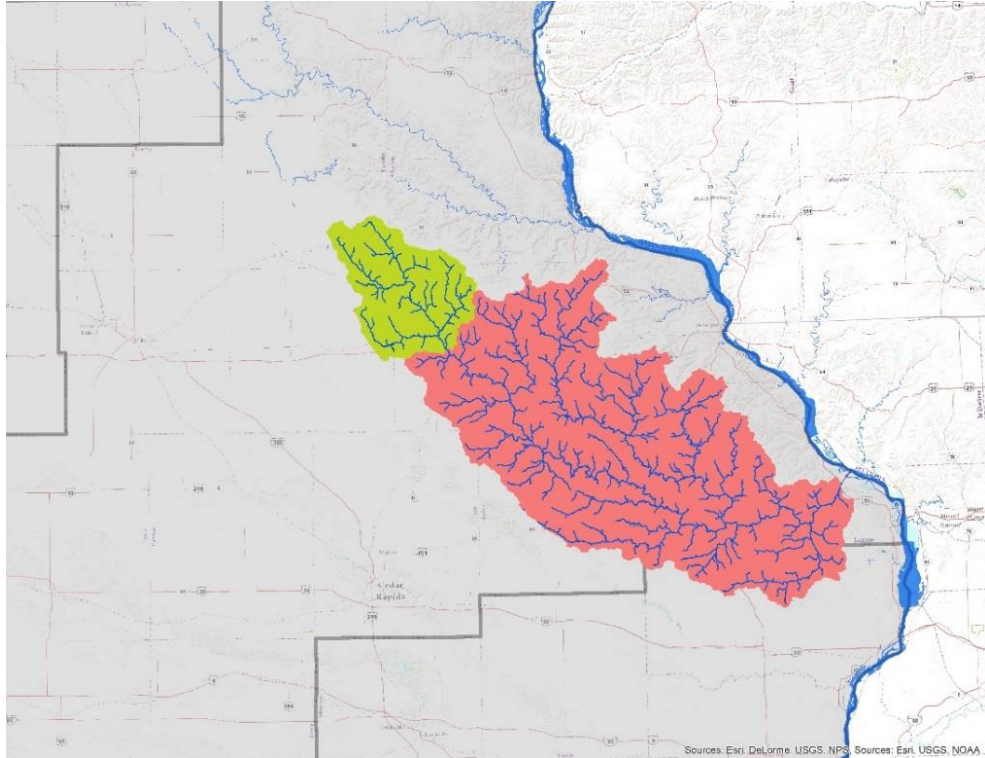


Figure 4. The Maquoketa River watershed (red) and the upper Maquoketa River watershed (green) drain into the Mississippi River at the northeastern border of Iowa.

The upper Maquoketa River drains over 275 square miles of agricultural land through downtown Manchester (Figure 5). The Maquoketa River flows directly through the city providing the locals with river-side properties, parks, and more recently a whitewater park.



Figure 5. The Maquoketa River drains directly through downtown Manchester where a whitewater park was installed in 2016.

Although the river brings the community opportunities for outdoor activities, it can also flood the homes and local businesses. Given its proximity to the river, the city often experiences major flooding caused by the river and upstream flows. Local flooding commonly occurs in the east side of the city where the natural drainage has been distorted by stormwater infrastructure. Recent flood events where the Maquoketa River has crested and caused major flooding in Manchester are recorded by the United States Geological Survey (USGS) and they are shown in Figure 6.

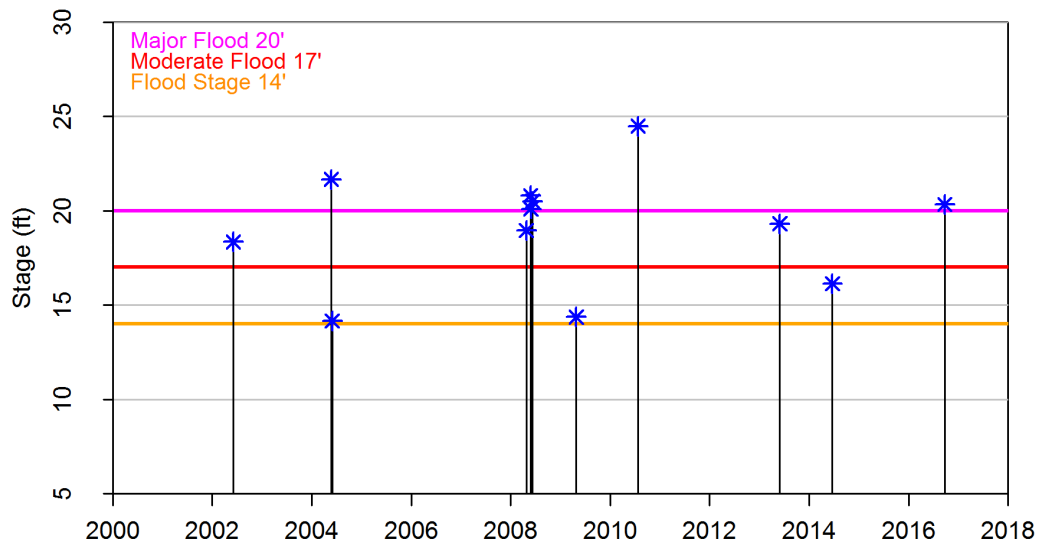


Figure 6. Historical crests that exceeded the NWS Flood Stage on the Maquoketa River at the Manchester USGS gauge from 2000-2018.

The annual normals for Delaware County (Table 1) were retrieved from Iowa Climate Normals Maps produced by the National Weather Service (NWS) using annual data from 1981-2010. The average precipitation during the summer months is 4.9-5.12 inches per month.

Table 1. Annual average climate normals for Delaware County

High Temperature (F)	57-58
Average Temperature (F)	46-47
Low Temperature (F)	36-37
Precipitation (inches)	35.5-37
Average Snowfall (inches)	30-34

The probable maximum precipitation (PMP) for the upper Maquoketa River watershed is between 15-18 inches as shown in Figure 7. This was calculated using a PMP analysis described in the report HMR-51 written by the National Oceanic and Atmospheric Administration (NOAA, 1978). Recorded storms near the site and an in-place moisture adjustment factor were used to estimate the maximized precipitation for the months of June and July.

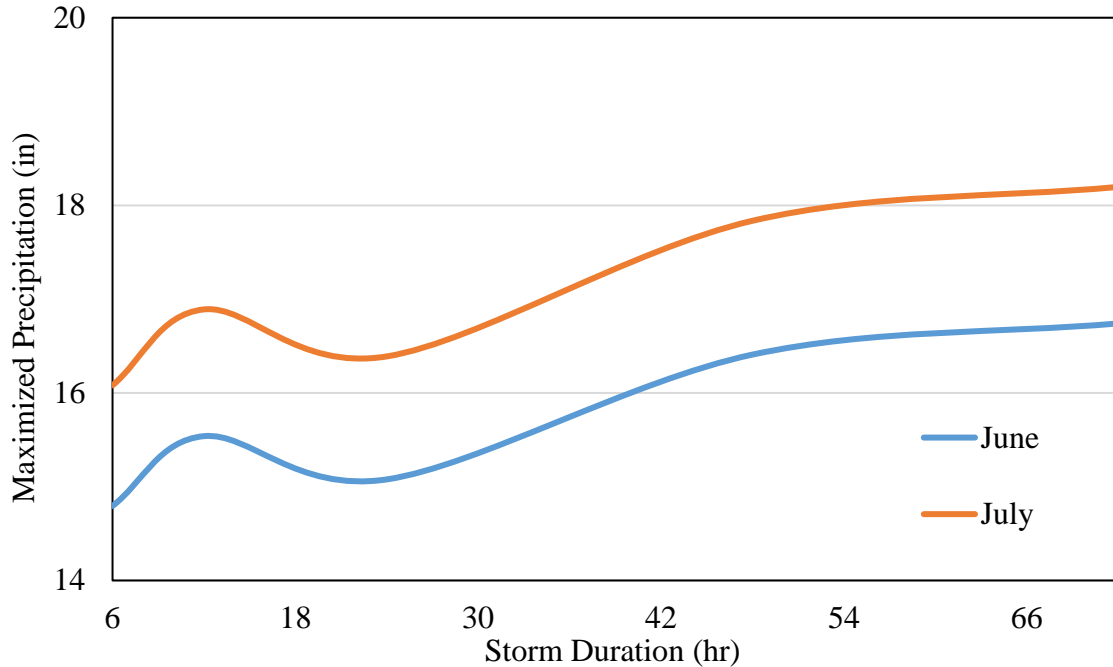


Figure 7. Maximized precipitation calculated using the method described in HMR-51 for the upper Maquoketa River watershed.

### 3.2 Models

The regional area, 275 mi<sup>2</sup> of rural land, was modeled with a computationally efficient physics-based model that operates on a high-performance computing environment. The outputs of the regional model are used as boundary conditions for the local model of the 5 mi<sup>2</sup> of Manchester. This approach has the advantages of creating a one-way connection between a model suitable for rural areas and a model more appropriate for urban landscapes. The area of interest for the regional model is the Upper Maquoketa River, Honey Creek, Coffins Creek, and the Eastern Tributary as shown in Figure 8. The area of interest for the local model is Manchester and the small rural areas located just east and west (Figure 8).



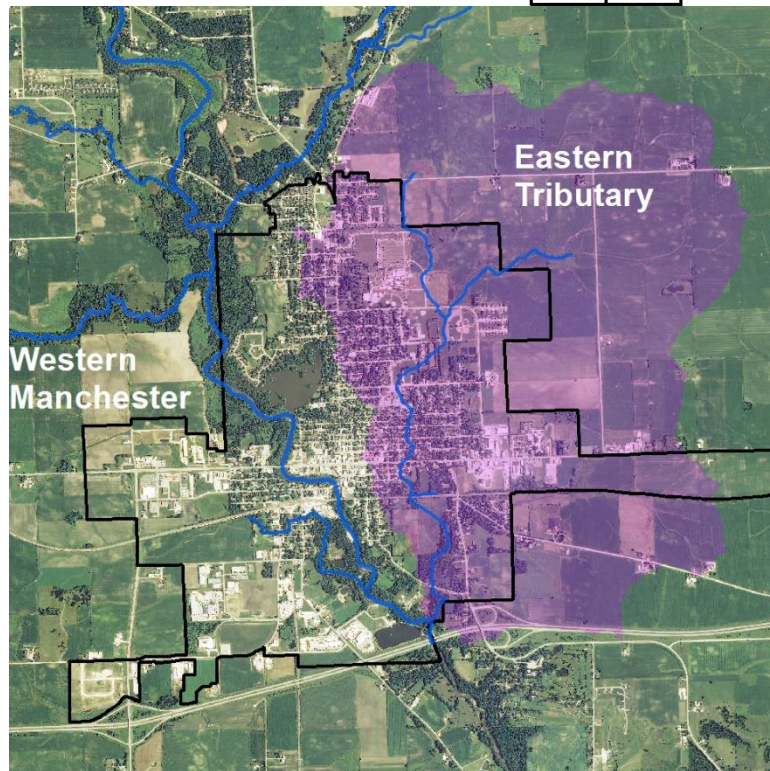
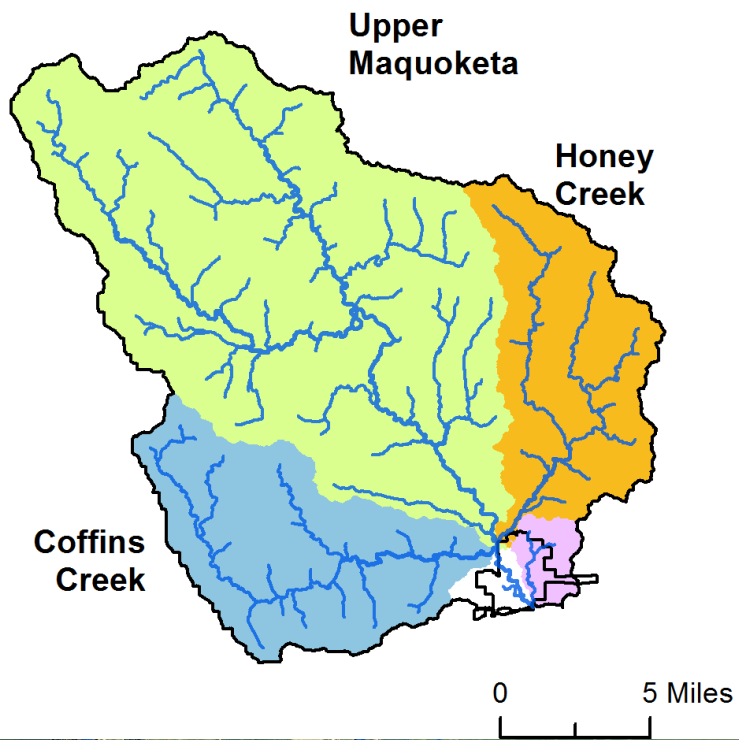


Figure 8. Areas of interest for the regional and local models are the upper Maquoketa River watershed and the city limits of Manchester, respectively.

### 3.2.1 Regional Model

The upper Maquoketa River watershed was modeled using the HLM which is a calibration-free, land surface model that decomposes the landscape into hillslopes and channels (Mantilla & Gupta, 2005) as shown in Figure 9.



Figure 9. The land surface representation as hillslopes and links by the HLM

Each hillslope is divided into four water storage components including channel storage, ponded surface water, water in the top soil, and water in the subsurface. Ordinary differential equations are used to solve the mass conservation equations within the hillslope layers and between the channels and hillslopes. A power law relation that describes flow velocity as a function of drainage area and discharge is used to route the streamflow through each channel link (Ayalew, Krajewski, & Mantilla, 2014). Additional



details about the HLM equations, configuration, and numerical solver can be found in Quintero et al. (2016) and Krajewski et al. (2013a).

### **3.2.2 Local Model**

To fully capture the physical processes in urban areas, XPSWMM was used to model the local area (Figure 8). Supported by the company Innovyze, XPSWMM is a 1D/2D integrated hydrodynamic model that is used to simulate natural rainfall-runoff processes and evaluate the performance of engineered systems that manage drainage systems, specifically in urban landscapes. XPSWMM allows for holistic modeling in urban areas because of its ability to efficiently model the interaction of all the system elements including channels, pipes, streets, control structures, ponds, weirs, catchments, groundwater flow, overland flow, infiltration, and more. Another advantage of this model is that it is constructed for efficient incorporation of GIS, HEC-RAS, EPA SWMM, and CAD. The source code for the solver is in FORTRAN and there is no record of the software running on a high-performance computing environment.

XPSWMM solves the complete St. Venant equations for gradually varied, one-dimensional, unsteady flow throughout the drainage network. The flow can be routed using kinematic or diffusive wave methods. The model can capture unique flow patterns including backwater effects, surcharging, flow reversal, pressure flow, tidal outfalls and interconnected ponds. Users can input inlet types, pumps, control structures and diversions. XPSWMM can simulate the complete hydrologic cycle including snowmelt, evaporation, infiltration, surface ponding and ground-surface water exchanges. XPSWMM has been dynamically linked to XP2D which is a computer program that solves the full two-dimensional, depth averaged, SWE for free-surface flow (Syme,

1991). The 2D domain is represented by a grid comprised of square elements where the computational timestep is described by the Courant Number (Syme, 1991). The computational engine is TUFLOW which uses an alternating implicit (ADI) finite difference method (xp2D Reference Manual). XPSWMM has the capability to dynamically link 1D network domains to 2D domains in a single model. This feature allows the user to model the interaction between stormwater flowing in the underground pipes or the land surface. Rainfall can be applied directly to the 2D domain, and the spatial and temporal changes of rainfall can be accounted for by using multiple polygons with different time series inputs. The cells are further characterized by 2D Land use types and soil types.

### **3.2.3 Model Comparison**

The local and regional models differ primarily on their method of routing water through the watershed via the drainage network and overland flow. The XPSWMM model solves the full set of SWE derived from depth-integrating the Navier-Stokes equations. This is suitable when the horizontal length scale is much greater than the vertical length scale. The vertical velocity component is small and the vertical pressure gradients are nearly hydrostatic. The 1D St. Venant equation can be solved using the dynamic wave, kinematic wave, and diffusive wave sets of the equation and is able to account for backwater effects. The HLM uses a power law relationship to calculate the nonlinearity of flow velocity as a function of the discharge and upstream drainage area. The HLM routing model is very simplistic and is based on scaling properties of the drainage network. It does consider variability of flow in the different channels of the network but it does not include local hydraulic considerations. Reservoirs and subsurface

drainage networks are not accounted for by the version of HLM used in this study. In Figure 10, the HLM hillslopes and drainage network can be seen over the small city of Manchester. It is evident that the overall drainage pattern of the natural surface is like the manufactured stormwater network. This indicates that design engineers attempt to harness the land's natural drainage patterns when channeling stormwater.

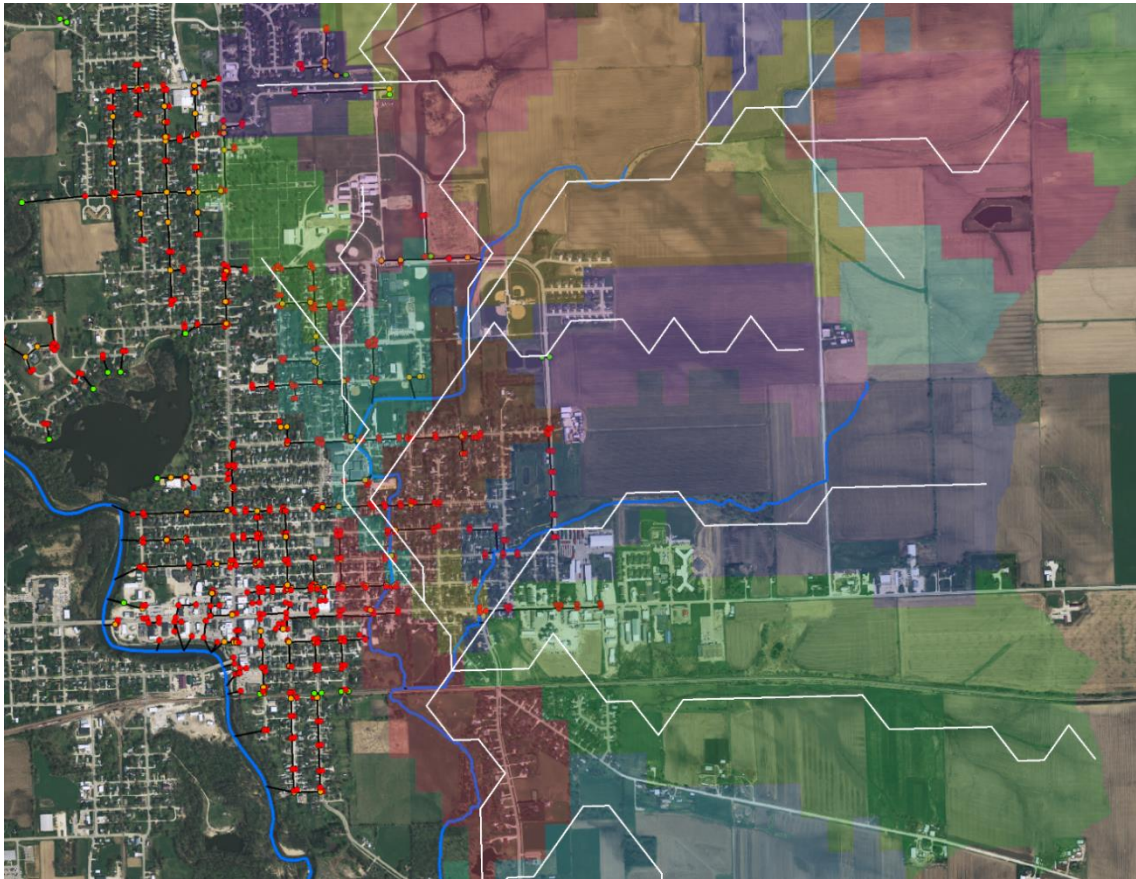


Figure 10. The HLM representation of eastern Manchester as hillslopes and links (white) compared to the actual stormwater network (black and blue)

Often coarse resolution models over-simplify the land surface representation. The average size of the hillslopes in the HLM are  $0.4 \text{ km}^2$  which may represent the land surface of rural areas, but it does not necessarily capture the unique drainage and land cover patterns common in urban areas (Quintero et al., 2016). The HLM hydrological model has three storage terms for every hillslope-link where (1) water is stored in the

channel, (2) water is ponded on the hillslope surface, and (3) the effective water depth in the hillslope surface. The fluxes between these different layers are calculated using principles of the conservation of mass with a runoff coefficient to describe the land surface. Using one runoff coefficient and soil type for a single hillslope is not realistic for hillslopes partially modeling an urban area. The 2D SWEs are used to calculate the sheet flow over the land surface at a fine resolution in XPSWMM, however this is numerically intensive.

In summary, the HLM routes water with a power law relation and water fluxes interact with 4 storage areas using the conservation of mass. XPSWMM solves the full set of the 1D St. Venant equations to route water in the drainage network and the overland flow is accounted for by solving the 2D SWE. These physics-based models are very different in their approaches to hydrological modeling. Computationally, the HLM can produce streamflow outputs at any link effortlessly whereas the XPSWMM model suffers from instabilities when numerically solving the equations. The speed of the HLM is ideal for real-time forecasting but the 2D outputs of the XPSWMM model provide decision-makers with more flood related data. Using a nested regional-local modeling approach will provide information on how models with varying spatial resolution perform in urbanized environments and for real-time flood warnings.

### **3.3 Streamflow Data**

Given a summary of the area of interest and the models being used, the streamflow and precipitation inputs are further explained. The model streamflow outputs are validated against discharge measurements at a USGS Stream Gauge (05416900-USGS, MCHI4-NWS) located directly south of State Highway 20 below the confluence

of the Maquoketa River and the Easter Tributary that drain through the city (Figure 8). Discharge records are available at this gauge from April 2000 to December 2002 and June 2003 to present. Over the period 2000 to 2017, the highest monthly average discharge measured is 623cfs occurring during June and the lowest during January of 145cfs. The spatial variability of rainfall across the upper basin causes different creeks (Honey, Coffin, or Eastern) to be the main contributors to flooding in Manchester. The IFC installed 3 streamflow bridge sensors in the upper Maquoketa River basin which provide real-time water surface elevation data that is converted to discharge using rating curves. The bridge sensor measurements will be useful for further validating the HLM model outputs and for customizing a flood forecasting and warning system for Manchester, but this will be discussed later in the report.

### **3.4 Precipitation Data**

In areas where rain gauge data is not present, radar rainfall is an ideal candidate for rainfall estimation in urban areas. In this study, we used rain gauge corrected MRMS QPE with a spatial resolution of 1 km and temporal resolution of 1 hour; Stage IV radar rainfall with a spatial resolution of 4km and a temporal resolution of 1 hour; and IFC radar rainfall with a spatial resolution of 500m and a temporal resolution of 1 hour and 5-min. The spatial resolution of the rainfall products over Manchester are shown in Figure 11. The radar rainfall estimates for Manchester were validated against daily accumulation records from an Iowa COOP Rain Gauge (Station ID: MHRI4) located directly south of Hwy 20, just outside the city limits. Information is collected at this site at 7am daily by the Iowa Environmental Mesonet.

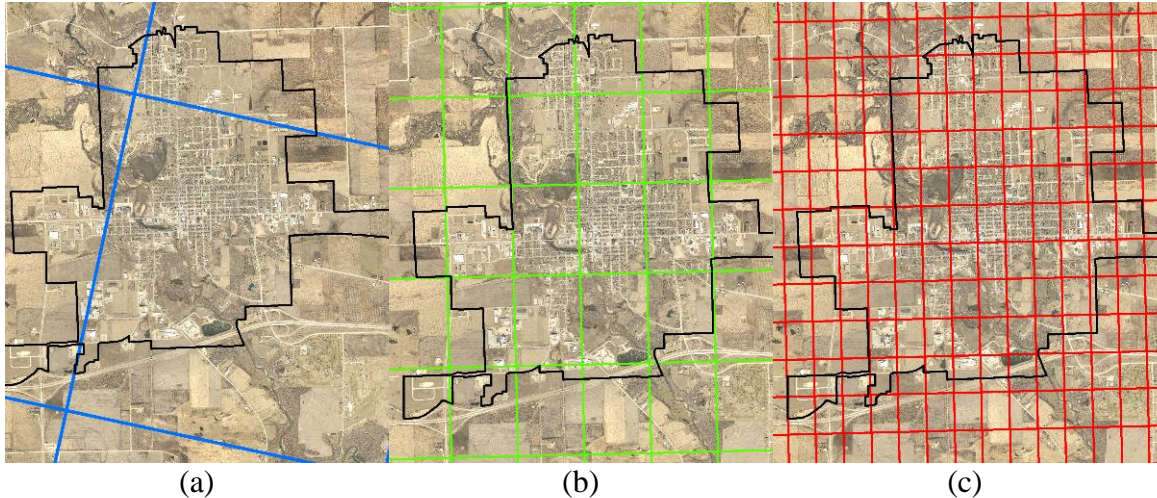


Figure 11. The spatial resolution of the radar rainfall products over Manchester including (a) StageIV-4km, (b) MRMS-1km and (c) IFC-500m

### 3.5 Flood Events Summary

Two historical flood events that both exceeded the NWS major flood stage were modeled for this study because of the availability of validation data and the unique hydrologic processes that occurred across the watershed. The peak USGS stage and discharge records for the July 2010 and September 2016 flood events are compared to the NWS flood categories in Table 2.

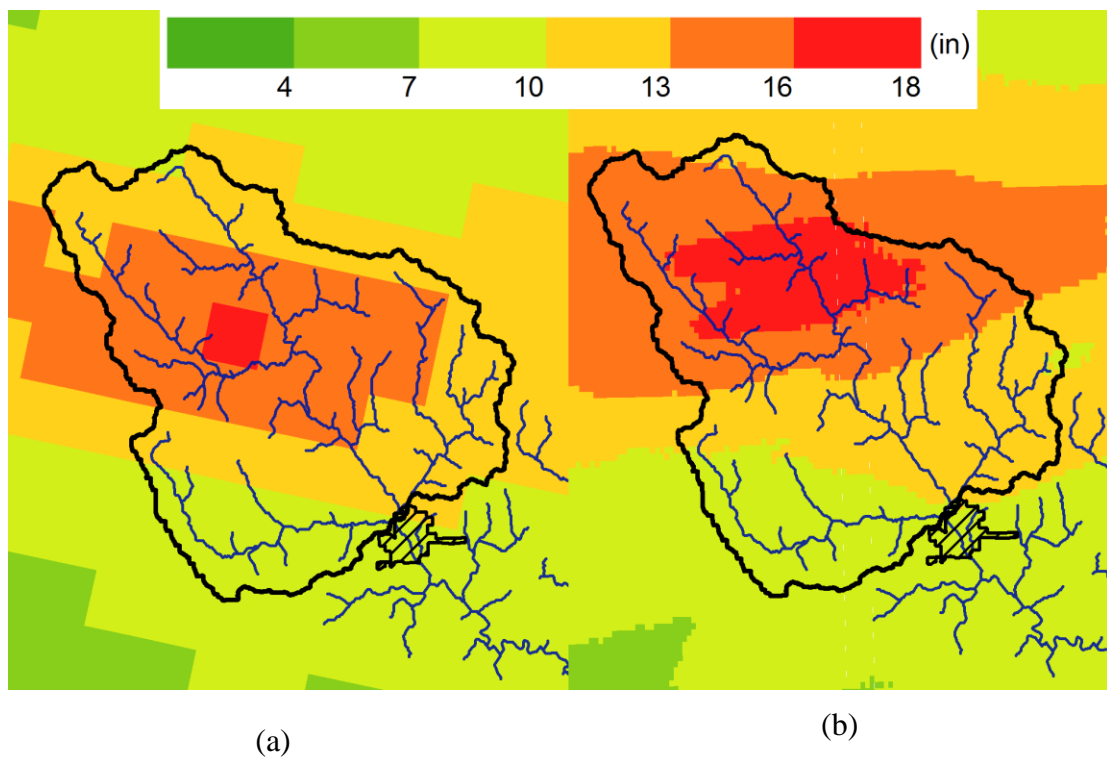
Table 2. Peak streamflow and stage records on the Maquoketa River at Manchester (USGS) compared to the NWS Flood Categories

Flood Level		Stage (ft)	Discharge (cfs)
Historic Crest	7/24/2010	24.48	26,600
	9/23/2016	20.34	15,800
NWS Flood Categories	Major Flood	20	14,758
	Moderate Flood	17	9,071
	Flood	14	4,977
	Action	12	3,284

In 2010, Manchester experienced disastrous flooding from the Maquoketa River after a three-pulse rainfall event that occurred over 3 days in July. The upper Maquoketa River basin experienced an excess of 16 inches of precipitation while the City of



Manchester received 8 inches of rainfall (Figure 12). Locally, the rainfall accumulated 1.6 inches over 8 hours on the 22<sup>nd</sup>, 3.13 inches over 13 hours on the 23<sup>rd</sup>, and 3 inches over 8 hours on the 24<sup>th</sup>. The heavy rain resulted in the highest crest recorded on the Maquoketa River at Manchester with a stage height of 24.5 ft and a discharge of 26,600 cfs (Figure 13). The annual flood probability range for the July 25, 2010 flood was 0.2-1% (a recurrence interval of 500 to 100 years) (Eash, 2012). The Iowa Public Assistance Program project costs for the Delaware County after the July 2010 floods was over \$850,000 with around \$110,000 used for emergency protective measures and over \$425,000 for roads and bridges (Eash, 2012).



(a) (b)  
Figure 12. A comparison of the accumulated precipitation over the upper Maquoketa watershed for the July 2010 flood event with (a) StageIV and (b) IFC radar rainfall estimates

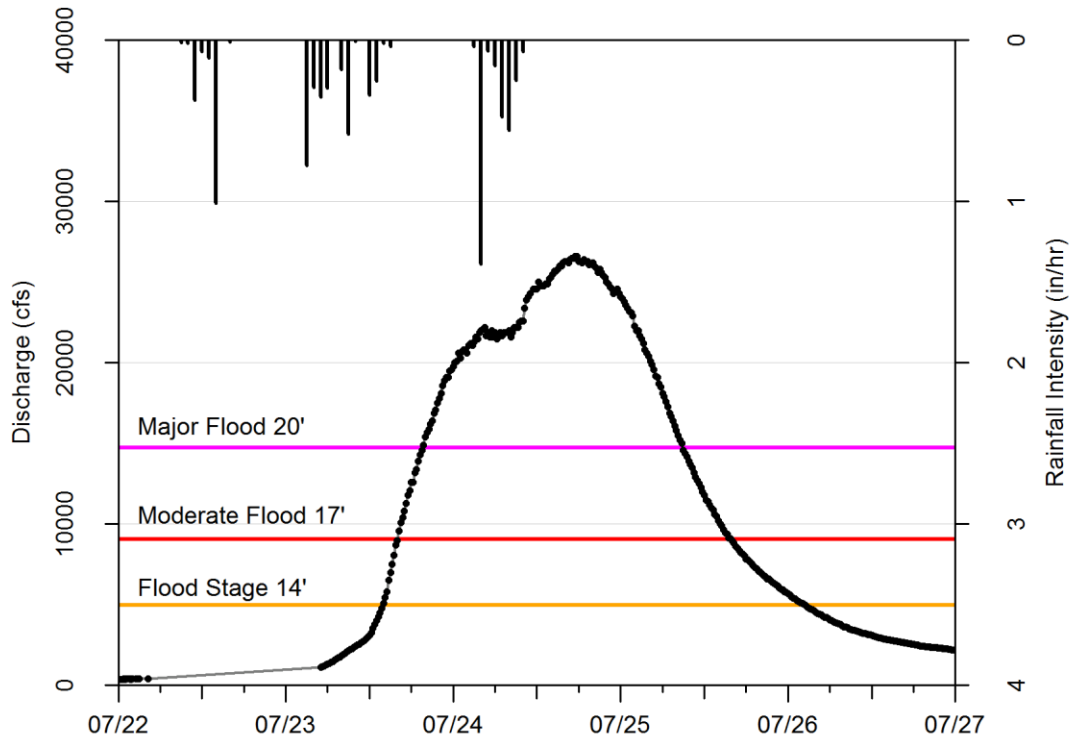


Figure 13. StageIV rainfall intensity, the NWS Flood Categories, and USGS discharge records on the Maquoketa River at Manchester for July 2010

During September of 2016, Manchester experienced over 6 inches of rainfall locally within 17 hours and the upper Maquoketa River basin received nearly 7 inches of rainfall in 21 hours (Figure 14). Downtown Manchester was flooded again when the Maquoketa River reached a stage height of 20.25 ft as shown in Figure 15. The two radar rainfall estimates show similar spatial patterns but slightly differ in the magnitude of rainfall estimates across the basin. This is a result of the different methods and approaches used to produce these rainfall products.



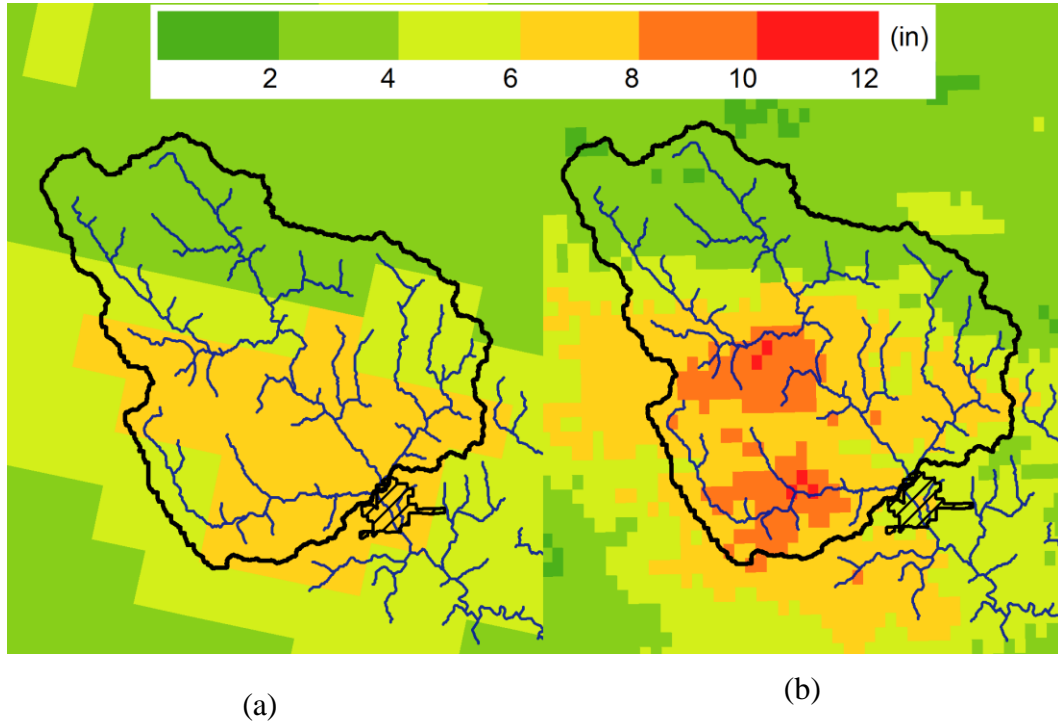


Figure 14. A comparison of the Accumulated precipitation over the upper Maquoketa watershed for the September 2016 flood event with (a) StageIV and (b) MRMS radar rainfall estimates

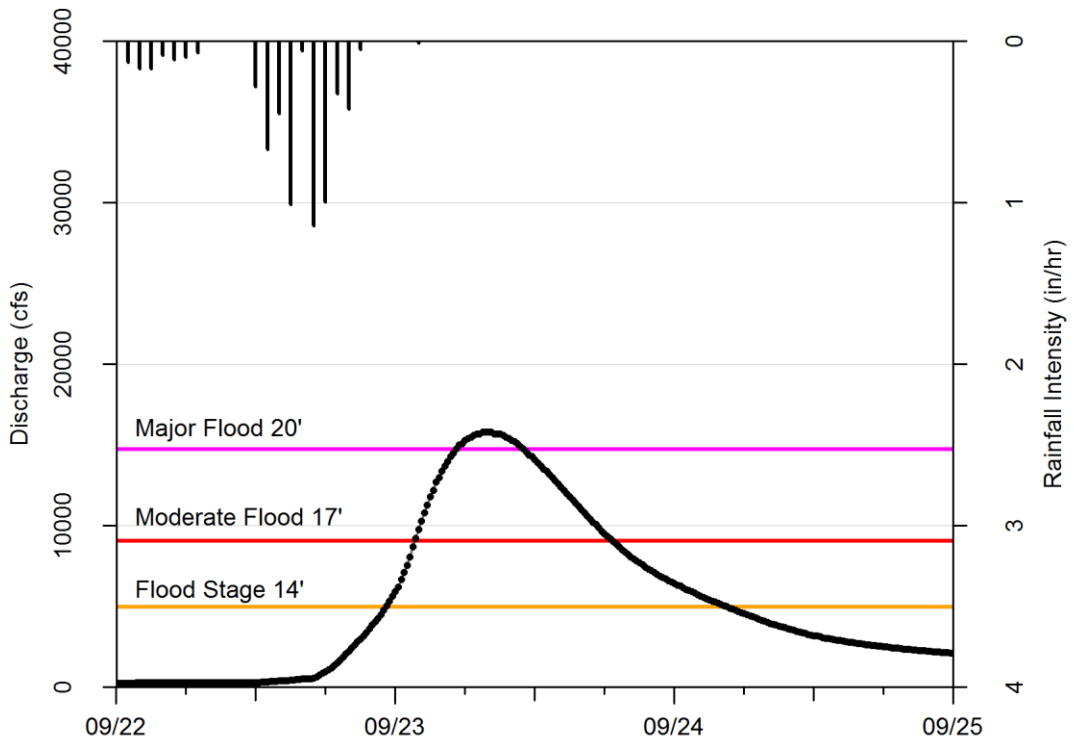


Figure 15. StageIV rainfall intensity, the NWS Flood Categories, and USGS discharge records on the Maquoketa River at Manchester for September 2016

## **CHAPTER 4: METHODOLOGY**

A nested regional-local modeling approach was used to incorporate the impacts of rainfall resolution and urban rainfall-runoff dynamics into streamflow predictions. This method has the advantage of using a high-resolution 1D/2D model in the local area and a coarse resolution in the regional model. The HLM was used to get streamflow boundary conditions for the local model created in XPSWMM. Instead of focusing on a single street or block (Arrault et al., 2016), this study uses the necessary detail to analyze how flooding propagates in a whole urban district.

### **4.1 Local Model**

XPSWMM uses a link-node scheme where the link (conduit) data is shared amongst all three modes (hydraulics, runoff, and sanitary), and each module routes flow differently (XPSWMM Technical Manual). Similarly, there are different parameters and settings for the nodal data depending on the mode (i.e. runoff or hydraulic). The XPSWMM 1D and 2D components unique to the local model of Manchester are described in this section.

#### **4.1.1 1D Domain**

In December of 2015, the USACE finished a hydraulic modeling and mapping project of the Maquoketa River at Manchester. As part of this study, a 1D river model was built using the Hydrologic Engineering Center's River Analysis System (HEC-RAS) software for the conditions in July 2010 (used for model calibration) and the proposed whitewater park changes. The natural tributaries on the east side of the city that drain to the Maquoketa River through a series of open and closed channels were modeled in HEC-RAS by the IDNR in 2013 (Figure 8). The detailed cross-sections of the channels

and bridge crossings in these models were derived from bathymetry and LIDAR. These river models were imported into XPSWMM, and modeled as 1D channels using the same link-node scheme that is used for the pipe networks. The 1D river models in XPSWMM included 3.90 mi of the Maquoketa River, 2.7 mi of the Tributary A, and 1.5 mi of Tributary 2 (Figure 17). Two XPSWMM models were created to simulate flooding in Manchester during 2010 and 2016 to present. The main difference between these models was a change in the routing of the Maquoketa River by adding cross-sections to describe the whitewater park built in 2016 (Figure 16).

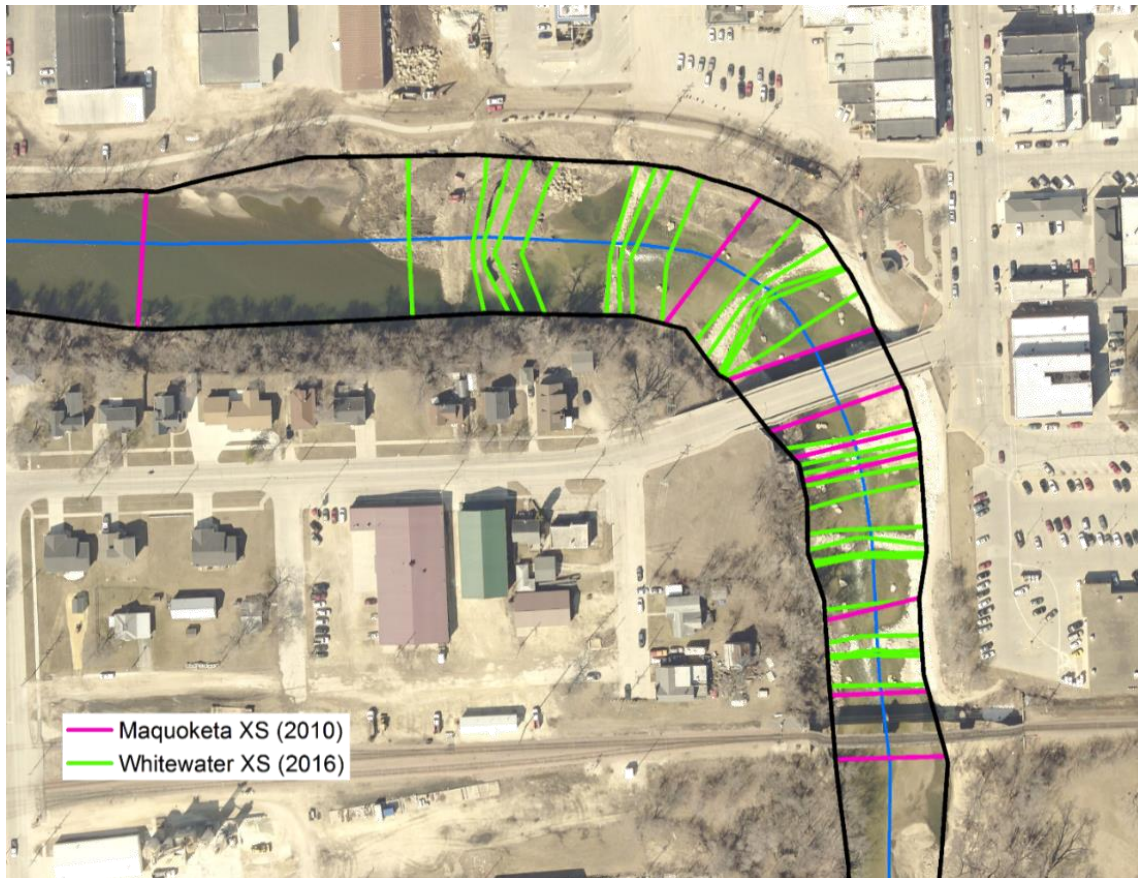


Figure 16. The density and layout of the Maquoketa River cross-sections used in XPSWMM before and after the whitewater park addition in 2016

Manchester is most vulnerable to flooding from the river, however the city engineers also explained that eastern Manchester experiences flooding due to surcharging

from the stormwater infrastructure. Given the significance of flooding issues in eastern Manchester and the extensive amount of time needed to gather, organize, and input the data the infrastructure included in the XPSWMM model was limited to the eastern area. The city provided a GIS shapefile of the spatial locations for the city's stormwater infrastructure and design plans dating back to 1980s. Using the design plans, the hydraulic information (invert elevations, pipe size, slope, etc.) for the network was manually input into a spatial database to be imported into XPSWMM. Finding and inputting this detailed information is time consuming because not all the information is available or easily found. Ideally, the model should include precise information on the key hydraulic controls (levees, embankments, bridges, culvert crossings, etc.) but it is often the case that additional survey work is required. Modeling these structures is important because they have a significant impact on the release and storage of stormwater.

Given that there is usually missing or conflicting hydraulic information on the components of the stormwater infrastructure (for example the size or invert of the pipe), decisions related to the layout and connectivity of the sewer system were based on standard design principles (i.e. matching crowns, minimum 2% slope, etc.). These decisions were made using previous consulting work experience and engineering judgement. All of the intakes were assumed to have the same capacity, equivalent to a 4-foot curb inlet. This was done because the aim of this model is to evaluate the flow behavior across the entire city, not at a specific intersection, and the design capacities for each inlet were not readily available. When intakes were adjacent to a manhole (< 10 ft away), they were merged into a single node to reduce model complexity. Additionally,

the pipes with shorter lengths require a smaller computational timestep which increases the instability of the model. A summary of the stormwater components included in the urban model are given in Table 3 and the overall layout is shown in Figure 17.

Table 3. The Manchester stormwater network components included in local XPSWMM model

Total Stormsewer (mi)	12.5
Stormsewer Diameter/Height (ft)	0.67-10.25
Intakes	492
Manholes	164
Culverts/Outfalls	15



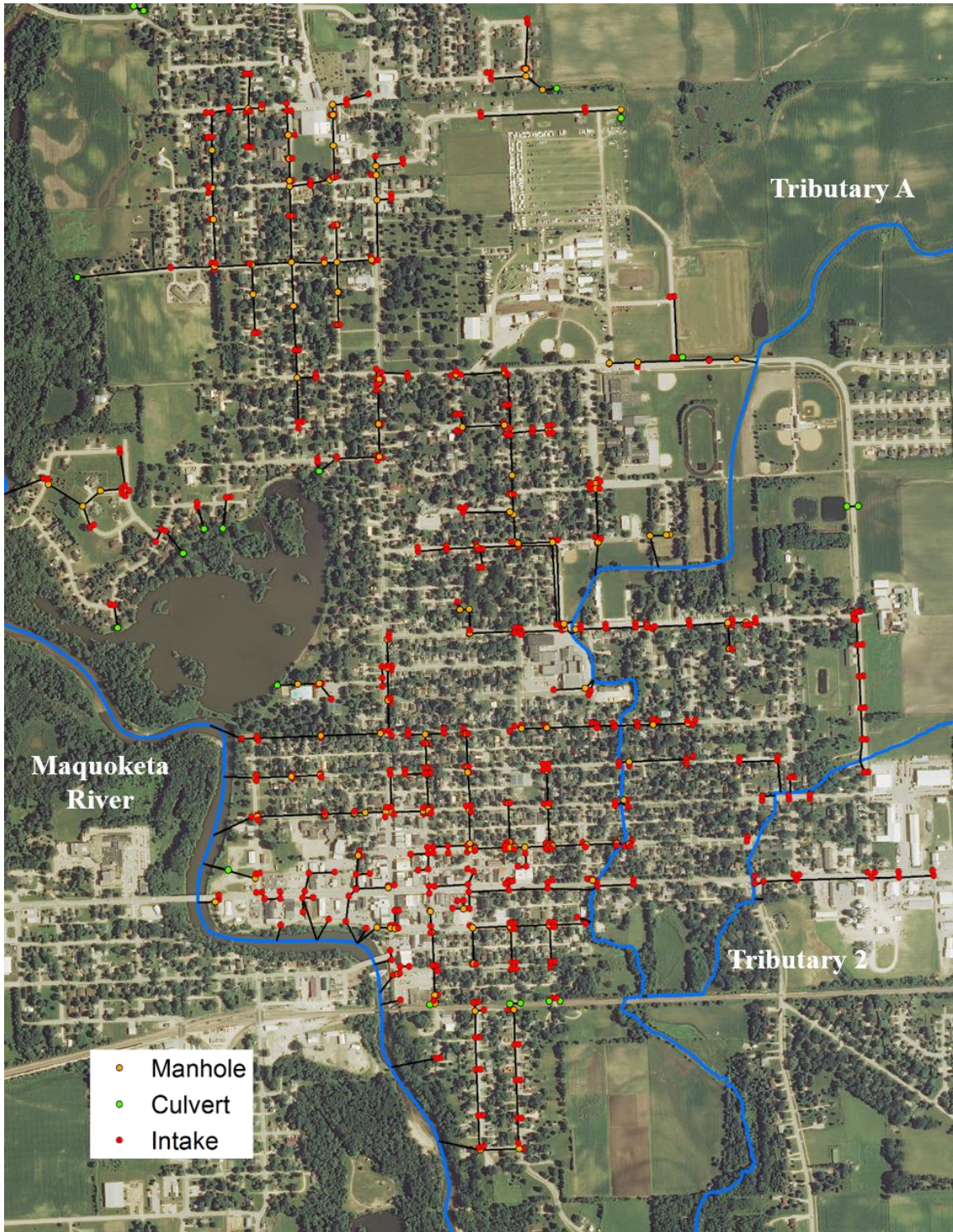


Figure 17. Manchester's stormwater network system modeled in the local XPSWMM model



The 2D domain was not applied across the entire urban area because of the computational requirements and limitations of the software license. For this reason, rainfall-runoff subcatchments were used model the inflows from the small, local basins as shown in Figure 18. Limitations of semi-distributed modeling of these catchments are that they each must be hydrologically homogeneous with land use and soil types. Often it is the case that 1D rainfall-runoff methods are calibrated by changing the parameters used to model the catchment while remaining within the bounds of allowable or expected values (Dotto et al., 2014; Petrucci & Bonhomme, 2014; Sun, Hall, Hong, & Zhang, 2014; Sun, Hong, & Hall, 2014). However, there is no direct explanation for the changes in the physical processes. For this reason, calibration was not used to correct the local model's behavior.

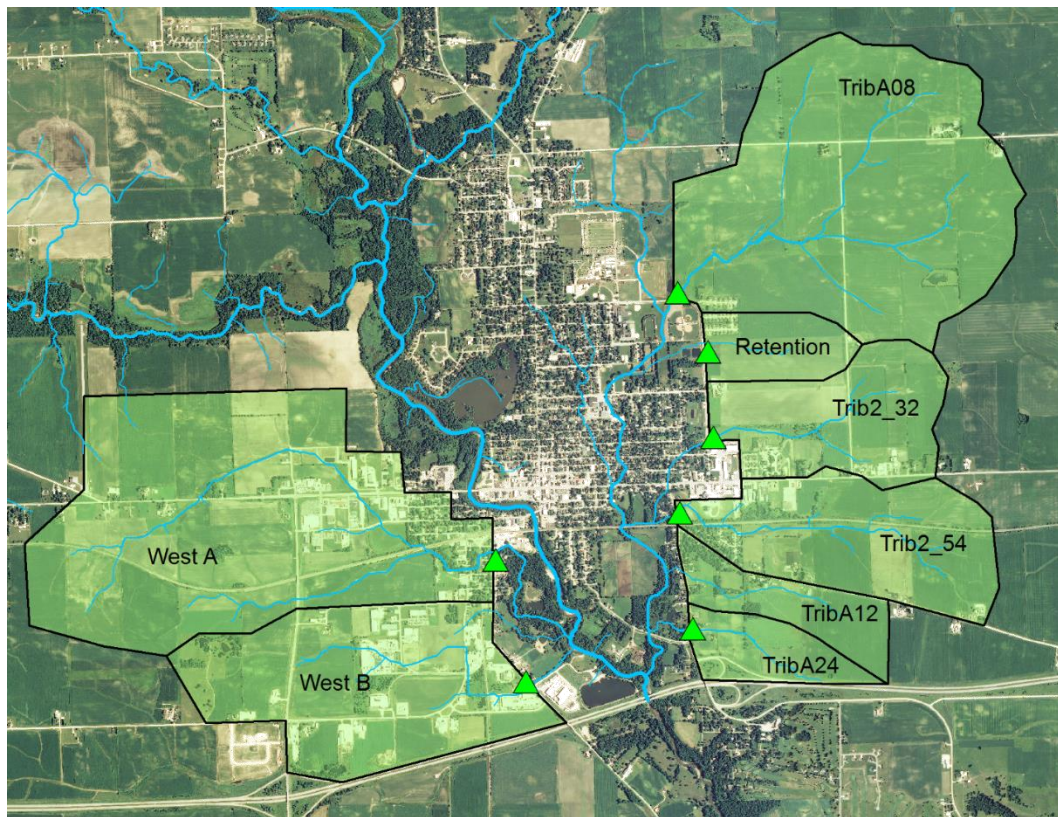


Figure 18. The location of XPSWMM runoff subcatchments, their connection to 2D Domain, and a visualization of the natural drainage for the landsurface.

Because the model is being used for a continuous simulation (longer than 24 hr), the Green and Ampt Infiltration Method was used to model the amount of rainfall that is stored in the soil prior to runoff. A description of the parameters required is listed below.

- The average capillary suction at the wetting front can be derived from soil moisture conductivity data if available.
- The initial moisture deficit, also known as the wilting point, is the fractional difference between the soil porosity and the actual moisture content. For dry antecedent conditions, the initial moisture deficit tends to be higher for sandy soils because the water is held weakly in the soil pores.
- Depression Storage is the volume that must be filled prior to the occurrence of runoff. It is used to represent the initial loss caused by surface ponding, surface wetting, interception and evaporation. This parameter is often treated as a calibration parameter to adjust runoff volumes. Separate depression storages are specified for both pervious and impervious areas.
- The impervious area depression storage is the water stored as depression storage on the impervious area that is depleted by evaporation.
- The pervious area depression storage is the water that is subject to both infiltration and evaporation. This parameter is best represented as the interception loss based on the type of surface vegetation.
- Manning's n roughness for the subcatchment pervious and impervious areas are not well known for overland flow, but recommended values are given in the XPSWMM Manual.
- Zero Detention is the percentage of the subcatchment impervious area with zero detention, in other words, immediate runoff. This parameter assigns a percentage of the impervious area as a zero depression storage to facilitate immediate runoff.



Soil data was gathered from the NRCS SSURGO database which contains spatial and tabular data on the soils collected by the National Cooperative Soil Survey over the course of a century. No additional quality control was conducted for the soil and land use data. Using the SSURGO database, the three prominent soil types in Manchester included loam, sandy loam and loamy sand (NRCS, 2006). The soil and subcatchment parameters used in the local model are listed in Table 4. These parameters are often difficult to estimate and the average (or typical) values provided in the XPSWMM manual were considered suitable for the local model (XPSWMM, 2017).

Table 4. XPSWMM subcatchment infiltration types

	Infiltration Types	East	West
Green-Ampt Parameters	Average Capillary Suction (in)	8	8
	Initial Moisture Deficit	0.36	0.36
	Sat. Hydraulic Conductivity (in/hr)	6	2
Impervious Area	Depression Storage (in)	0.2	0
	Manning's n	0.014	0.014
	Zero Detention (%)	10	45
Pervious Area	Depression Storage (in)	0.5	0.5
	Manning's n	0.05	0.045

The local subcatchments used the Kinematic Wave method for routing where they are modeled as idealized rectangular areas with the slope of the catchment perpendicular to the width (XPSWMM, 2017). The Kinematic Wave method has been found to provide reasonable estimates of the runoff hydrograph (Akram et al., 2014). The area, percent impervious, and width were calculated using tools in XPSWMM and GIS. The width of the subcatchment was estimated as the area of the subcatchment divided by the average path length of the overland flow. The parameters used to describe the land cover and storage in the local subcatchments are given in

Table 5.

Table 5. XPSWMM runoff subcatchment information

Subcatchment Node ID	Slope	% Impervious	Width (ft)	Area (ac)	Infiltration
TribA08	0.007	2	4,850	1,009	East
TribA12	0.003	15	1,502	152	East
TribA24	0.005	7	1,264	124	East
Trib2_32	0.003	6	2,875	319	East
Trib2_54	0.002	8.5	2,367	414	East
Retention	0.003	7	2,737	124	East
West A	0.003	21.5	4,828	1,124	West
West B	0.003	21.5	6,450	597	West

#### 4.1.2 2D Domain

The minimum data requirements of setting up a 2D hydrodynamic model are a high resolution DEM and land cover data. The topography of Manchester is shown in Figure 19, where the flat terrain and low elevation of downtown results in frequent flooding from the river because the west bank of the river is approximately 50 feet higher than the east bank.

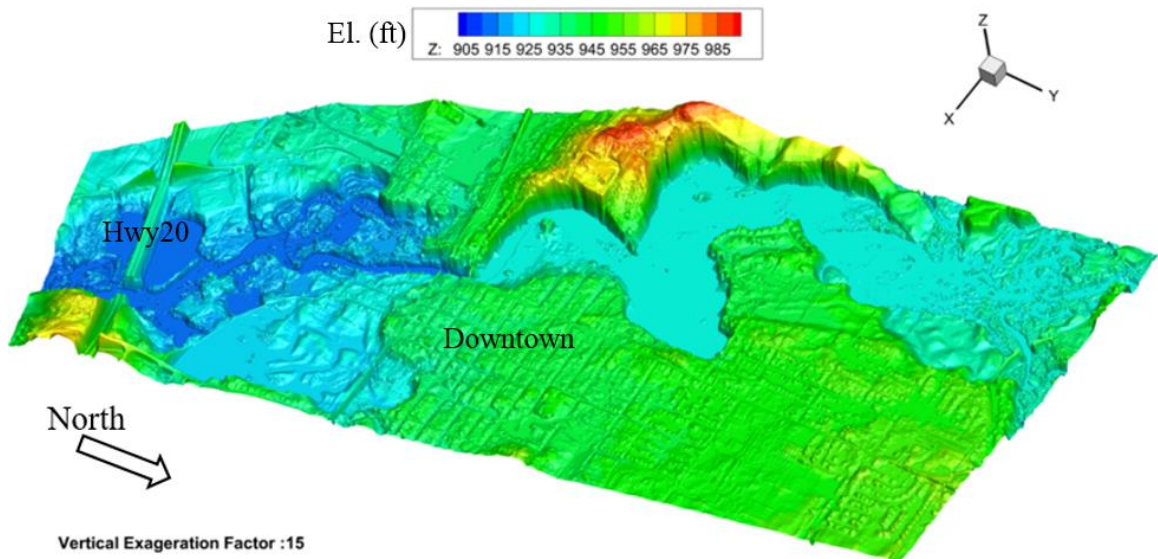


Figure 19. The topography of downtown Manchester and the Maquoketa River as represented by a 1m DEM

The model topography is defined by the elevations at the cell centers, mid-sides, and corners which are interpolated (extrapolated) from a digital terrain model (DTM). The DTM used in the XPSWMM model was created from a 5 ft DEM which was resampled from a 1 m DEM created from LIDAR. A 5 ft DEM was used instead of the 1 m DEM because it was easier to load into XPSWMM without sacrificing detail of the terrain. The 2D domain is made up of square cells that are the same size and orientation. The domain is automatically discretized into a grid where each element is assigned characteristics related to the terrain including elevation, land cover, and soil type. The 2D domain must have sufficiently small cell sizes for it to accurately reproduce the hydraulic behavior of flooding in urban areas. However, a grid resolution finer than 2 m will have adverse impacts on the computation efficiency and reduce model stability (Neelz & Pender, 2013). A compromise must be made between the level of detail and computational effort of the model because a finer resolution requires longer computing time. Because the historical events of interest were continuous simulations (greater than 24 hr), cells sizes of 15 ft and 30 ft were used in the local model to improve the run time. Using a cell size of 5 ft was not an option because the number of cells exceeded those available with the IFC's XPSWMM license. A cells size of 10 ft was briefly tested but resulted in an unstable simulations.

The land cover for the 2D domain was determined using the High Resolution Landcover (HRLC) for Delaware County in 2009. The land cover types used in the local model of Manchester are shown in Figure 20. Each cell in the 2D domain is assigned a resistance parameter and soil type based on the land cover so that the overland flow and infiltration can be accurately modeled.

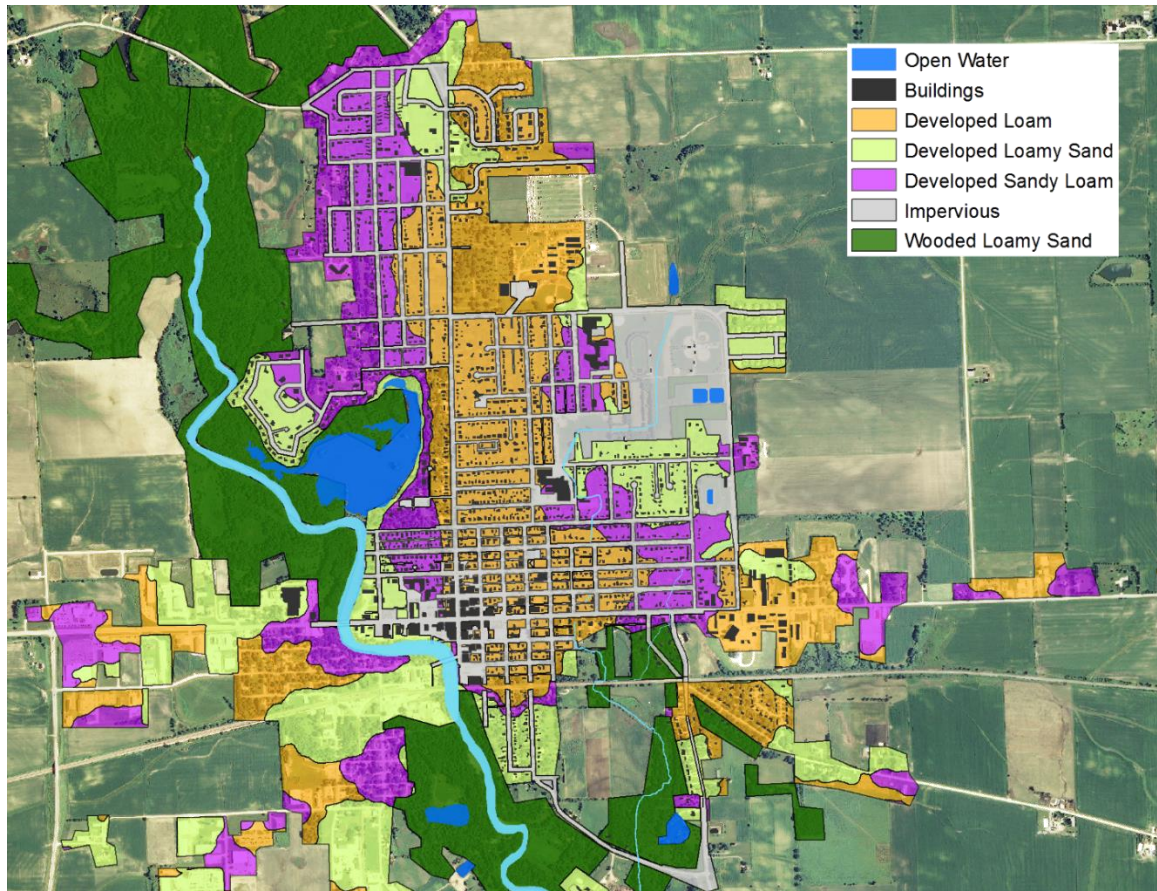


Figure 20. The XPSWWM 2D landuse types used in the Manchester model

The Manning's roughness ( $n$ ) describes how the sheet flow moves over the gridded surface. There are difficulties for estimating the roughness parameters which vary significantly in space, particularly in floodplains (Arrault et al., 2016). The typical range of values for the Manning's roughness values are listed below (Engineering, 2016; Janses & SCE, 2016).

- impervious, concrete surfaces ( $n = 0.01-0.014$ )
- wooded, forested areas dominated by trees generally greater than 5 meters tall and greater than 20% of total vegetation cover ( $n = 0.01-0.16$ )
- short grass and prairie ( $n = 0.10-0.20$ )
- developed areas, medium intensity with impervious surfaces accounting for 50-70% of the total cover ( $n = 0.06-0.14$ )
- open water, generally with less than 25% cover, vegetation, or soil ( $n = 0.2-0.35$ )

To account for rainfall-runoff and flood storage, the buildings were modeled as a land cover with varying roughness. At depths between 0 and 1 ft the roughness was set to a high value ( $n = 3$ ) so that water could be released, but at depths greater than 1 ft the roughness values was set to a low value ( $n = 0.05$ ) to mimic ponded water in the buildings (Syme, 2008). The final list of land covers, percent impervious, and roughness parameters are given in Table 6.

Table 6. XPSWMM 2D landuse types and parameters used in the Manchester model

2D Landuse	Manning's Roughness (n)	% Impervious
Impervious/concrete	0.015	100
Open Water	0.35	100
Wooded Loamy Sand	0.40	0
Grass Loam	0.15	0
Developed Loam	0.03	50
Developed Sandy Loam	0.03	50
Developed Loamy Sand	0.03	50
Buildings	Variable	100

There are a wide range of potential saturated hydraulic conductivities that are detected in urban areas after the land surface has experienced varying levels of soil compaction (Knighton, White, Lennon, & Rajan, 2014). The soil type, given in Table 7, and corresponding infiltration parameters were average values recommended by the XPSWMM Manual and from Rawls, Brakensiek, and Miller (1983).

Table 7. XPSWMM 2D soil types and parameters used in the Manchester model

Soil Properties	Sandy Loam	Loamy Sand	Loam
Porosity	0.453	0.437	0.434
Suction (in)	4.335	2.413	3.500
Initial Moisture (in)	0.330	0.320	0.310
Hydraulic Conductivity (in/hr)	0.429	1.177	0.134
Max Ponding Depth (ft)	0.203	16.88	0.072

The simplest approach for linking the 1D and 2D domains is to insert 1D storm networks below (stormsewers) and replace the 2D domain with a 1D channel (rivers, creeks). This technique has the benefit of integrating existing detailed 1D river models with an overland flow model appropriate for the floodplain. The water surface in the channels is interpolated along a polyline interface located at the bank where water can flow between the channel and the floodplain. The spillcrest of the intakes (nodes) are connected to the 2D domain so that water can flow into the subsurface network of pipes or be surcharged into the streets. The inverts of culverts and outfalls were linked to the 2D domain so that stormwater could drain out of the pipe network into a ditch or headwaters could create negative flow in the pipe.

#### **4.1.3 Model Settings**

The 1D minimum timestep is controlled by the minimum channel length while the 2D timestep is a function of the grid cell size. The minimum grid cell size for urban applications is roughly equal to the shortest length scale of the urban structures (Fewtrell, T.J., Bates, P.D., Horritt, M. and Hunter et al., 2008; Mignot et al., 2006). Generally, model accuracy is improved with a finer resolution (1 to 5 m) but it requires a longer computational time. The model run time is directly proportional to the number of timesteps required for calculating the model behavior for the selected period. The 2D scheme in XPSWMM operates at a Courant Number (Equation 1), indicates the stability of the model based on the cell size ( $\Delta x$  in meters), timestep ( $\Delta t$  in seconds), and average water depth ( $H$  in meters) (Syme, 1991).

$$C_r = \frac{\Delta t \sqrt{2gH}}{\Delta x} \quad \text{Equation 1}$$

The selected 2D timestep is typically 1/4 or 1/8 the cell size in meters. The 2D overland flow was calculated by solving the dynamic wave version of the SWE. Flows in urban areas are supercritical with high Froude numbers which usually require smaller timesteps (Arrault et al., 2016; Dottori & Todini, 2013). The flow is subject to viscous effects of the frictional surfaces. The effect of small-scale motions in the 2D domain that cannot be modeled directly are accounted for with the eddy viscosity parameter. The Smargorinsky Formulation is used by XP2D engine to adjust the velocity based on the viscous forces on the flow from the frictional surfaces (XPSolutions, n.d.). A constant eddy viscosity value (or Smargorinsky Coefficient) of 0.2 was used as recommended in the XP2D manual since the cell size was generally much larger than the depth of the water and the overland roughness is the dominant force.

## 4.2 Model Combinations

The model combinations are specified in terms of the rainfall input and the regional-local model connection. The regional areas upstream of Manchester are modeled using the HLM which generates streamflow time series that are used as the boundary conditions to the local domain. For a single nested model simulation, the rainfall in the upper Maquoketa River watershed was applied to the HLM and the streamflow time series outputs at the links representing the Coffins Creek, Upper Maquoketa, and Eastern Tributary were used as input into the urban model. The local rainfall was applied directly to the 2D domain in XPSWMM and the pre-simulated HLM streamflow was input to the XPSWMM 1D river nodes. The models were forced with different radar rainfall products

with varying spatial resolutions including IFC, StageIV, and MRMS (see Section 3.4). An overview of the nested regional-local modeling approach is shown in Figure 21.

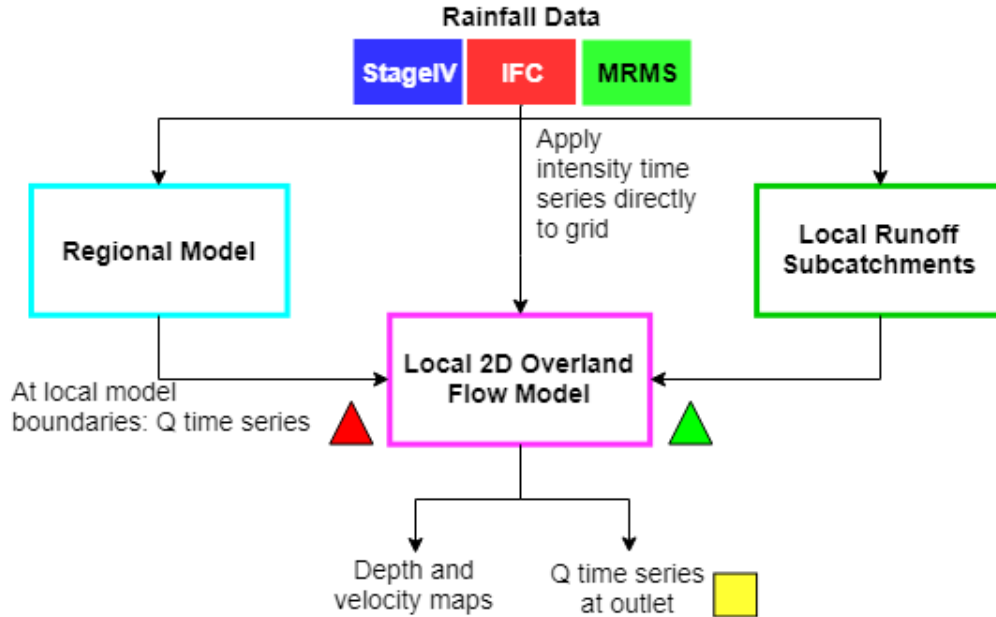


Figure 21. A flow diagram of the overall approach to the nested regional-local model

The base drainage network of the HLM was derived at a spatial scale that was appropriate for the entire state of Iowa while providing streamflow outputs at the community level. The local model of Manchester requires a higher detail of discretization in order to provide runoff results for the eastern and western subcatchments. However, the HLM does model the eastern tributary (now of a larger magnitude because of the upstream area) when it connects to the Maquoketa River. This provides an opportunity to test a configuration of the nested model with the eastern tributary model in by HLM and XPSWMM. The three model combinations include:

- HLM - the regional model only
- XP-C1 – the nested regional-local model with the eastern tributary modeled using HLM shown in Figure 22
- XP-C2 – the nested regional-local model with the eastern tributary modeled by XPSWMM as shown in Figure 23



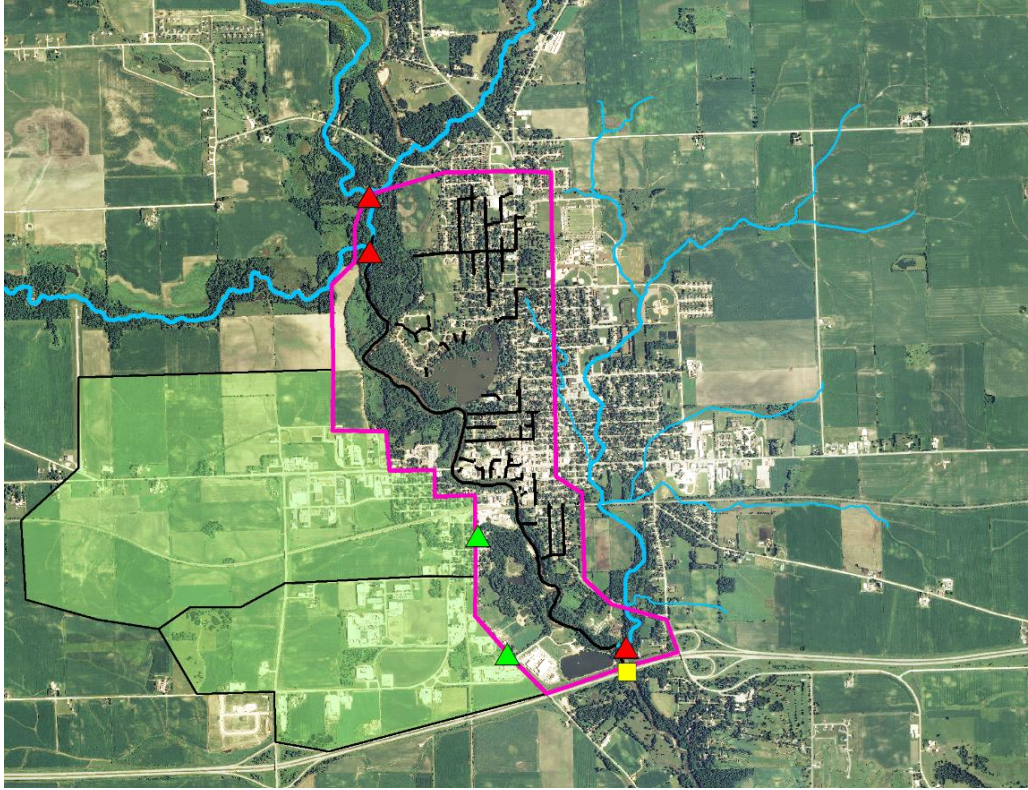


Figure 22. Nested regional-local model configuration XP-C1

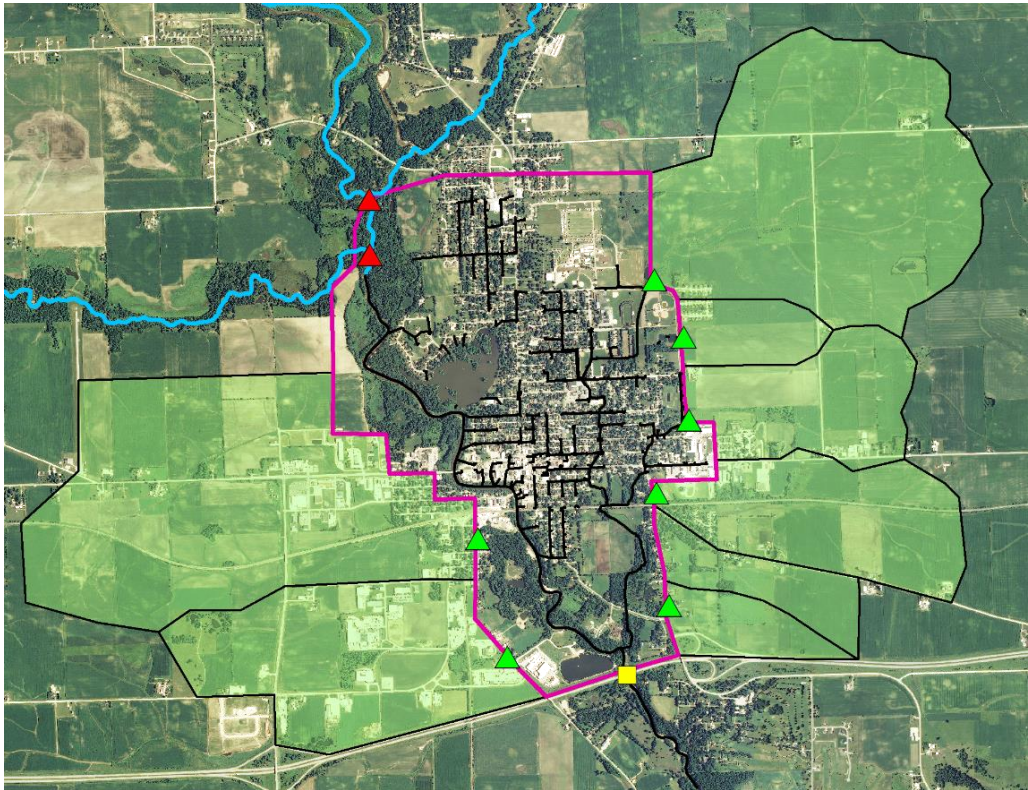


Figure 23. Nested regional-local model configuration XP-C2

Two model combinations were used to better understand how a coarse resolution model of an urban area compares to a detailed, high-resolution model of the same area. The components of the two model configurations are given in Table 8.

Table 8. XPSWMM model components for configurations XP-C1 and XP-C2

Configuration	XPSWMM Configuration 1 (XP-C1)	XPSWMM Configuration 2 (XP-C2)
HLM Streamflow	Upper Maquoketa, Coffins Creek, Eastern Tributary	Upper Maquoketa, Coffins Creek
XP Subcatchment	Western Manchester	Western Manchester, Eastern Rural
XP Nodes	495	862
XP Links	473	841
XP2D Domain	1.70 sq. mi.	2.90 sq. mi.

The initial soil moisture conditions for the regional area were obtained using a spinup of the HLM. The model simulated the hydrological processes in the watershed starting on April 1<sup>st</sup>, at least 3 months before the events. The soil moisture conditions for the XPSWMM models are given in Table 7. The local model simulation started at least 6 hours before the first pulse of rainfall allowing time for the streamflow in the Maquoketa River to fill. The initial state of the stormsewers and eastern tributary was empty or dry. For each model combination (rainfall + model configuration) the streamflow time series output was compared with streamflow records at the downstream USGS gauge.

## **CHAPTER 5: MODEL EVALUATION**

The advantage of having a 1D/2D flood inundation model is its ability simulate flow spreading across the city giving water depths and velocities at any location in the model (Henonin et al., 2013). The resulting maps can provide decision-maker with data on the risks and hazards of the encroaching flood. The models were evaluated based on their ability to reproduce the historical flood events as documented by the locals and the potential as a real-time forecasting tool. For the floods of July 2010 and September 2016, the flood extent and depth of the model simulations are compared and validated against drone footage and photos. A simple statistical analysis was completed to compare the discharge and stage values observed to those simulated. The uncertainty of the results and the impacts of rainfall inputs and model structure are discussed.

### **5.1 Model Validation**

The radar rainfall estimates for the three products are compared to the NWS Coop Rain Gauge data located near the USGS gauge. The daily accumulated rainfall measured at the gauge is reported at 7am. The accumulated precipitation, maximum rainfall intensity, and duration of the storm over Manchester are given in Table 9. These were calculated by averaging the values of the rainfall grids located directly over the city limits.

Table 9. Comparison of the NWS COOP rain gauge accumulated precipitation measurements to the radar rainfall estimates for July 2010 and September 2016

<b>Flood Event</b>	<b>Dates</b>	<b>Rainfall Product</b>	<b>Local Cumulative Rainfall (in)</b>	<b>Maximum rainfall intensity (in/hr)</b>	<b>Duration (hr)</b>
July 2010	7/22/10 4:00	StageIV	7.72	1.39	50
	7/24/10 5:00	IFC	8.81	1.65	50
		NWS Coop	7.33	---	---
September 2016	9/22/16 3:00	StageIV	6.23	1.14	31
		MRMS	6.24	1.32	31
	9/23/16 21:00	IFC	6.59	1.09	31
		NWS Coop	5.69	---	---

The rainfall estimates agree across the radar rainfall products. The spatial pattern of accumulated precipitation over the region for the July 2010 and September 2016 flood events are shown in Figure 12 and Figure 14, respectively. The finer resolution rainfall products (IFC and MRMS) provide more detail on the spatial distribution of rainfall over the basin but the overall pattern is similar to Stage IV. These measurements do not give information on the temporal patterns of the different radar rainfall products. The movement of the storm across the basin will affect the runoff and response of the watershed. Any variances between the model outputs could be due to the uncertainty of the radar rainfall estimates caused by the spatiotemporal movement of the storm.

The simulated flood depths and extent are compared to photos to evaluate the performance of the model to capture the flooding in both July 2010 and September 2016. Additionally, the flood extents for the local area were generated for stages of 16, 18, 20, 22, and 24 ft using a calibrated, 1D HEC-RAS model for the Maquoketa River. The riverine flooding mostly affects River Street, Main Street (downtown), and Hwy 20 and the Wastewater Treatment Plant (WWTP) which are highlighted in Figure 24. The local



rainfall-runoff mechanisms are important because at high river levels, the stormwater network is overwhelmed and is not able to drain the urban areas, specifically downtown. Eastern Manchester experiences flooding at the Beckman Sports Complex from Tributary A. For extreme local events, the stormwater network will be overwhelmed and overland flow through the streets will hydraulically connect Tributary A and 2. The models ability to reproduce this phenomena will be discussed in Section 6.2.

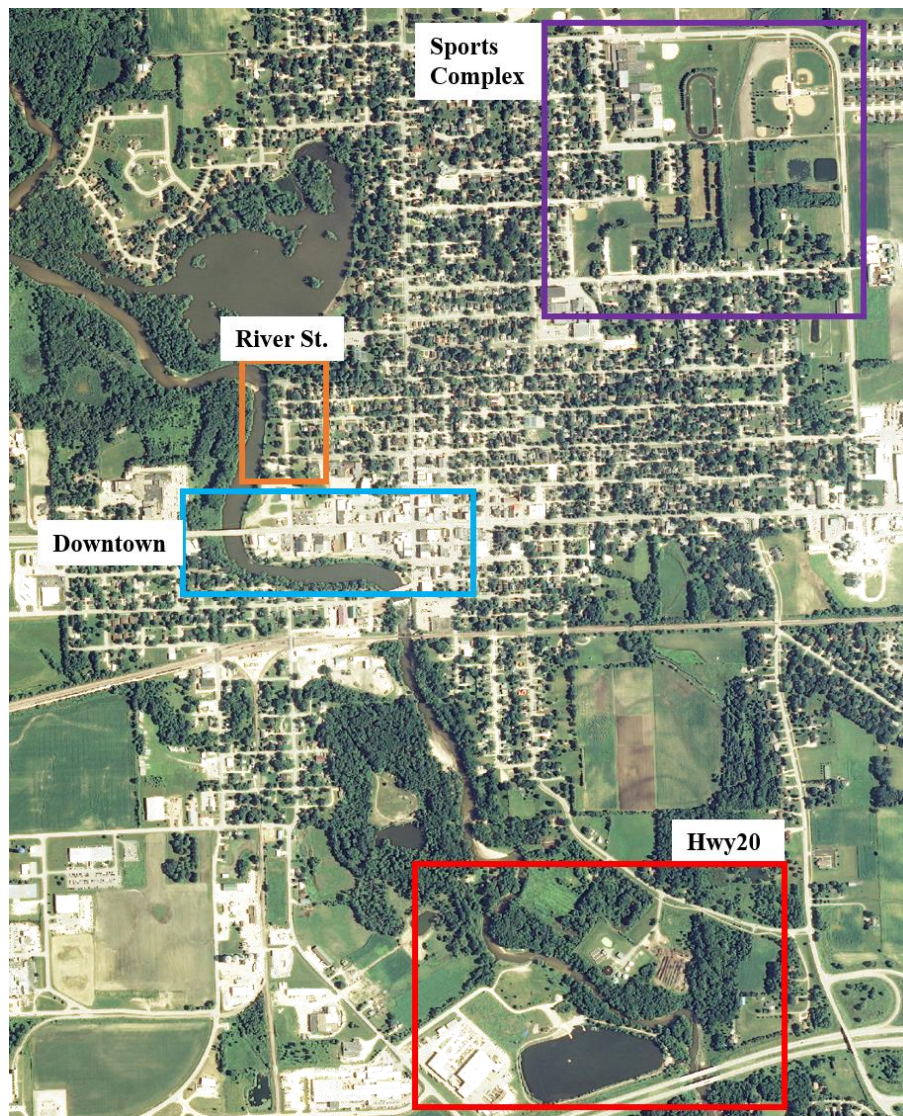


Figure 24. Areas of interest for model validation including the Sports Complex, River St., Main St., and north of Hwy 20

### 5.1.1 July 2010

The max flood extent and depth do not vary largely between the different model structures or rainfall inputs. However, the time to peak and duration of flood inundation is significantly different between the different models. This will be discussed in the following section. In Figure 25, the max flood extent of the XP-C2 IFC model is compared to the outputs of a 1D HEC-RAS model. There is good agreement of the peak flood extent of the XPSWMM model when compared to the flood photos and 1D HEC-RAS flood extents. The XP-C2 IFC simulation crested on 7/23/10 22:15 (CST) and the flood extents and depths are shown in Figure 26. The model reproduces the flooding that is seen in the photos from the flood event in Figure 27 which are described below:

- Looking south from the Track and Baseball fields at Tributary A which is flowing full.
- There is 2-4 ft of water inundating many homes on River Street and cross streets.
- Drone footage of flood waters show up to 7 ft of water on Main Street.
- Drone footage of water backed up behind Hwy 20 inundating the WWTP and business park.



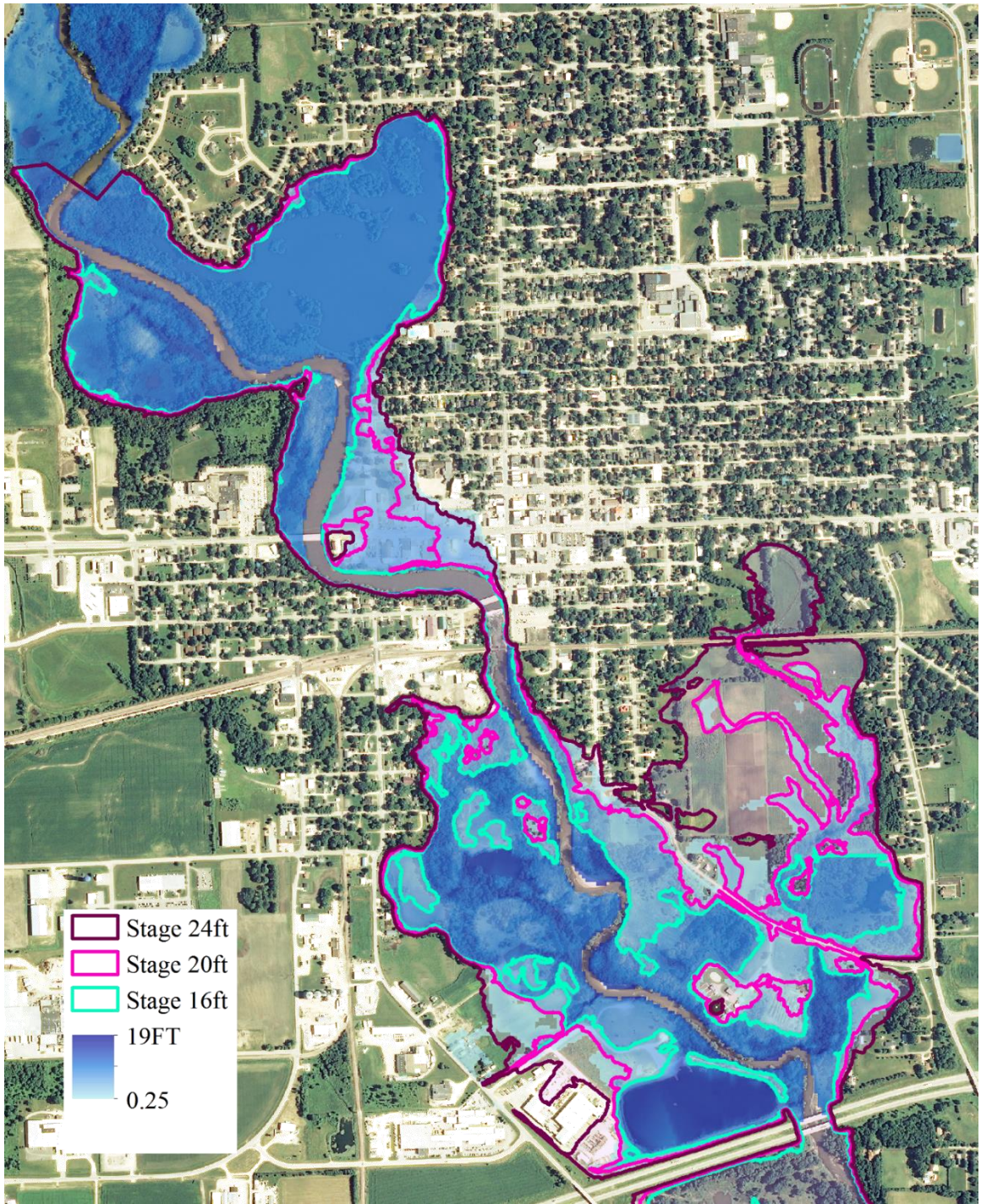


Figure 25. The output max flood extent for stages 16, 20, and 24 ft from a 1D HEC-RAS river model compared to the output of XP-C2 IFC for July 2010



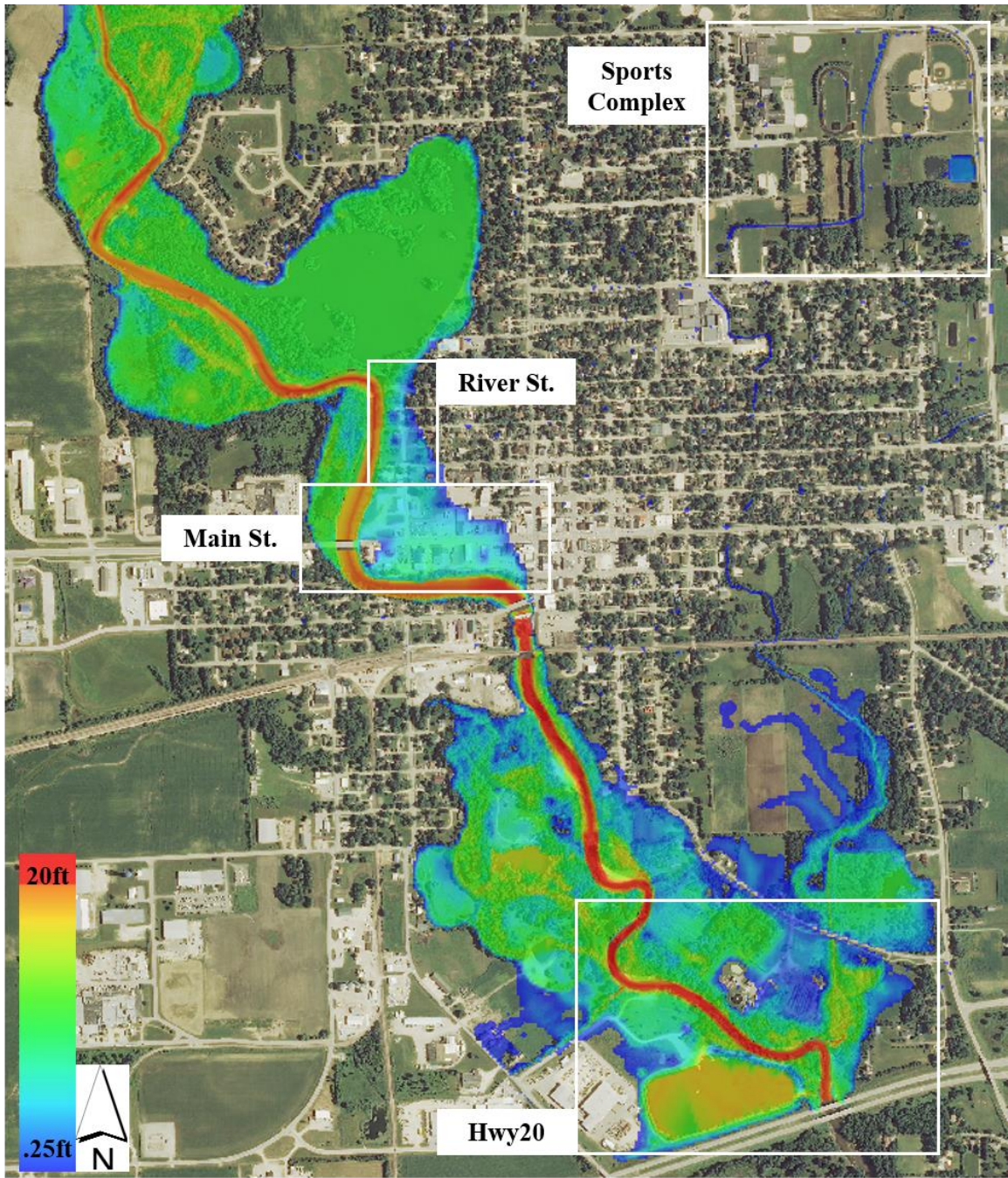


Figure 26. Model results for XP-C2 IFC including flood depths at the time of peak flow (7/23/10 22:15) for July 2010





(a) Looking south, Tributary A at the sports complex



(b) Looking south down River St.



(a) Looking west at Main St.



(a) Looking west at Hwy 20

Figure 27. July 2010 flood event photos used for validation against model outputs at (a) the Sports Complex, (b) River St., (c) Main St., and (d) Hwy 20

### 5.1.2 September 2016

In the summer of September 2016, the dam downstream of Marion Bridge was removed and a whitewater park was constructed in the Maquoketa River near downtown (Figure 5). Additionally, a bike and pedestrian path was added along the river bank and the elevation was raised approximately two feet. Land cover, cut and fill, and building removal was accounted for in the model. The XP-C2 MRMS simulation crested on 9/22/16 14:30 (CST) and the flood extents and depths are shown in Figure 28. The model reproduces the results as seen in the photos from the flood event shown in Figure 29, more specifically:

- Looking west onto River Street from Howard Street there is approximately 1ft of water.
- The homes on the west side of River Street are not yet inundated, but are surrounded by water.
- Downtown, Main Street and the buildings are inundated but the pedestrian path south of Main Street is acting as a spillway but also hindering the release of the water ponded on the properties downtown.
- The ponded and natural area west of the river and north of Hwy 20 is flooded. The small, park structure is surrounded by 2-3 feet of water.
- Looking south from Brewer St. the open area surrounding the WWTP is inundated.



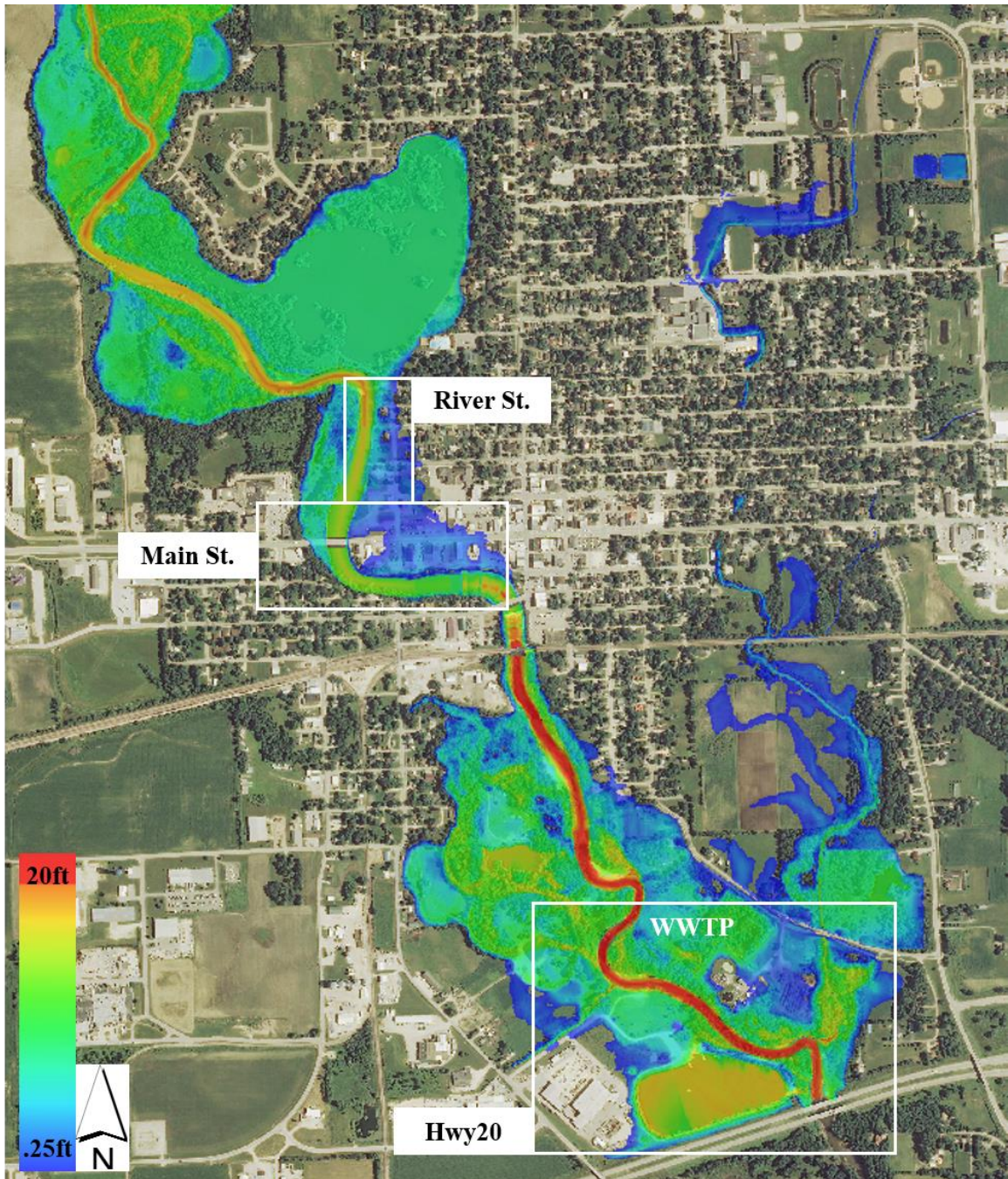


Figure 28. Model result of XP-C2 MRMS including flood depths at the time of peak flow (9/23/16 14:30) for September 2016







Figure 29. September 2016 flood event photos used for validation at (a) River St., (b) the Reservoir, (c) Main St., (d) Hwy 20, (e) the WWTP

## 5.2 Model Performance

When evaluating the performance of the different model combinations, the variables that are important for flood forecasting include the magnitude and timing of (1) the rising limb of the hydrograph, (2) the peak, and (3) the falling limb of the hydrograph. The time to crest of the major flood level and the duration above the major flood level are more useful information to emergency responders who have a thorough understanding of

the flooding to expect at a given stage. These topics will be addressed in the context of the different model configurations and rainfall inputs.

The simulated time series were compared to the observed data with a few general statistics. The Root Mean Square Error (RMSE) is used to measure the difference between the values predicted by the model and the values observed from the environment that is being modelled. The RMSE is calculated using Equation 2 where  $Obs_i$  are the observed values (discharge or stage) and  $Sim_i$  are the modeled values at the number of timesteps ( $n$ ).

$$RMSE = \sqrt{\frac{\sum_{i=1}^n (Obs_i - Sim_i)^2}{n}} \quad \text{Equation 2}$$

The RMSE values can be used to distinguish model performance in a simulation period with that of a validation period as well as to compare the individual model performance to that of other predictive models. The Mean Absolute Error (MAE) is a common measure of forecast error in time series analysis and can be calculated using Equation 3.

$$MAE = \frac{\sum_{i=1}^n |Obs_i - Sim_i|}{n} \quad \text{Equation 3}$$

Another statistical measure used to measure the deviation is the coefficient of determination ( $R^2$ ) where  $\overline{Obs}_1$  and  $\overline{Sim}_1$  are the mean value of the observed and simulated, respectively, depth or discharge during the time period (Equation 4).

$$R^2 = \frac{[\sum_{i=1}^n (\text{Obs}_i - \overline{\text{Obs}}_i) \times (\text{Sim}_i - \overline{\text{Sim}}_i)]^2}{\sum_{i=1}^n (\text{Obs}_i - \overline{\text{Obs}}_i)^2 \times \sum_{i=1}^n (\text{Sim}_i - \overline{\text{Sim}}_i)^2} \quad \text{Equation 4}$$

The variables of interest during the peak include the peak error (PE) and the time to peak error (TPE) which are calculated for both the stage and discharge using Equation 5 and Equation 6.

$$\text{PE} = \max(\text{Obs}_i) - \max(\text{Sim}_i) \quad \text{Equation 5}$$

$$\text{TPE} = t\{\max(\text{Obs}_i)\} - t\{\max(\text{Sim}_i)\} \quad \text{Equation 6}$$

For July of 2010 and September 2016 flood events, the stage and discharge of the models was compared to the measured values at the USGS location on the Maquoketa River.

### 5.2.1 July 2010

A model with accurate performance should be able to predict, at a given time, the quantity and location of flood waters. The hydrograph shown in Figure 30 tells us that the HLM and HLM-XP models have skill when predicting the peak flow and time of peak flow. The overall shape of the simulated hydrographs indicates that the model detects and responds to additional rainfall at the second peak, but there is a significant volume of water unaccounted for. This extra volume in the hydrograph is potentially due to the downstream boundary conditions of the local model which do not account for a reservoir located 11 miles downstream at the Delhi Dam. The reservoir is approximately 440 acres of area with storage volume of 9,900 acre-ft. The Delhi Dam was breached at noon on July 24, 2010 resulting in a maximum flow of 69,200 cfs to be released (IDNR, 2010).



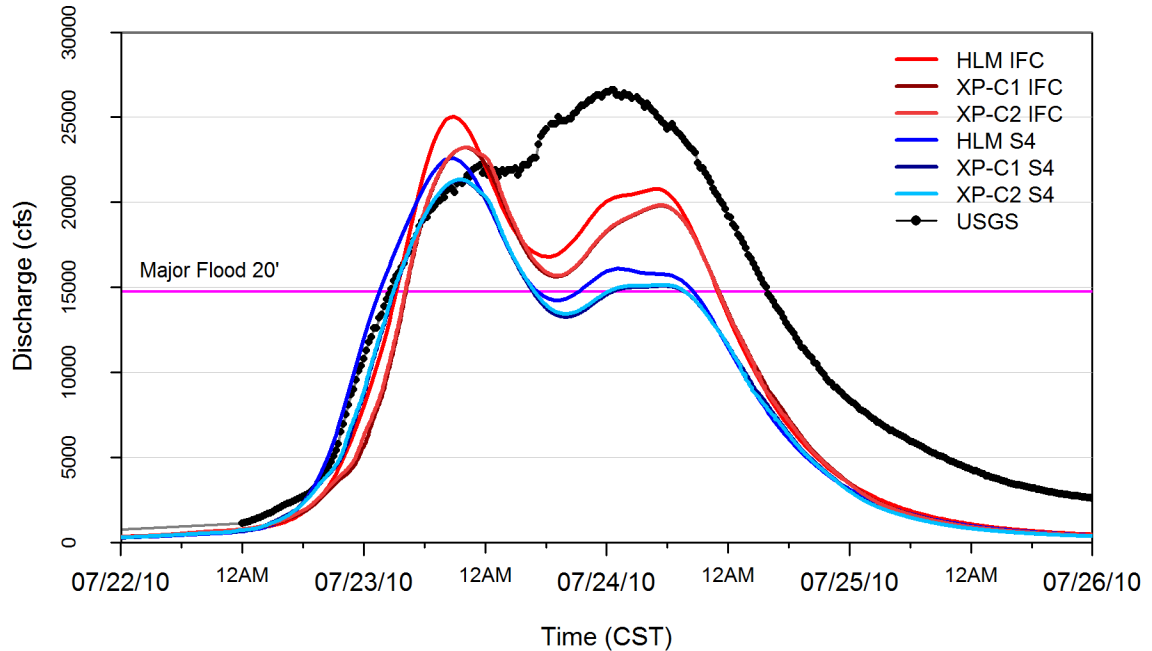


Figure 30. Comparison of the observed USGS hydrograph and the model results for the July 2010 flood

For the July 2010 flood, the simulated results underestimate the stage of the rising limb by 1-2 feet (Figure 31). The models predict the flood stage for the first peak of July 2010, slightly quicker than what was observed (1-2hours). After the first peak, the models' simulated the recession of the flood waters but in reality the flood stage increased. This is may be due to using a rating curve that has been updated since the flood of 2010. The discharge at the second peak is underestimated by 4,500-6,500cfs and the stage by 2-4ft. Though precise forecasts are desired, planning for the worst possible flood is a suitable option; the model simulations do this by overestimating the initial peak flow and earlier than observed (Table 10).

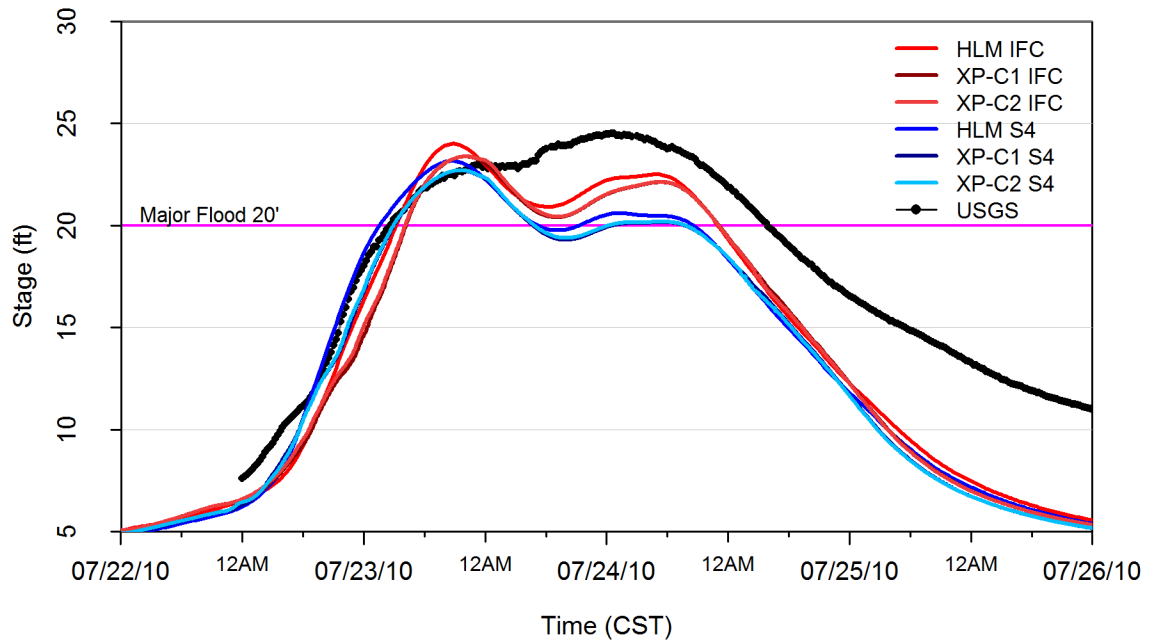


Figure 31. Comparison of the USGS stage records and the model results for the July 2010 flood

The model is not able to reproduce the receding limb of the hydrograph. The inclusion of this portion of the hydrograph into the statistical analysis will indicate an overall poor performance of the models. The models were compared to the observations for the first and second peak of the hydrograph separately (Table 10 and Table 11). The model is able to predict the flood stage within 2-3 feet which is typically the error for issuing flood warnings (Zalenski, Krajewski, Quintero, Restrepo, & Buan, 2017). This flood event was especially destructive to the infrastructure of the city because the flood waters remained at the major flood stage for approximately 37 hours (Table 12). In the case of the Maquoketa River at Manchester, the flood depth and extent does not drastically change once above the major flood level. The fact that the models can simulate the time to major flood stage and the duration above flood stage shows that the model has skill despite the various uncertainties of rainfall input.

Table 10. Statistical analysis to evaluate model performance in predicting the discharge at the outlet for the flood of July 2010

<b>Rainfall</b>	<b>Model Configuration</b>	<b>RMSE</b>	<b>MAE</b>	<b>R<sup>2</sup></b>	<b>Observed Peak Q (cfs)</b>	<b>Simulated Peak Q (cfs)</b>	<b>PE (cfs)</b>	<b>Time of Peak Observed (CST)</b>	<b>Time of Peak Simulated (CST)</b>	<b>TPE (hr)</b>
July 2010 Peak 1										
StageIV	HLM	1,738	1,386	1,738	22,200	22,598	-398	7/23 23:30	7/23 20:45	2.8
	HLM-XP-C1	1,525	1,025	1,525	22,200	21,303	897	7/23 23:30	7/23 21:30	2.0
	HLM-XP-C2	1,474	991	1,474	22,200	21,343	857	7/23 23:30	7/23 21:30	2.0
IFC	HLM	2,173	1,815	2,173	22,200	25,030	-2,830	7/23 23:30	7/23 20:45	2.8
	HLM-XP-C1	2,438	1,900	2,438	22,200	23,212	-1,012	7/23 23:30	7/23 22:00	1.5
	HLM-XP-C2	2,263	1,780	2,263	22,200	23,214	-1,014	7/23 23:30	7/23 22:15	1.3
July 2010 Peak 2										
StageIV	HLM	6,226	5,450	6,226	26,600	16,241	10,359	7/24 12:30	7/24 3:15	9.3
	HLM-XP-C1	6,577	5,688	6,577	26,600	16,206	10,394	7/24 12:30	7/24 3:15	9.3
	HLM-XP-C2	6,552	5,681	6,552	26,600	16,290	10,310	7/24 12:30	7/24 3:15	9.3
IFC	HLM	4,562	4,212	4,562	26,600	20,787	5,813	7/24 12:30	7/24 16:45	-4.3
	HLM-XP-C1	4,948	4,492	4,948	26,600	19,789	6,811	7/24 12:30	7/24 17:15	-4.8
	HLM-XP-C2	4,952	4,499	4,952	26,600	19,827	6,773	7/24 12:30	7/24 17:15	-4.8

Table 11. Statistical analysis to evaluate model performance in predicting the stage at the outlet for the flood of July 2010

<b>Rainfall</b>	<b>Model Configuration</b>	<b>RMSE</b>	<b>MAE</b>	<b>R<sup>2</sup></b>	<b>Observed Peak Stage (ft)</b>	<b>Simulated Peak Stage (ft)</b>	<b>PE (ft)</b>	<b>Time of Peak Observed (CST)</b>	<b>Time of Peak Simulated (CST)</b>	<b>TPE (hr)</b>
July 2010 Peak 1										
StageIV	HLM	1.1	0.9	1.1	23.01	23.15	-0.14	7/23 23:30	7/23 20:45	2.8
	HLM-XP-C1	1.0	0.8	1.0	23.01	22.68	0.33	7/23 23:30	7/23 21:30	2.0
	HLM-XP-C2	1.0	0.8	1.0	23.01	22.70	0.31	7/23 23:30	7/23 21:30	2.0
IFC	HLM	1.4	1.3	1.4	23.01	23.99	-0.98	7/23 23:30	7/23 20:45	2.8
	HLM-XP-C1	1.8	1.5	1.8	23.01	23.37	-0.36	7/23 23:30	7/23 22:00	1.5
	HLM-XP-C2	1.6	1.4	1.6	23.01	23.37	-0.36	7/23 23:30	7/23 22:15	1.3
July 2010 Peak 2										
StageIV	HLM	4.8	4.7	4.8	24.51	20.66	3.85	7/24 12:30	7/24 3:15	9.3
	HLM-XP-C1	5.1	5.0	5.1	24.51	20.65	3.86	7/24 12:30	7/24 3:15	9.3
	HLM-XP-C2	5.1	5.0	5.1	24.51	20.69	3.82	7/24 12:30	7/24 3:15	9.3
IFC	HLM	4.3	4.1	4.3	24.51	22.49	2.02	7/24 12:30	7/24 16:45	-4.3
	HLM-XP-C1	4.5	4.3	4.5	24.51	22.11	2.40	7/24 12:30	7/24 17:15	-4.8
	HLM-XP-C2	4.6	4.3	4.6	24.51	22.13	2.38	7/24 12:30	7/24 17:15	-4.8

Table 12. Statistical analysis to evaluate model performance in predicting the Major Flood Stage at the outlet for the flood of July 2010

<b>Rainfall</b>	<b>Model Configuration</b>	<b>Flood Stage Crest Time Observed (CST)</b>	<b>Flood Stage Crest Time Simulated (CST)</b>	<b>Crest Time Error (hr)</b>	<b>Duration Above Major Flood Stage Observed (hr)</b>	<b>Duration Above Major Flood Stage Simulated (hr)</b>	<b>Duration Above Major Flood Stage Error (hr)</b>
StageIV	HLM	7/23 14:45	7/23 13:45	-1.0	37	30.8	-6.3
	HLM-XP-C1	7/23 14:45	7/23 15:00	0.3	37	28.5	-8.5
	HLM-XP-C2	7/23 14:45	7/23 15:00	0.3	37	28.8	-8.3
IFC	HLM	7/23 14:45	7/23 15:15	0.5	37	31.5	-5.5
	HLM-XP-C1	7/23 14:45	7/23 16:15	1.5	37	30.8	-6.3
	HLM-XP-C2	7/23 14:45	7/23 16:15	1.5	37	30.8	-6.3

### 5.2.2 September 2016

For the September 2016 event, the local area experienced more rainfall in a smaller period of time. Though the magnitude and duration of the flood is not as significant as the July 2010 event, the quick hydrologic response of the watershed makes this flood event memorable to the local officials. The spatiotemporal variability of rainfall and the resulting uncertainty is evident in the model results for the flood of September 2016. The discharge at the outlet of the model simulations is compared to the observed streamflow in Figure 32. The difference in timing and peak volume simulated with the different model configurations and rainfall inputs is more pronounced in this flood event (Table 13). The multiple model realizations form an uncertainty band or envelope around the observed values. The ensemble of hydrographs obtained with the different rainfall inputs is implicitly accounting for the uncertainty in the rainfall estimation.

The models are able to reproduce the rising limb of the hydrograph, though overestimating the stage at a given time by 2-3 feet (Figure 33). The simulated peak discharge is highly overestimated using MRMS and StageIV rainfall inputs, but the peak stage is within 1-3 feet of the measured peak (Table 14). These same rainfall inputs resulted in models that simulated the major flood level 2-3.5 hours early and the flood duration nearly twice as long as what was observed (Table 15). On the other hand, the HLM IFC simulation simulates the shape and volume of the hydrograph but shifted ahead by 2-3 hours. The IFC-5min and IFC-1hr were applied to the nested models but there was no significant change in the results, so much so that the hydrographs lie directly on top of each other (Figure 32).

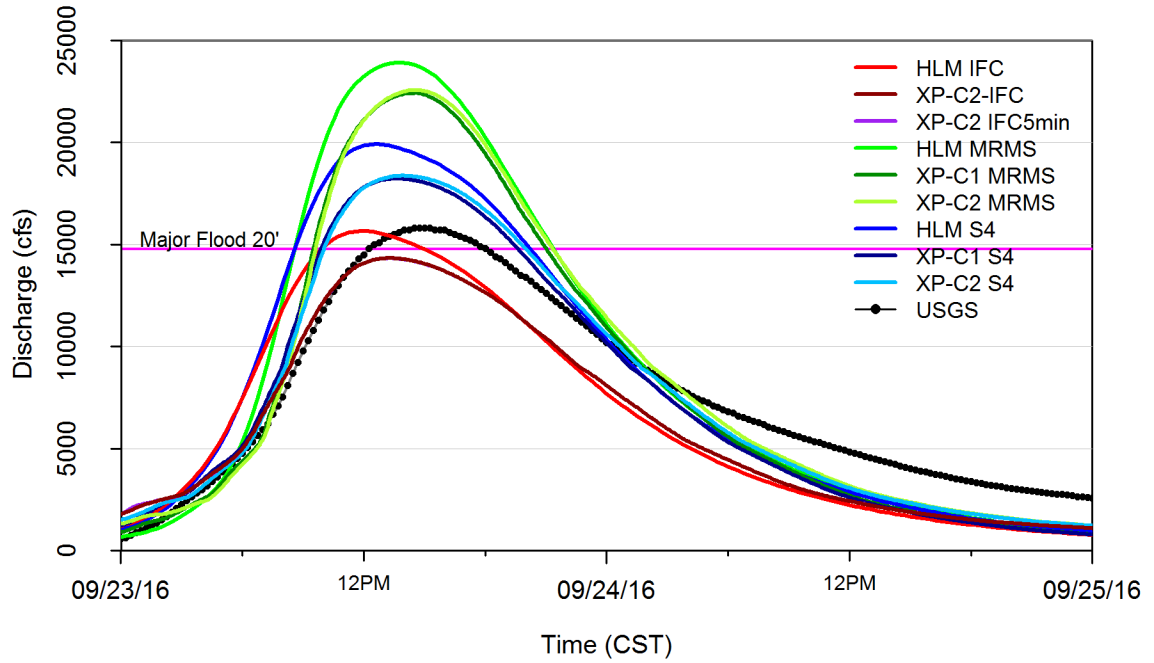


Figure 32. Comparison of the observed USGS hydrograph and the model results for the September 2016 flood

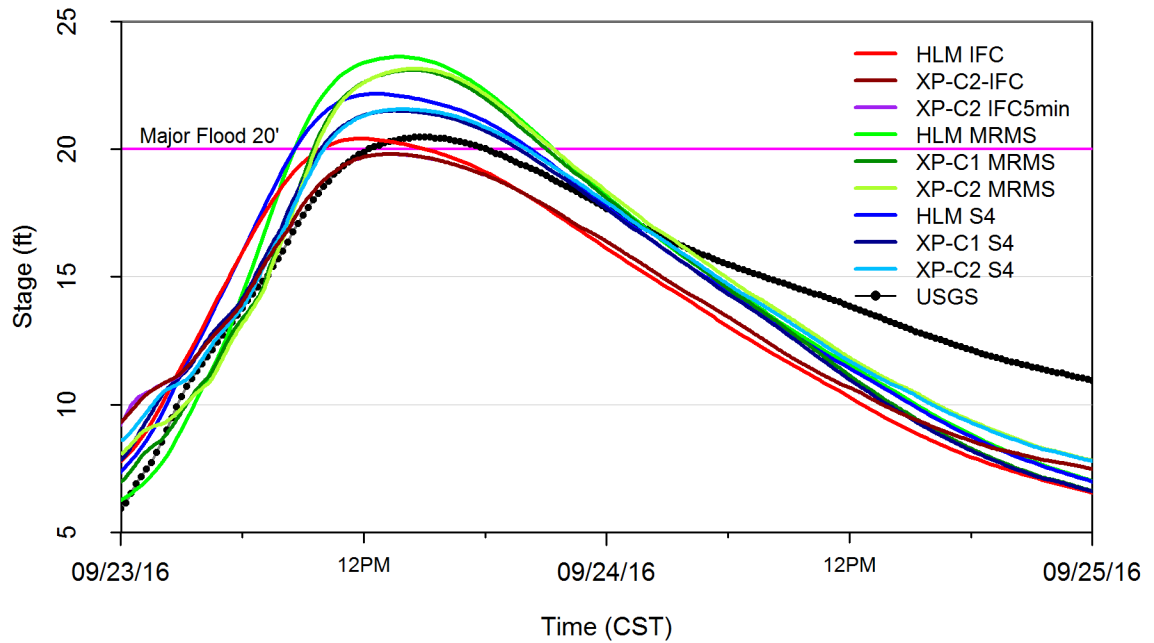


Figure 33. Comparison of the USGS stage records and the model results for the September 2016 flood

Table 13. Statistical analysis to evaluate model performance in predicting the discharge at the outlet for the flood of September 2016

<b>Rainfall</b>	<b>Model Configuration</b>	<b>RMSE</b>	<b>MAE</b>	<b>R<sup>2</sup></b>	<b>Observed Peak Q (cfs)</b>	<b>Simulated Peak Q (cfs)</b>	<b>PE (cfs)</b>	<b>Time of Peak Observed (CST)</b>	<b>Time of Peak Simulated (CST)</b>	<b>TPE (hr)</b>
StageIV	HLM	2,105	1,486	2,105	15,800	19,905	-4,105	9/23 14:30	9/23 12:30	2.0
	HLM-XP-C1	1,498	1,189	1,498	15,800	18,219	-2,419	9/23 14:30	9/23 13:30	1.0
	HLM-XP-C2	1,328	1,075	1,328	15,800	18,360	-2,560	9/23 14:00	9/23 14:30	0.5
MRMS	HLM	2,977	1,847	2,977	15,800	23,901	-8,101	9/23 14:30	9/23 13:45	0.8
	HLM-XP-C1	2,365	1,578	2,365	15,800	22,404	-6,604	9/23 14:30	9/23 14:30	0.0
	HLM-XP-C2	2,321	1,527	2,321	15,800	22,553	-6,753	9/23 14:30	9/23 14:30	0.0
IFC-5min	HLM	1,851	1,487	1,851	15,800	15,651	149	9/23 14:30	9/23 12:00	2.5
	HLM-XP-C2	1,502	1,282	1,502	15,800	14,328	1,472	9/23 14:30	9/23 13:15	1.3
IFC-1hr	HLM-XP-C2	1,501	1,282	1,501	15,800	14,332	1,468	9/23 14:30	9/23 13:15	1.3



Table 14. Statistical analysis to evaluate model performance in predicting the stage at the outlet for the flood of September 2016

<b>Rainfall</b>	<b>Model Configuration</b>	<b>RMSE</b>	<b>MAE</b>	<b>R<sup>2</sup></b>	<b>Observed Peak Stage (ft)</b>	<b>Simulated Peak Stage (ft)</b>	<b>PE (ft)</b>	<b>Time of Peak Observed (CST)</b>	<b>Time of Peak Simulated (CST)</b>	<b>TPE (hr)</b>
StageIV	HLM	2.3	1.8	2.3	20.47	22.16	-1.69	9/23 14:30	9/23 12:30	2.0
	HLM-XP-C1	2.7	2.0	2.7	20.47	21.49	-1.02	9/23 14:30	9/23 13:30	1.0
	HLM-XP-C2	1.9	1.6	1.9	20.47	21.55	-1.08	9/23 14:30	9/23 14:00	0.5
MRMS	HLM	2.4	1.9	2.4	20.47	23.61	-3.14	9/23 14:30	9/23 13:45	0.8
	HLM-XP-C1	2.7	2.1	2.7	20.47	23.08	-2.61	9/23 14:30	9/23 14:30	0.0
	HLM-XP-C2	2.0	1.8	2.0	20.47	23.14	-2.67	9/23 14:30	9/23 14:30	0.0
IFC-5min	HLM	2.6	2.0	2.6	20.47	20.40	0.07	9/23 14:30	9/23 12:00	2.5
	HLM-XP-C1	2.3	2.0	2.3	20.47	19.80	0.67	9/23 14:30	9/23 13:15	1.3
IFC-1hr	HLM-XP-C2	2.3	2.0	2.3	20.47	19.80	0.67	9/23 14:30	9/23 13:15	1.3

Table 15. Statistical analysis to evaluate model performance in predicting the major flood stage at the outlet for the flood of September 2016

<b>Rainfall</b>	<b>Model Configuration</b>	<b>Flood Stage Crest Time Observed (CST)</b>	<b>Flood Stage Crest Time Simulated (CST)</b>	<b>Crest Time Error (hr)</b>	<b>Duration Above Major Flood Stage Observed (hr)</b>	<b>Duration Above Major Flood Stage Simulated (hr)</b>	<b>Duration Above Major Flood Stage Error (hr)</b>
StageIV	HLM	9/23 12:15	9/23 8:45	-3.5	5.8	11.3	5.5
	HLM-XP-C1	9/23 12:15	9/23 9:55	-2.3	5.8	9.7	3.9
	HLM-XP-C2	9/23 12:15	9/23 10:05	-2.2	5.8	9.9	4.2
MRMS	HLM	9/23 12:15	9/23 8:45	-3.5	5.8	12.5	6.8
	HLM-XP-C1	9/23 12:15	9/23 9:30	-2.8	5.8	11.5	5.8
	HLM-XP-C2	9/23 12:15	9/23 9:40	-2.6	5.8	11.7	5.9
IFC-5min	HLM	9/23 12:15	9/23 10:00	-2.3	5.8	5.0	-0.8

### **5.3 Uncertainty**

Having compared the model outputs with photos and streamflow observations at the USGS gauge, it is evident that none of the model combinations can reproduce the exact hydrologic response observed. However, the overall shape of the simulated hydrographs and the max flood extent obtained are very close to what was observed which shows that model does have skill. The uncertainty of the model structure, rainfall inputs, and other sources are discussed.

#### **5.3.1 Model Structure**

Some of the key hydraulic features in urban areas include the subsurface conveyance through stormsewers and overland flow paths through streets and between buildings. Locally, the extension of the 2D grid and stormwater network did not significantly change the results of the discharge at the outlet, as seen by the small differences between the peak flows and time to peak for XP-C1 and XP-C2. The nested regional-local modeling approach had reduced flows at the outlet when compared to the regional HLM output. Overall, the rising and falling limb of the hydrographs are not significantly improved with the nested modeling approach. For extreme flood events, the flows from the upper Maquoketa River watershed are the dominant source of flooding in Manchester resulting in a minor impact from the urban area. For these flood events, the max flood extent produced by the urban models is mostly influenced by the streamflow boundary conditions from the regional model. The hydrologic response of the regional watershed has significant uncertainty associated with it which overwhelmed the local model results.

### 5.3.2 Rating Curve

During extreme flood events, typically the conveyance of the channel is exceeded resulting in the overflow into the floodplain where water is stored and transported until it reenters the channel. With historical streamflow data and LIDAR derived cross-sections, rating curves can be created for a channel relating the measured water stage to the discharge. The discharge in the channel is determined using a rating curve and the measured flood stages. The uncertainty associated with rating curves, specifically at extreme flood levels, is prominent because of the lack of measurements at high flows and the uncertainty in the volume of water stored in the floodplain.

A large increase in discharge through the river does not necessarily mean a large increase in flood stage. The model output, usually a discharge, is converted to a stage which is what local officials use to make decisions for evacuation or road closures. The land adjacent to rivers are low and flat so the water that spills out of the river banks and spreads like a sheet over a large section of land. The observed peaks for both events were above the major flood stage. The models predict that the flood stage will remain above the Major Flood Stage for the entirety of the July 2010 event (Table 12), however they overestimate the duration of the Major Flood Stage by a factor of 2 for the September 2016 event (Table 15). Having an accurate picture of the channel and overbank cross-section will improve the rating curves. The uncertainty of the rating curves propagates into the model results when the discharge or stage is interpolated from the gauge rating curve.

### 5.3.3 Rainfall

Errors in the rainfall inputs are one of the most important sources of uncertainty in urban hydrological models. The extreme rainfall events of July 2010 and September 2016 in the Maquoketa River basin is an example of how there is a large uncertainty using radar to estimate the volume of rainfall for high return periods. When evaluating the performance of the model based on the individual rainfall products used as inputs for the two events, there is not systematic error. This highlights the large uncertainty of rainfall inputs that is a result of the non-linear, spatiotemporal patterns of rainfall. However, the ensemble of model simulations using different radar rainfall inputs creates an uncertainty band around the observed hydrograph, implicitly accounting for the uncertainty in the rainfall.

When the regional watershed experienced heavy rainfall, the rainfall-runoff volume from Manchester is not crucial for predicting flood levels at the outlet. However, the urban catchment is sensitive to the temporal resolution of the rainfall while the regional streamflow output is less sensitive. The spatial and temporal resolution of the rainfall applied to the XPSWMM model did impact the hydrologic response of the urban area. This is evident looking at the discharge at the confluence of Tributary A and Tributary 2 occurs at the railroad crossing as shown in Figure 17. For July 2010, the model discharge of the Eastern Tributary for the IFC and StageIV rainfall estimates show a similar rainfall-runoff response for the urban catchment (Figure 34).

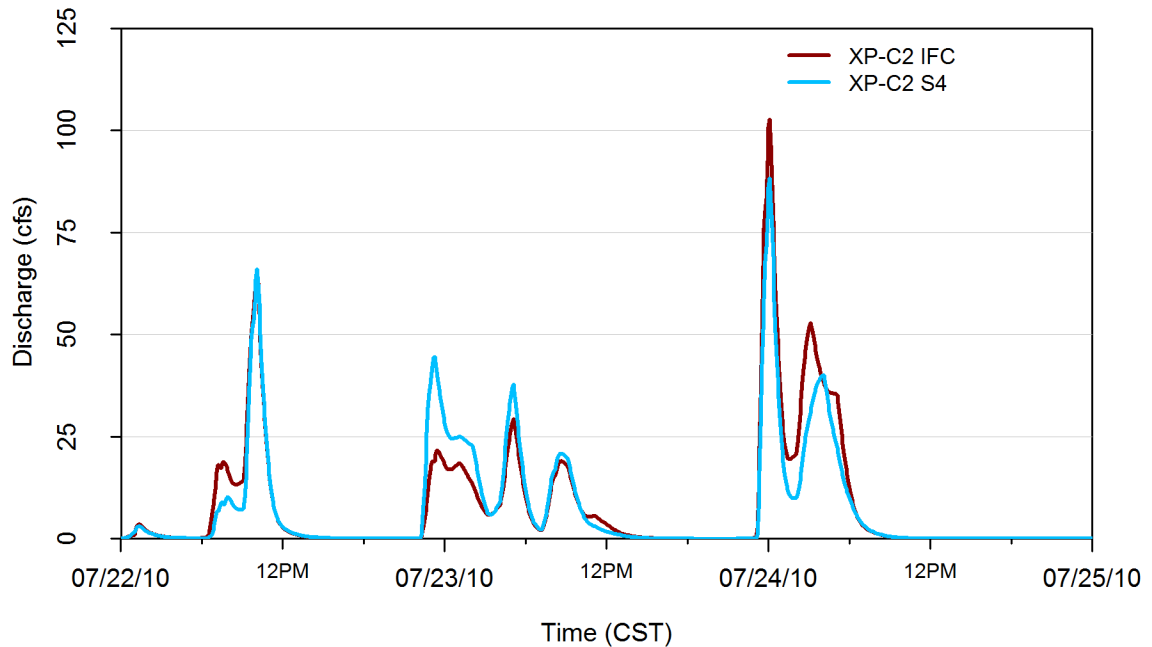


Figure 34. The effect of the rainfall temporal and spatial resolution on the hydrologic response of eastern Manchester up to the railroad crossing for the July 2010 flood

Recall that during the September 2016 flood, the streamflow predictions of the nested model at the USGS gauge did not significantly change with the use of hourly and 5-min IFC rainfall (Section 5.2.2). The temporal and spatial resolution of the rainfall does change the hydrologic response of the urban area as shown in Figure 35. The uncertainty in the resolution of rainfall makes predicting the rainfall-runoff volume in urban areas difficult, but it is important because of the significant changes in the potential flood risks.

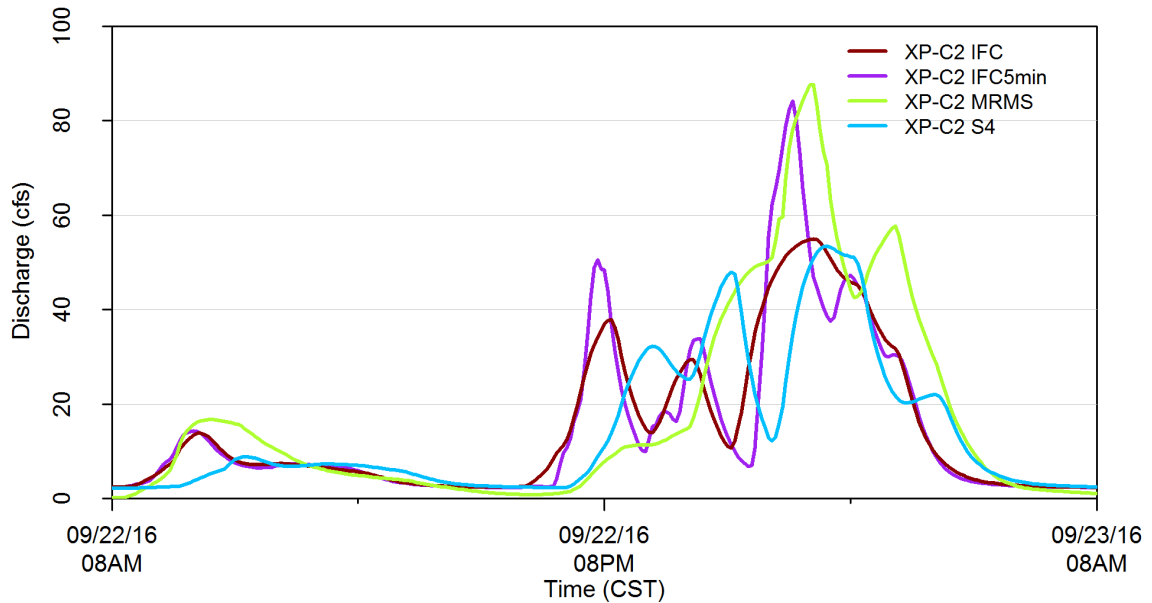


Figure 35. The effect of the rainfall temporal and spatial resolution on the hydrologic response of eastern Manchester up to the railroad crossing for the September 2016 flood

#### 5.4 Discussion

The streamflow observations at the USGS gauge are within the predictions of all the different model realizations. The nested model has skill in reproducing the flood extent as shown in Section 0. Assuming each rainfall product is valid, together the model configurations provide an accurate prediction of the flood. For real-time forecasting, the main value of using a nested modeling approach is to take advantage of the hazard related information from the local 1D/2D model. However, cities that experience riverine flooding might find it most useful to have warnings associated with rainfall amount and river stages upstream. Most of the flood risks for urban areas in Iowa are the buildings and stormwater infrastructure interacting directly with the channel or overbanks. The buildings or roadways that are adjacent to the streams or reservoirs would most benefit from the XPSWMM model overland flow results.

## **CHAPTER 6: MODEL APPLICATION**

An objective of this project was to assist the small community of Manchester with improving their flood preparedness. In this section, the various causes of local flooding in Manchester are evaluated and general mitigation options are proposed based for areas at risk. Maps of the duration of the flood waters at high depths and velocities can provide information to the city engineer on potential debris, sediment transport, and scouring that might occur around bridges or other structures.

### **6.1 Design Storms**

The stormwater infrastructure standards in Iowa are set by the Statewide Urban Design and Specifications (SUDAS) program which is overseen by a statewide steering committee comprised of various stakeholders (Iowa DOT, cities, counties, and consultants). All urban drainage networks are designed to manage a maximum rainfall with the use of design storms. This implies that there is an accepted flood risk for any greater rainfall event, but this risk is underestimated. With changes in urbanization, land cover, and more frequent heavy rainfalls the infrastructure may no longer be able to cope (Henonin et al., 2013).

A design event or design storm is used as a basis for determining the requirements of new stormwater improvements or for evaluating an existing project. It is assumed that the stormwater conveyance components will be able to function properly and accommodate the design event at full capacity. The frequency of a rainfall event is the average recurrence interval of storms having the same duration and precipitation volume (absolute depth). If a storm event has a 2% chance of occurring in any given year, then it has a return period of 500 years and a probability of exceedance of 0.02. The exceedance



probability is the probability that a storm event with a specified duration and volume will be exceeded in one given period. The return period is the average length of time between the events that have the same duration and volume. The design criteria relevant to urban stormwater infrastructure from SUDAS Section 2A-3 are summarized in Table 16. To learn more about Iowa's stormwater regulations, permitting, and management criteria see the Iowa SUDAS Design Manual or the Federal Highway Administration Urban Drainage Design Manual (S. A. Brown et al., 2013). Design storms were used as input into the XPSWMM model to test the overall capabilities of Manchester's stormwater network. The performance of the model will be compared to the minimum design standards for the capacity of the system as prescribed by SUDAS. However, the design storms used to design urban conveyance networks do provide information on how the intensity varies during the storm and they do not consider how much rain fell before the period in question.

Table 16. Summary of Statewide Urban Design and Specifications (SUDAS) for Stormwater

Intakes	<ul style="list-style-type: none"> <li>▪ Should have the minimum capacity to convey the 5yr storm under developed conditions during the peak flow rate</li> </ul>
Storm sewers	<ul style="list-style-type: none"> <li>▪ Should have the minimum capacity to convey a 5yr storm under developed conditions within the pipe</li> <li>▪ Additional conveyance should be made for the 100yr storm in areas where overland flow is not allowed or available to prevent damaging private property</li> </ul>
Culverts	<p>Should have the capacity to convey:</p> <ul style="list-style-type: none"> <li>▪ A 10yr storm without headwater depth exceeding the diameter of the culvert</li> <li>▪ A 50yr storm without the headwater depth exceeding 1 foot over the top of pipe</li> <li>▪ A 100yr storm without the headwater depth exceeding 1 foot below the low point of the roadway</li> </ul>
Ditches	<ul style="list-style-type: none"> <li>▪ Should have the capacity to convey a 50yr storm within the banks</li> <li>▪ Surface water flowage easements should provide conveyance for the 100yr storm to manage overland flow</li> </ul>
Detention Basins	<ul style="list-style-type: none"> <li>▪ Should have the capacity to retain a 100yr storm at critical duration or by safely discharging over an auxiliary spillway</li> <li>▪ The top of any detention embankments should be a minimum of 1 foot above the 100yr ponding elevation</li> </ul>
Street Flow	<ul style="list-style-type: none"> <li>▪ For local roads, there should be no curb overtopping. Flow may spread to the crown of the street.</li> <li>▪ The initial design storm runoff is a depth of 6 inches at the crown and 9 inches for the 100yr design storm.</li> </ul>

A rainfall frequency analysis is performed to obtain the precipitation-frequency estimate (PFE) for an individual location using historical records gathered from NOAA's Precipitation Frequency Data Server or Atlas 14. Because of the wide use of design storms, regional intensity-duration-frequency (IDF) tables corresponding to the climatic sections in Bulletin 71 were developed for regions of Iowa by averaging the county PFE values. Manchester is in Delaware County which is in the Northeast climatic section (code 3) of Iowa. Tables of the rainfall depth and intensity for various returns periods for Iowa can be found in the SUDAS Manual Section 2B online. Using the SCS type II curve for Iowa, the rainfall hyetograph was created for the 5, 10, 50, 100, and 500 yr design storms with a duration of 6 hr as shown in Figure 36. The accumulated precipitation for each design storm is 2.98, 3.56, 5.17, 5.97, and 8.07 inches, respectively.

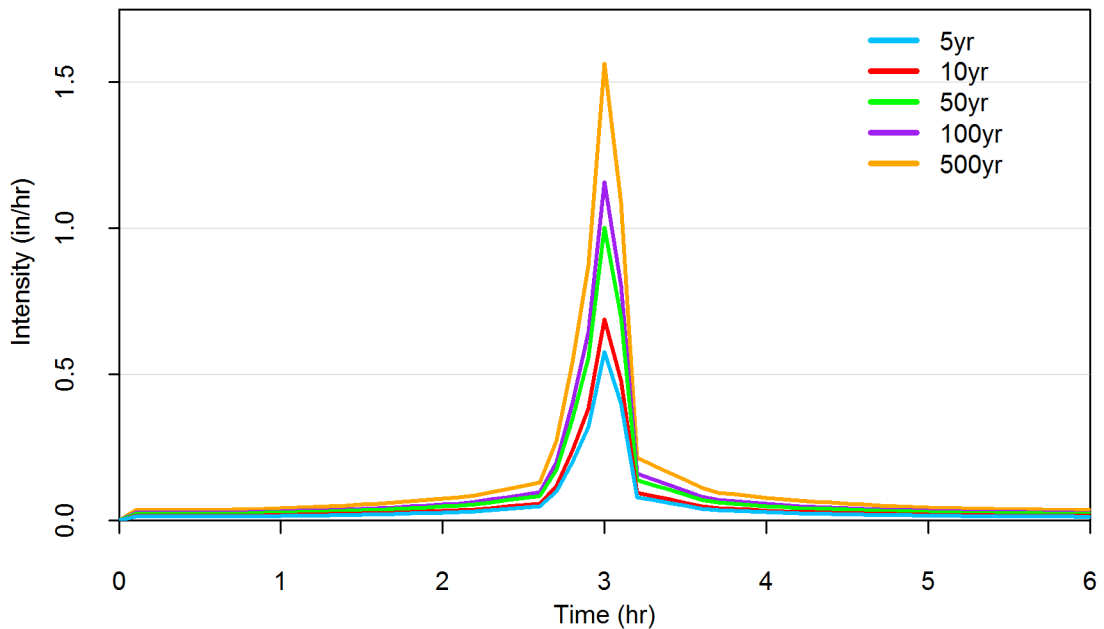


Figure 36. Design storms for 5, 10, 50, 100, and 500yr return periods with a 6hr duration for northeast Iowa

For the design storm scenarios, the Maquoketa River was modeled with a constant inflow of 500 cfs which is the approximately the average discharge for the summer months (USGS), and the initial conditions of the model were set to dry. The advantage of a holistic XPSWMM model of Manchester is there is opportunity for evaluating the capacity of the stormwater network for design storms. Model outputs can be used to identify areas that do not meet current stormwater design criteria outlined in Table 16. For example, in Figure 37 the stormwater infrastructure can be evaluated using model outputs from the 100-yr design storm scenario. The culverts and ditches along Tributary A are not able to handle the 100-yr flows whereas further downstream above the railroad the stormwater drainage functions as designed.

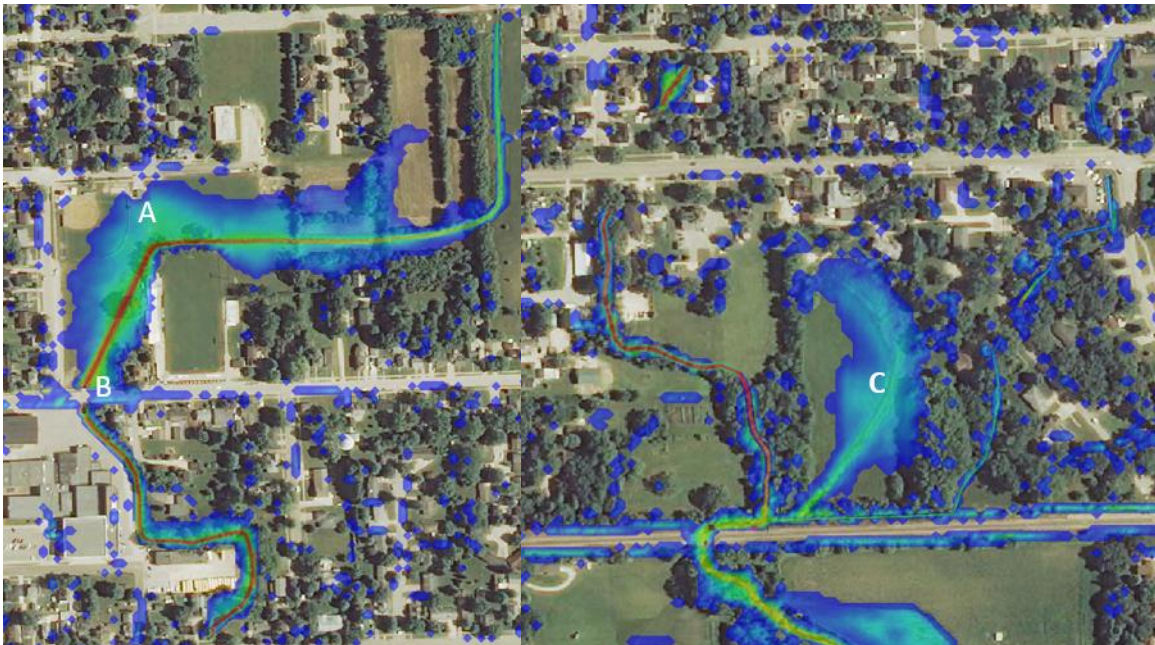


Figure 37. Model results for the 100yr-6hr design storm scenario shows (a) ditch capacity is exceeded, (b) culvert is overtopped into streets, and (c) detention pond is able to store excess flows

Catchments with short times of concentration may cause a greater runoff rate because they are sensitive to high-intensity rainfall. The volume of runoff from the urban

catchment will change depending on the initial conditions and also the rainfall intensity. The uncalibrated XPSWMM model output from the five design storm scenarios was compared to the local flows generated during the July 2010 and September 2016 floods. The model discharge at the railroad for the 6hr design storm scenarios with dry initial conditions is shown in Figure 38.

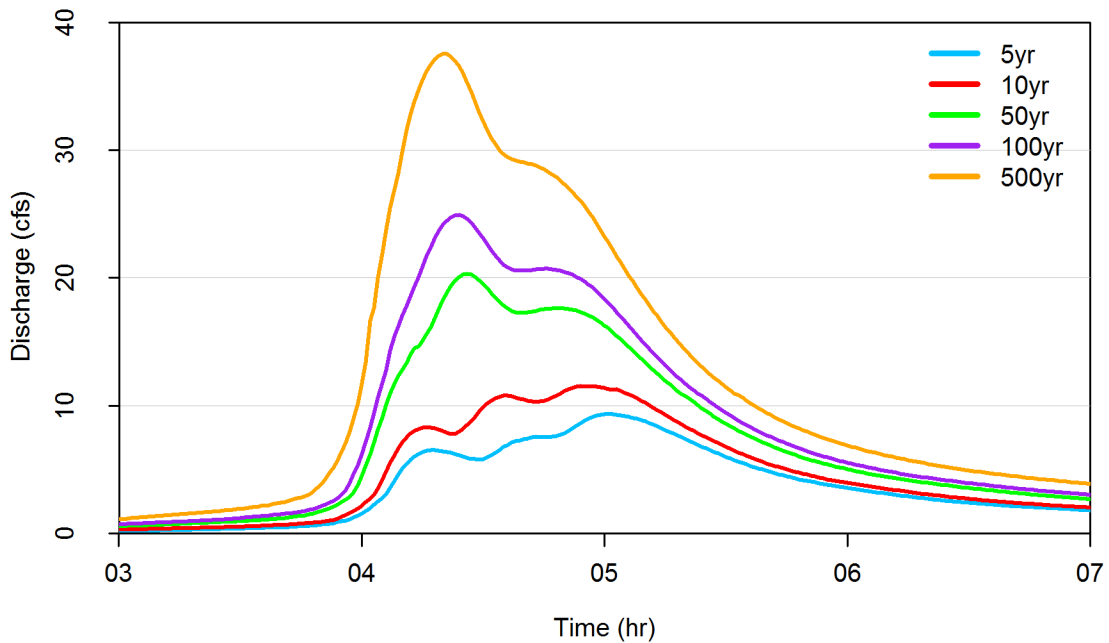


Figure 38. Flow in Eastern Tributary at Railroad Crossing for the 6hr design storms with a return interval of 5, 10, 50, 100, 500yr

The peak flow for the 500yr scenario is less than 40 cfs, nearly half the flow simulated for the July 2010 and September 2016 flood events (Figure 34 and Figure 35). The significant difference in total volume indicates that the urban runoff generated from design storms may underestimate the runoff for the “worst case”. The disadvantage of design storms is they do not properly account for the spatiotemporal variability of rainfall or how much rain fell before the period in question.

## 6.2 Local Flooding

For local rainfall extremes, the hydrologic characteristics of the local subcatchments and the initial conditions will change the flood risk of the urban area. Saturated or frozen conditions can result in a larger volume of runoff from the eastern subcatchments. In October of 2007, the eastern area of Manchester experienced extreme flooding where the overland flow in the streets hydraulically connected Tributary A and Tributary 2, but the Maquoketa River only reached the Flood Stage (14 ft). Though the storm event of October 2007 is smaller compared to the 2010 or 2016 event, it also caused a flood risk for the community. The duration of rainfall the city experienced was approximately 4 hours, but the intensity was very high ranging up to 2 inches per hour. Two scenarios with different initial conditions (dry and saturated) were simulated using StageIV rainfall from October 7, 2007 to test the urban catchment's sensitivity to initial conditions. Using the saturated condition, two scenarios were simulated, one with the stormsewer system active and one with overland flow. This will provide insight into the capabilities of XPSWMM to capture the hydrologic response with different initial conditions and flood routing mechanisms.

The dry initial conditions were used for the model scenario called XP-C2 Dry, these were also used for the July 2010 and September 2016 model simulations. The model parameters were adjusted so that the ground was saturated for the simulation XP-C2 Saturated and XP-C2 Sat-Overland. To model frozen or saturated (nearly impermeable) ground the percent impervious of the 2D Landuse types were altered to increase the volume of runoff as shown in Table 17.

Table 17. Change in 2D landuse percent impervious for saturated ground during October 2007 flood

2D Landuse	Average Conditions % Impervious	Saturated/Impervious Conditions % Impervious
Impervious	100	100
Open Water	100	100
Wooded Loamy Sand	0	80
Grass Loam	0	80
Developed Loam	50	90
Developed Sandy Loam	50	90
Developed Loamy Sand	50	90
Buildings	100	100

The infiltration parameters of the local rainfall-runoff subcatchments were changed so that there would be an immediate runoff response. XP-C2 Dry used the Green-Ampt parameters from Table 4. XP-C2 Saturated and XP-C2 Sat-Overland subcatchments were modeled using the uniform loss method and the depression and detention storages of the subcatchments were changed so that direct runoff was dominant (Table 18). The definitions of these parameters used in XPSWMM are provide in Section 4.1.1.

Table 18. Uniform loss method of infiltration used for saturated ground during October 2007 flood

	Parameter	East	West
Uniform Loss Method	Initial Loss (in)	0	0
	Continuing Loss (in)	0	0
Impervious Area	Depression Storage (in)	0.2	0.2
	Manning's n	0.014	0.014
	Zero Detention (%)	90	90
Pervious Area	Depression Storage (in)	0	0
	Manning's n	0.05	0.045



The discharge of the model at the outlet was compared to USGS records as shown in Figure 39. The XPSWMM model was not calibrated for any of the simulations. The regional model and the local model both have skill in reproducing the hydrologic response of the urban catchment. However, it is evident that the initial conditions and parameter selection for the local model can influence the hydrologic response.

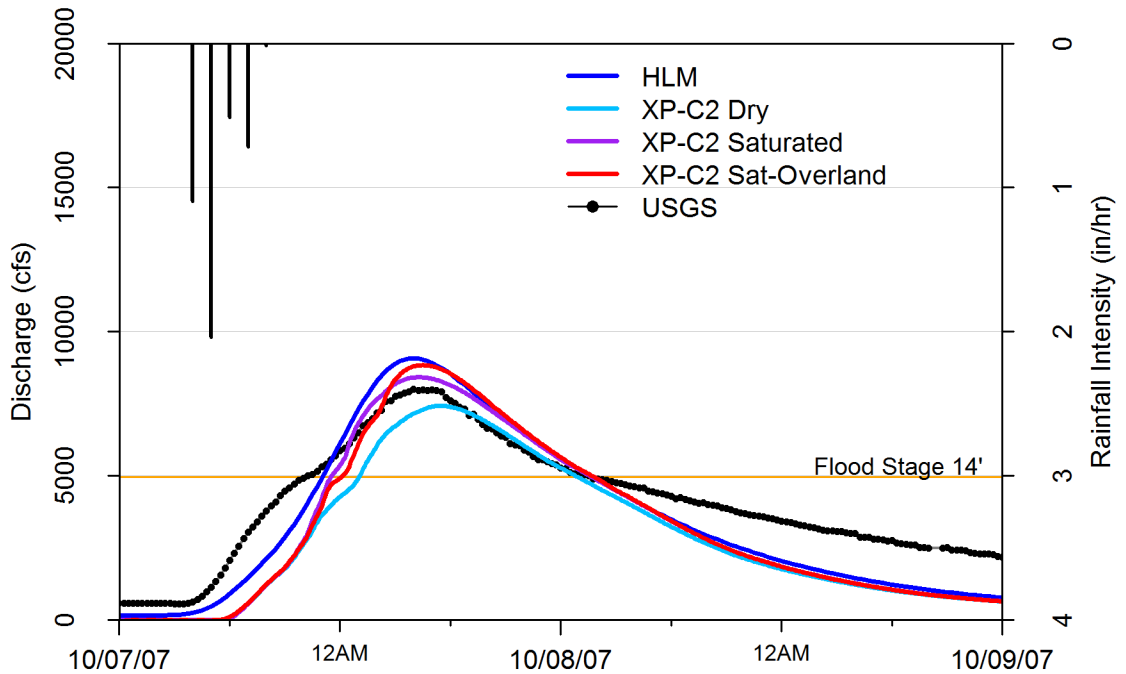


Figure 39. Stage IV rainfall and USGS streamflow records for October 2007 compared with HLM and XP simulations

Correctly modeling the amount of water that can be stored, whether in the soil or ponded in depressions in the land surface, will change the flood potential. Additionally, the inclusion of the stormwater network alters the rising limb of the hydrograph by allowing the water to drain quickly from the residential areas. With saturated conditions, the time to peak flow is improved with the stormwater network included in the model. It is evident from the XPSWMM simulations that the initial conditions are important for accurately accounting for the volume of runoff (Table 19).

Table 19. Statistical analysis of the simulated discharge and the USGS observed streamflow for October 7, 2007

Model Configuration	RMSE	MAE	R <sup>2</sup>	Obs Peak Q(cfs)	Sim Peak Q(cfs)	PE (cfs)	TOP Sim (CST)	TPE (min)
HLM	956	938	956	8,020	9,083	-1,063	4:00	0
XP-Average	2,850	2,537	2,850	8,020	7,434	586	5:30	-90
XP-Frozen	3,110	2,681	3,110	8,020	8,426	-406	4:15	-15
XP-Overland	3,103	2,681	3,103	8,020	8,845	-825	4:30	-30

The runoff production and timing of hydrologic response do play a role in the storm event response (B. K. Smith et al., 2013). The model’s sensitivity to the parameter selection is evident by the large change in runoff volume between the eastern modeled with dry versus saturated conditions (Figure 40).

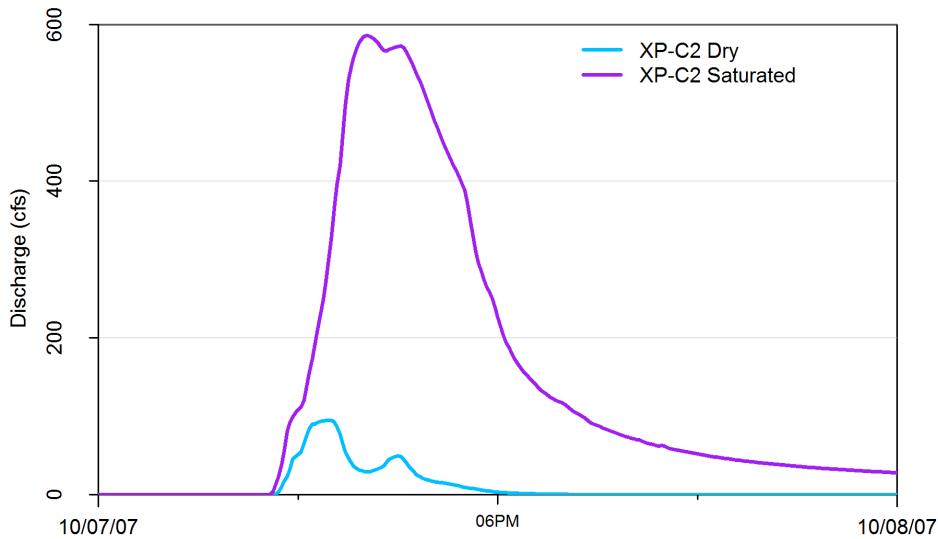


Figure 40. Streamflow for the October 2007 flood event at the confluence of Tributary A and Tributary 2 at the railroad tracks in the east

The locals recalled that during the October 2007 flood, the water surcharged from Tributary A and traveled south down Iowa St. and east on E. Howard St. to Tributary 2. This flood behavior is reproduced by the model as shown in Figure 41. The influence of the subsurface utilities on reducing urban flooding is evident by the difference in inundation between the XP-C2 Saturated and XP-C2 Sat-Overland.

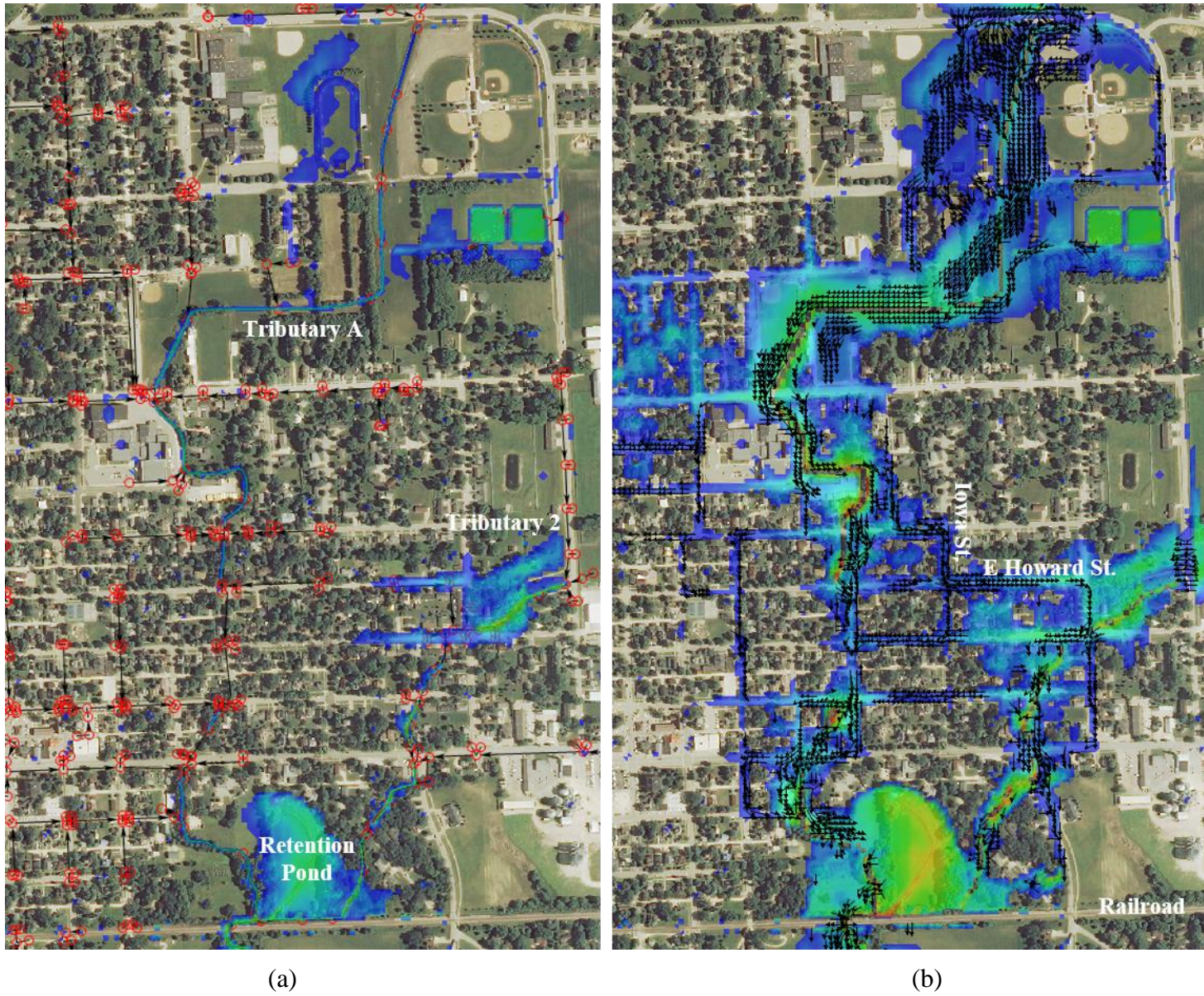


Figure 41. XPSWMM output for Oct 2007: saturated conditions with (a) the stormwater system active and (b) overland flow only



In urban areas, ponds and low, flat areas are often designed to have the capacity to store extra water during extreme flood events (SUDAS Manual). Including the effects of storage and release of water in urban areas is important in the same way that accounting for reservoirs in rural models is needed. Typically, any changes or updates to the city infrastructure must “work around” any existing railroads. At two locations in Manchester, on the Maquoketa River and on the eastern tributary, stormwater is forced through a single channel underneath the railroad as shown in Figure 42.



Figure 42. High water levels in the Maquoketa River nearly touching the low-chord of the railroad crossing during the July 2010 flood

To reduce local flooding, measures can be taken to add extra storage by increasing the depth of the retention pond located north of the railroad tracks or the one northeast of E. Howard St. Another means to divert water that is bottlenecked at the railroad would be to regrade or redesign the ditches that run along the railroad. Additionally, a large culvert can be installed under the railroad southeast of the retention pond so that excess flows from Tributary 2 can be diverted to the open areas south of the railroad. This may reduce surcharging of the stormwater network system upstream.

### 6.3 Hazard and Flood Maps

The actions taken in the initial minutes of an emergency are critical and real-time information is crucial for emergency managers deciding how to allocate their resources. The disadvantage of 1D models is they exclusively give information on the maximum flood extent but not the temporal progression of flooding (Figure 25). The advantage of a 1D/2D model is it can produce flood risk maps over time. Using velocity and depth outputs, maps can be generated that provide spatial and temporal flood information useful to planners or emergency managers. If the model is unable to operate in real-time, pre-simulated scenarios are helpful but they are unable to give information on the evolution of the flood extent or drainage network capacity (Henonin et al., 2013). The XPSWMM flood modeling tools available to aid decision making in an emergency can be generated at a given timestep or the maximum, worst case scenario. The types of risk map outputs from XPSWMM are listed below.

- Max water depth maps highlight the maximum depth predicted in each cell of the 2D domain.
- Max hazard maps can be calculated with user defined hazard expressions as functions of the depth, velocity, and debris factor.
- Mapping time to peak velocity and water surface elevations can help identify areas that will be affected by flood water most quickly.
- Time to inundation and duration of flood mapping enables assessment of the time flood depths will be above certain levels and identify the timing at which flood waters will prevent safe evacuation. The maps are calculated and displayed for depth, elevation, flow, velocity, and hazard for a given threshold value.
- Max property risk maps give the city planners and insurance companies an idea of what buildings have a high chance of flood damage.
- Max road safety risk maps provide emergency responders with a basis prioritizing what area should be evacuated and barricaded because flows will be unsafe.
- Other map results can display results on bed shear stress, stream power, mass balance, bathymetry, and more.

The XP-C2 IFC model outputs for the July 2010 flood are used to demonstrate the capabilities of XPSWMM in generating maps that provide useful flood information. The maximum flood depth and velocity map for the areas near River Street and downtown Manchester are shown in Figure 43. Compared to the photos after the 2010 flood waters had receded, it is evident that knowing the water depth and velocity can provide information on the potential destruction to infrastructure. By classifying the hazard level of the flood as a function of the water depth and horizontal velocity component, a hazard map can be generated highlighting the overall flood risks (Figure 44).

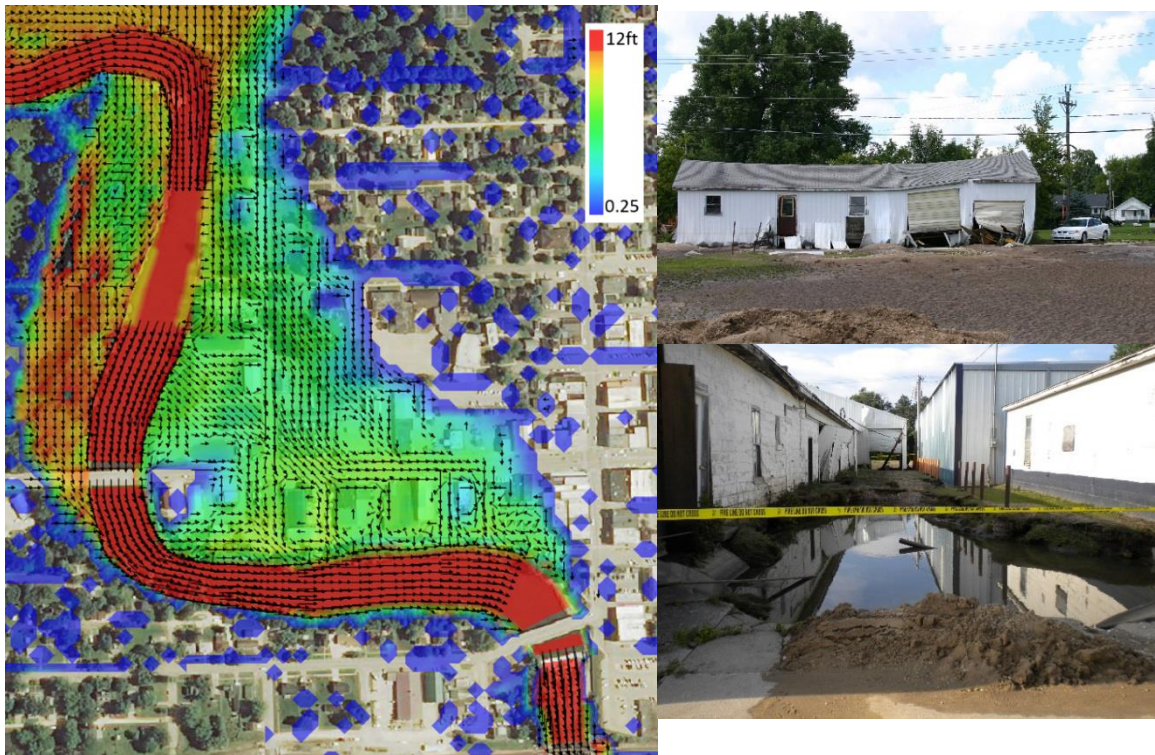


Figure 43. XP-C2 IFC max depth and velocity map output for July 2010 compared to photos



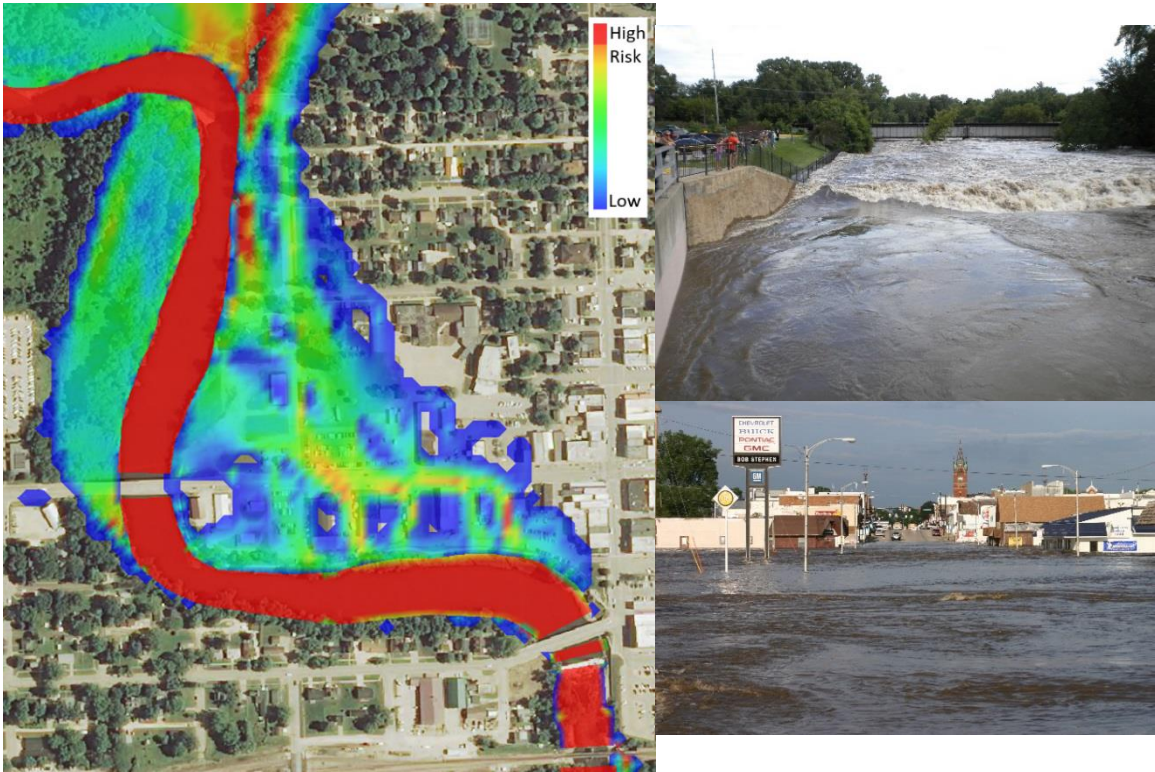


Figure 44. XP-C2 IFC max hazard (VxD) map for the July 2010 event compared to photos

The road and property safety risk maps (Figure 45 and Figure 46) can be used to help decision makers when planning to evacuate a specific area or to barricade certain roads. It is often the case that people underestimate the depth of flood waters when they try to drive across inundated roads. The road inundation maps also are useful for emergency vehicles trying to answer a distress call and transport to someone to a hospital. By identifying the safety risk in certain areas, the public will be more informed on the risks of driving on certain roads or remaining in buildings that could potentially be flooded.





Figure 45. XP-C2 IFC max road safety risk for the July 2010 event compared to photos

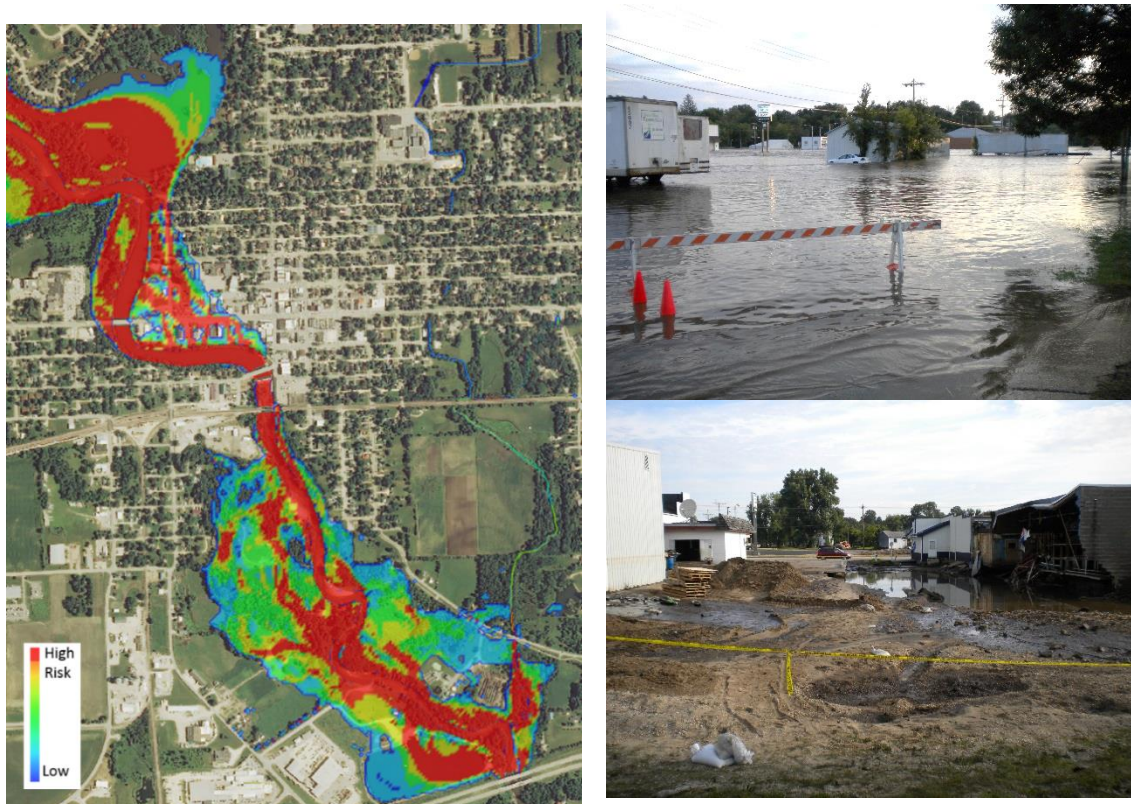


Figure 46. XP-C2 IFC max property safety risk for the July 2010 event compared to photos



Lastly, the XPSWMM model provides maps on the time of peak water surface elevation or velocity. The map shown in Figure 47 can be used to aid decision-makers to prepare at risk areas of the city before the flood reaches that location. Additional capabilities of the XPSWMM model include water quality and sediment transport modeling. Extreme flooding events typically result in sediment transported in the river and deposited downstream or potentially clogging the stormwater network. There is also a risk of structural failure for bridges due to scouring at the bridge piers or even dam failure (Delhi Dam breach of July 24, 2010). The XPSWMM model results, specifically maps, are a useful tool that can be integrated into IFIS to better communicate flood risks to the Manchester community.



Figure 47. XP-C2 IFC time to peak water surface elevation (hr) for the July 2010 event compared to photo

## **CHAPTER 7: RECOMMENDATIONS AND CONCLUSIONS**

To conclude this report, recommendations are given to the City of Manchester on ways for them to use the nested model results and existing IFC's tools to monitor their flood risk. Advice is given on the types of data and information that can be documented and shared with IFC for extended development of a flood warning system for the community. The advantages and disadvantages of using the nested regional-local modeling approach for flood modeling and real-time applications is discussed. Recommendations to IFC for future work to incorporate urban areas into the statewide forecasting system are given.

### **7.1 Recommendations for Manchester**

The documentation of flooding at various locations along the Maquoketa River during the July 2010 and September 2016 flood event were invaluable for validating the performance of the model. The community is encouraged to continue taking photos of floods where the river stage exceeds the Flood Stage (14 ft). This will provide information on model performance during the less extreme flood events. For example, October 2007 may not have attracted as much attention because the river stage had not crested the Major Stage, but the mechanisms of flooding are important and flood model needs to be able to reproduce all potential flood dynamics. With timestamped measurements, researchers can test and diagnose models to see if there is agreement with the observations. The local officials and citizens should continue to record water levels, flood extents, and flood depths along with the time the measurement was taken. With a catalogue of this information, the IFC will be better equipped to test the success of the flood tools created for the benefit of the community.

Bill Cappuccio from the IDNR provided useful crest data throughout the upper Maquoketa River watershed for several historical storm events that occurred during the years 2013 to 2016. The crest measurements taken during the flood of September 2016 were compared to the HLM discharge which was converted to stage using the rating curves estimated at the IFC. The bridge sensors of interest for this event are (1) MQ-4 located on the Maquoketa River in Dundee, (2) HY-1 located in on Honey Creek, (3) CF-1 located on Coffins Creek, and (4) MQ-7 located downstream of Manchester and Delhi Dam as shown in Figure 48. The observations are compared to the HLM outputs in Figure 49.

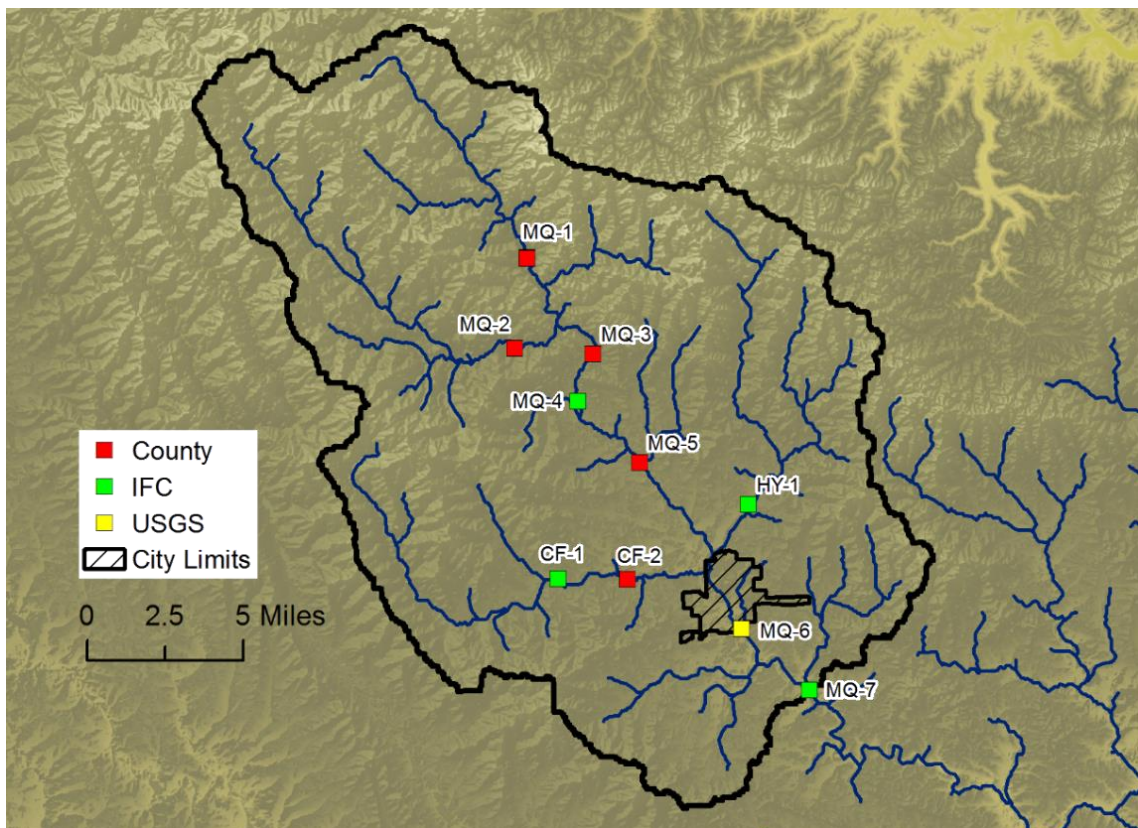


Figure 48. Locations of crest measurement across the upper Maquoketa River Watershed

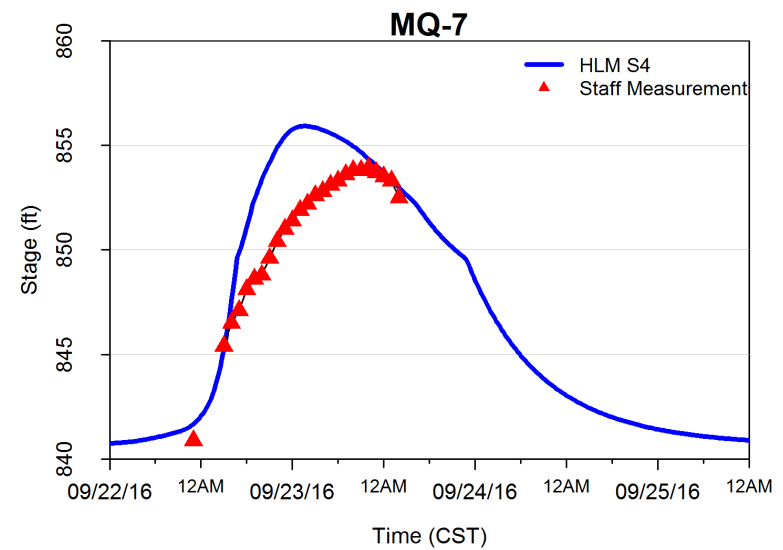
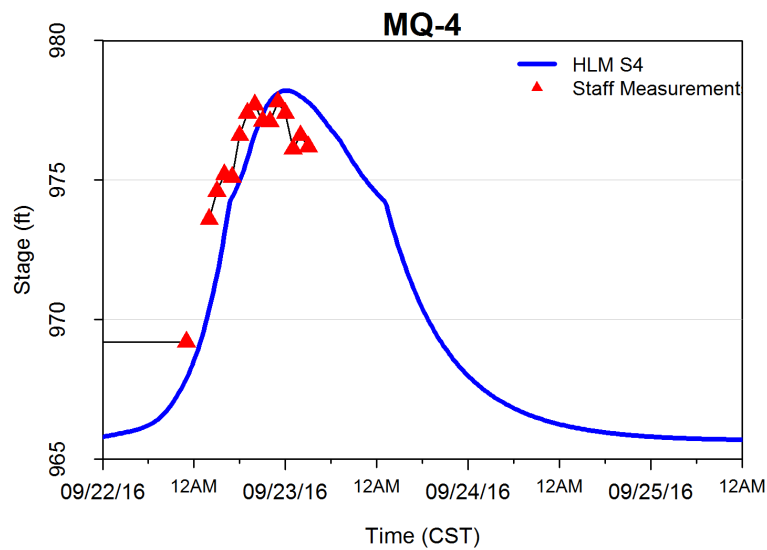
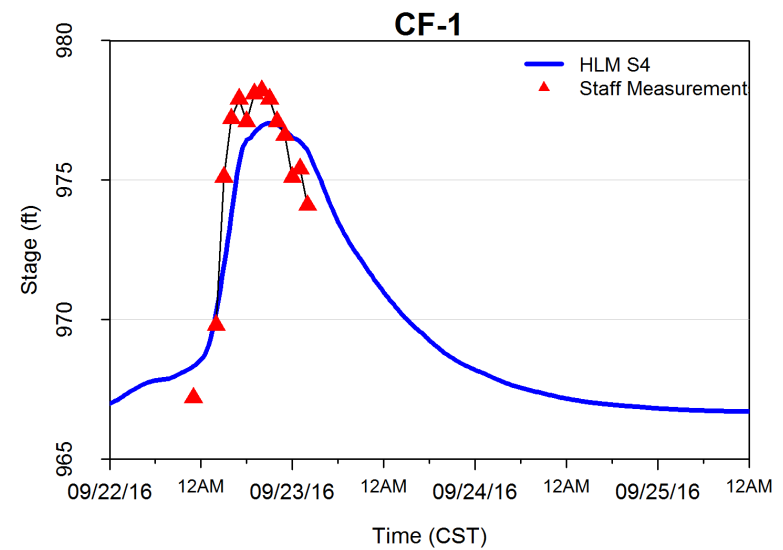
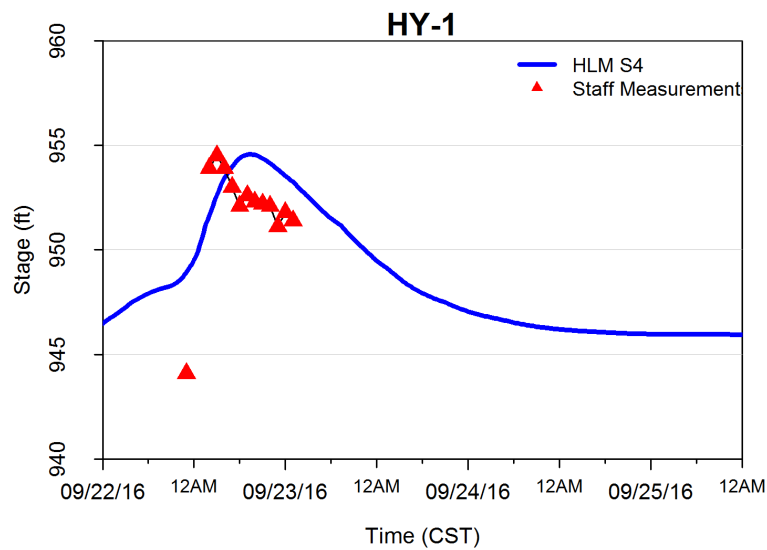


Figure 49. HLM forced with StageIV output compared to stage measurements across the upper Maquoketa River basin during September 2016

The HLM model has skill in reproducing the hydrologic response of the watershed at the various locations. At the USGS gauge at Manchester (Figure 33) the model is quick to predict the peak flow. Downstream at the IFC sensor MQ-7, the HLM does not capture the slow, rising limb of the hydrograph (Figure 49). This might be because of the reservoir upstream. The stage measurements were compared with the simulated results as shown in Table 20.

Table 20. HLM stage output compared to measurements across the upper Maquoketa River basin for September 2016

	<b>CF-1</b>	<b>HY-1</b>	<b>MQ-4</b>	<b>MQ-6</b>	<b>MQ-7</b>
<b>RMSE</b>	1.69	1.79	0.76	1.02	1.95
<b>MAE</b>	1.38	2.12	1.45	2.87	2.30
<b>R<sup>2</sup></b>	1.69	1.79	0.76	1.02	1.95
<b>Peak Obs Stage (ft)</b>	978.20	954.50	977.80	20.20	853.90
<b>Peak Sim Stage (ft)</b>	977.04	954.55	978.21	22.96	855.91
<b>PE (ft)</b>	1.16	-0.05	-0.41	-2.76	-2.01
<b>TP Sim (CST)</b>	9/23 9:00	9/23 7:00	9/23 12:00	9/23 13:00	9/23 14:00
<b>TP Obs (CST)</b>	9/23 8:00	9/23 3:00	9/23 11:00	9/23 14:00	9/23 22:00
<b>TPE (min)</b>	-60	-240	-60	60	480

For this specific flood event, the HLM estimates the peak occurring earlier than what was observed. The simulated stages are within 1-2 ft of the measured stage. Given the HLM model's ability to predict the flood stage upstream of Manchester, the locals can monitor the streamflow forecasts on IFIS at these bridge sensors. When high water levels in the tributaries are predicted or being measured, the city can prepare for potential flooding downstream. The travel times for the peaks measured and observed to those measured and observed at the USGS gauge at Manchester are given in Table 21.

Table 21. Travel times for observed and measured peaks throughout the upper Maquoketa River basin for September 2016

<b>Upstream Location</b>	<b>Discharge Obs (cfs)</b>	<b>Discharge Sim (cfs)</b>	<b>Downstream Location</b>	<b>Distance (mi)</b>	<b>Travel Time Obs (hr)</b>	<b>Travel Time Sim (hr)</b>
CF-1	8,637	5,890	MQ-6	9.9	6	4
HY-1	4,693	4,769	MQ-6	6.0	11	6
MQ-4	7,621	8,587	MQ-6	12.9	3	1
MQ-6	15,194	22,067	MQ-7	3.7	8	1

The travel times observed were significantly longer than those simulated by the HLM.

The time to peak is important and the city should use their experience to judge the amount of time before upstream flood peaks will propagate downstream. The inconsistency in travel time is a result of the spatiotemporal variability of the rainfall across the basin and the hydrologic response of the land surface. The local officials and agencies should continue to work together to gather crest measurements throughout the basin during flood events. The IFC aims to assist communities in developing tools that will aid them make decisions, and having additional data will improve the IFC's ability to predict floods in real-time.

When creating a 1D/2D detailed urban model, the construction of the stormwater layout can be cumbersome. The city engineers provided documentation of the stormwater network that was integral for the incorporation of the subsurface utilities in XPSWWM. For easy import into modeling software, the construction and content of GIS shapefiles of the stormwater drainage system is listed in Table 22.



Table 22. Useful stormwater network data for building a 1D/2D hydrodynamic model for an urban area

Stormsewers	<ul style="list-style-type: none"> <li>▪ Upstream and downstream invert elevation</li> <li>▪ Length</li> <li>▪ Material</li> <li>▪ Slope</li> <li>▪ Shape (circular, rectangular, etc.)</li> <li>▪ Crown Elevation</li> </ul>
Intakes/Manholes	<ul style="list-style-type: none"> <li>▪ Invert elevation</li> <li>▪ Intake type</li> <li>▪ Size and depth (storage)</li> </ul>
Outfalls	<ul style="list-style-type: none"> <li>▪ Invert elevation</li> <li>▪ Material</li> </ul>
Ditches	<ul style="list-style-type: none"> <li>▪ Cross-sectional shape</li> <li>▪ Spatial location (centerline)</li> <li>▪ Material</li> </ul>
Detention/Retention	<ul style="list-style-type: none"> <li>▪ Cross-sectional shape</li> <li>▪ Outlet location and invert</li> <li>▪ Material</li> </ul>
Pavement	<ul style="list-style-type: none"> <li>▪ Cross-section</li> <li>▪ Curb and gutter specifications</li> <li>▪ Street slopes</li> <li>▪ Sheet flow direction</li> </ul>
GIS Tips	<ul style="list-style-type: none"> <li>▪ Links are drawn in the direction of flow</li> <li>▪ Links should connect to nodes</li> </ul>

## 7.2 Recommendations for IFC

One of the main issues with flood risk management is the ability to forecast urban flooding in real-time. An essential tool to do this are hydrologic and hydraulic models, and the most common models are physically based with 2D capabilities. The more detailed the model, the greater the computational expense. The balance between accuracy and model complexity will vary depending on the desired model outputs. A nested regional-local model is a suitable approach for real-time applications but additional consideration should be given to the type of model that is appropriate for the urban areas.

There are no records of XPSWMM being run on a high-performance computer or if the source code can be modified to be linked to the HLM. The computational requirements for the XPSWMM model simulations running on a Windows 7 desktop with 32 GB of RAM is given in Table 23. It should be noted that multiple XPSWMM models (up to 10) could be simulated at a given time. The main constraint on model computation time was the cell size.

Table 23. Computational requirements for individual XPSWMM model simulations

<b>Rainfall</b>	<b>Model Configuration</b>	<b>Clock Time (hr)</b>	<b>x faster than real-time</b>	<b>Cell Size (ft)</b>	<b>Active 2D Cells</b>	<b>Active Area (mi<sup>2</sup>)</b>
October 2007, Simulation Time = 72 hr						
StageIV	HLM-XP Average	4.8	14.9	30	89,818	2.9
	HLM-XP Frozen	5.5	13.2	30	89,818	2.9
	HLM-XP Overland	5.4	13.4	30	89,818	2.9
July 2010, Simulation Time = 120 hr						
StageIV	HLM-XP-C1	6.1	19.8	30	57,398	1.9
	HLM-XP-C2	8.5	14.2	30	89,818	2.9
IFC	HLM-XP-C1	7.4	16.1	30	57,398	1.9
	HLM-XP-C2	8.9	13.5	30	89,818	2.9
September 2016, Simulation Time = 84 hr						
StageIV	HLM-XP-C1	18.3	4.6	15	214,614	1.7
	HLM-XP-C2	24.7	3.4	15	359,147	2.9
MRMS	HLM-XP-C1	18.4	4.6	15	213,562	1.7
	HLM-XP-C2	24.1	3.5	15	359,174	2.9
IFC-5min	HLM-XP-C2	21.9	3.8	15	359,174	2.9
IFC-1hr	HLM-XP-C2	21.1	4.0	15	359,174	2.9

For 1D/2D models like XPSWMM, they have the advantage of easily incorporating components unique to urban areas (pumps, weirs, channels of any shape, etc.) but the model construction can be tedious. For real-time applications, the advantages of using the XPSWMM model do not outweigh the time requirements for model construction and simulation. Furthermore, the XPSWMM model created for Manchester

was simplified in the sense that a single inlet capacity was used and the topography was not significantly adjusted to account for ponds and ditches. This was due to a lack of data and time. The unique geometries of inlets, ditches, streets and other components is only necessary for making design decisions or when completing a mitigation study. The minimum hydrologic information relevant to real-time flood modeling throughout an entire urban district is the rainfall-runoff mechanism from impervious surfaces and the surface and subsurface flow paths, around buildings and through the stormwater network.

Advances in hardware, data processing methods, and models of radar rainfall data are being made so that this product can be applied in areas where there are not rain gauges. Rainfall adjustments techniques can be used to reduce error in the prediction. If flood inundation models are to provide accurate, real-time predictions, it is crucial that the radar rainfall inputs are adjusted in real-time to reflect the movement storms (Thorndahl et al., 2017). To take advantage of the nested regional-local model developed in the upper Maquoketa River watershed, IFC can work with the community to investigate the installation of rain gauges to provide spatiotemporal information crucial for flood prediction.

To better understand the hydrologic response of the nested model during the July 2010 event, the backwater of effects of the Delhi Dam can be incorporated by extending the river model downstream or imposing downstream boundary conditions. The IDNR has operational and dam breach reports for the Delhi Dam and a HEC-RAS model of the Maquoketa River reach at the dam. Additional studies can be completed to determine a way to use remote sensing techniques to identify and characterize the key features in urban landscapes. Currently, there is no clear method for easily identifying the subsurface

pipes or other drainage components unique to urban areas. However, the an urban model should at minimum represent impervious area and large stormsewers (greater than 30 inches) because of their impact on the quick hydrologic response of the urban catchment. A few successful case studies have shown the ability of a synthetic pipe network to operate like the actual storm sewer network (Henonin et al., 2013; Rossel et al., 2014; Sitzenfrei, 2012).

If flood forecasting in all Iowan cities is the goal, the inclusion of subsurface utilities may not be worth the data and time requirements. An alternative would be to include the main channels and ditches that redirect overland and subsurface flows, such as the Tributary A and Tributary 2. The IWA is developing a tool in GIS that can detect ponds and channels that are from a DEM given certain constraints. This might be useful to identify the main channels or ponds in the urban drainage network. It is likely that hydraulic models already exist for many small tributaries that drain through urban areas. In the case of Manchester, 1D HEC-RAS models had already been created for the Maquoketa River from Manchester to the Delhi Dam and the Eastern Tributaries. The XPSWMM model has the advantage of providing meaningful flood-related maps that give information on the potential risks. It is important that the real-time flood model results can be clearly communicated to the user.

### **7.3 Conclusions**

The future of hydrology is real-time forecasting and predictions, especially in populated areas. Flood simulation models can provide accurate predictions about pending flood disasters with advances in computational resources. Nesting the HLM regional model to a local, urban model has the advantage of outputting flood risk maps with

information on the temporal and spatial changes of water depth and velocities. These maps can be used by emergency management and decision-makers to make appropriate decisions related to the safety of the community.

The uncalibrated, nested model of Manchester was validated against streamflow records and photos for the extreme flood events of July 2010 and September 2010. The model was able to reproduce the flow behavior documented by the locals, and the model had good skill in reproducing the overall shape and peak of the hydrographs. The model was able to predict the stage levels on the rising limb of the hydrographs, within less than 3 feet of error (Figure 31 and Figure 33). While the HLM does a good job of providing real-time streamflow information, the local model has the ability to represent the flow behavior throughout the entire urban district. The fine resolution model has the advantage of being able to capture the hydrologic response of the urban landscape specifically in eastern Manchester, where the HLM model output is not available for the rural subcatchments draining to Tributary A or 2 (Figure 10).

The two local configurations of the nested model did not significantly impact the streamflow results at the downstream USGS gauge. The small rainfall-runoff volume from eastern Manchester was negligible compared to the high discharges in the Maquoketa River during the July 2010 and September 2016 floods. However, the inclusion of the stormwater network is important because it does change the flood risk within the urban district as evident in Figure 41.

The main source of uncertainty that effects the performance of the nested model is the spatiotemporal resolution and variability of the rainfall input. For the flood events of July 2010 and September 2016, there is no rainfall-model combination that consistently

outperforms the others. Interestingly, the temporal resolution of the rainfall input does not significantly impact the streamflow predictions on the Maquoketa River. For the September 2016 event, the nested model was forced with both the IFC-hourly and IFC-5min intensity time series. The streamflow output of the nested model was significantly impacted by the spatial resolution of the rainfall input but was less sensitive to the temporal resolution (Section 5.2). In contrast, the urban catchment was sensitive to the spatial and temporal resolution of the rainfall which significantly impacted the hydrologic response.

Accounting for urban areas using a nested regional-local modeling approach is a valid method for the IFC to integrate the operational HLM with a model more suitable for the local scale. However, every detail of the urban landscapes may not need to be modeled. Since most cities are at risk for riverine flooding, a 2D porous model is an option for a quick simulation of flood depths and velocities near the floodplain. The stormwater network should not be removed from the modeling process, but methods for creating or generating equivalent networks should be evaluated to reduce model construction requirements. For real-time forecasting purposes, the value added by increasing model complexity reaches a point where the added detail does not significantly affect the hydrologic response of the catchment. The results of local models can be practically applied in decision-making processes using actual information but with data and time constraints, it is not feasible to create a high resolution, 1D/2D local models for every urban area in Iowa. Identifying and characterizing the sources of uncertainty, primarily in rainfall inputs and model complexity, will be integral for the successful implementation of an accurate, real-time flood model in all urban areas.



## REFERENCES

- Akram, F., Rasul, M. G., Masud, M., Khan, K., Imam, S., & Amir, I. (2014). Comparison-of-Different-Hydrograph-Routing-Techniques-in-XPSTORM--A-Case-Study. *International Journal of Environmental, Ecological, Geological and Mining Engineering*, 8(3), 213–223.
- Arrault, A., Finaud-Guyot, P., Archambeau, P., Bruwier, M., Erpicum, S., Piroton, M., & Dewals, B. (2016). Hydrodynamics of long-duration urban floods: Experiments and numerical modelling. *Natural Hazards and Earth System Sciences*, 16(6), 1413–1429. <https://doi.org/10.5194/nhess-16-1413-2016>
- Ayalew, T. B., Krajewski, W. F., & Mantilla, R. (2014). Connecting the power-law scaling structure of peak-discharges to spatially variable rainfall and catchment physical properties. *Advances in Water Resources*, 71, 32–43. <https://doi.org/10.1016/j.advwatres.2014.05.009>
- Barco, J., Wong, K. M., Stenstrom, M. K., & Asce, F. (2008). Automatic Calibration of the U.S. EPA SWMM Model for a Large Urban Catchment. *Journal of Hydraulic Engineering*, 134(4), 466–474. [https://doi.org/10.1061/\(ASCE\)0733-9429\(2008\)134:4\(466\)](https://doi.org/10.1061/(ASCE)0733-9429(2008)134:4(466))
- Bellos, V., & Tsakiris, G. (2015). Comparing Various Methods of Building Representation for 2D Flood Modelling In Built-Up Areas. *Water Resources Management*, 29(2), 379–397. <https://doi.org/10.1007/s11269-014-0702-3>
- Bennett, N. D., Croke, B. F. W., Guariso, G., Guillaume, J. H. A., Hamilton, S. H., Jakeman, A. J., ... Andreassian, V. (2013). Characterising performance of environmental models. *Environmental Modelling & Software*. <https://doi.org/10.1016/j.envsoft.2012.09.011>
- Bermúdez, M., Neal, J. C., Bates, P. D., Coxon, G., Freer, J. E., Cea, L., & Puertas, J. (2017). Quantifying local rainfall dynamics and uncertain boundary conditions into a nested regional-local flood modeling system. *Water Resources Research*, 53(4), 2770–2785. <https://doi.org/10.1002/2016WR019903>
- Bisht, D. S., Chatterjee, C., Kalakoti, S., Upadhyay, P., Sahoo, M., & Panda, A. (2016). Modeling urban floods and drainage using SWMM and MIKE URBAN: a case study. *Natural Hazards*. <https://doi.org/10.1007/s11069-016-2455-1>
- Brown, J. D., Spencer, T., & Moeller, I. (2007). Modeling storm surge flooding of an urban area with particular reference to modeling uncertainties: A case study of Canvey Island, United Kingdom. *Water Resources Research*, 43(6), 1–22. <https://doi.org/10.1029/2005WR004597>

- Brown, S. A., Schall, J. D., Morris, J. L., Doherty, C. L., Stein, S. M., & Warner, J. C. (2013). Urban Drainage Design Manual, 2009(22), 478. Retrieved from [http://www.fhwa.dot.gov/engineering/hydraulics/library\\_arc.cfm?pub\\_number=22&id=140](http://www.fhwa.dot.gov/engineering/hydraulics/library_arc.cfm?pub_number=22&id=140)
- Bruni, G., Reinoso, R., Van De Giesen, N. C., Clemens, F. H. L. R., & Ten Veldhuis, J. A. E. (2015). On the sensitivity of urban hydrodynamic modelling to rainfall spatial and temporal resolution. *Hydrology and Earth System Sciences*, 19(2), 691–709. <https://doi.org/10.5194/hess-19-691-2015>
- Chang, T. J., Wang, C. H., & Chen, A. S. (2015). A novel approach to model dynamic flow interactions between storm sewer system and overland surface for different land covers in urban areas. *Journal of Hydrology*. <https://doi.org/10.1016/j.jhydrol.2015.03.014>
- Chen, A. S., Evans, B., Djordjević, S., Savić, D. A., Djordjević, S., & Savić, D. A. (2012). A coarse-grid approach to representing building blockage effects in 2D urban flood modelling. *Journal of Hydrology*, 426–427, 1–16. <https://doi.org/10.1016/j.jhydrol.2012.01.007>
- Czajkowski, J., Cunha, L. K., Michel-Kerjan, E., & Smith, J. A. (2016). Toward economic flood loss characterization via hazard simulation. *Environmental Research Letters*, 11(8), 84006. <https://doi.org/10.1088/1748-9326/11/8/084006>
- Di Lazzaro, M., Zarlenga, A., & Volpi, E. (2016). Understanding the relative role of dispersion mechanisms across basin scales. *Advances in Water Resources*, 91, 23–36. <https://doi.org/10.1016/j.advwatres.2016.03.003>
- Dotto, C. B. S., Kleidorfer, M., Deletic, A., Rauch, W., & McCarthy, D. T. (2014). Impacts of measured data uncertainty on urban stormwater models. *Journal of Hydrology*, 508, 28–42. <https://doi.org/10.1016/j.jhydrol.2013.10.025>
- Dottori, F., & Todini, E. (2013). Testing a simple 2D hydraulic model in an urban flood experiment. *Hydrological Processes*, 27(9), 1301–1320. <https://doi.org/10.1002/hyp.9370>
- Eash, D. A. (2012). *Floods of July 23 – 26 , 2010 , in the Little Maquoketa River and Maquoketa River Basins , Northeast Iowa.*
- Emmanuel, I., Andrieu, H., Leblois, E., Janey, N., & Payrastre, O. (2015). Influence of rainfall spatial variability on rainfall-runoff modelling: Benefit of a simulation approach? *Journal of Hydrology*, 531, 337–348. <https://doi.org/10.1016/j.jhydrol.2015.04.058>
- Engineering, T. R. W. (2016). Manning’s n Values for Overland Flow, *I*(January), 2016.

- Falter, D., Vorogushyn, S., Lhomme, J., Apel, H., Gouldby, B., & Merz, B. (2013). Hydraulic model evaluation for large-scale flood risk assessments. *Hydrological Processes*, 27(9), 1331–1340. <https://doi.org/10.1002/hyp.9553>
- Fewtrell, T.J., Bates, P.D., Horritt, M. and Hunter, N. M., Fewtrell, T. J., Bates, P. D., Horritt, M., & Hunter, N. M. (2008). Evaluating the effect of scale in flood inundation modelling in urban environments. *Hydrological Processes*, 22(November 2008), 5107–5118. <https://doi.org/10.1002/hyp>
- Fletcher, T. D., Andrieu, H., & Hamel, P. (2013). Understanding, management and modelling of urban hydrology and its consequences for receiving waters: A state of the art. *Advances in Water Resources*, 51, 261–279. <https://doi.org/10.1016/j.advwatres.2012.09.001>
- Garcia, L., Barreiro-Gomez, J., Escobar, E., Tellez, D., Quijano, N., & Ocampo-Martinez, C. (2015). Modeling and real-time control of urban drainage systems: A review. *Advances in Water Resources*, 85(18), 120–132. <https://doi.org/10.1016/j.advwatres.2015.08.007>
- Gires, A., Tchiguirinskaia, I., Schertzer, D., Ochoa Rodriguez, S., Willems, P., Ichiba, A., ... ten Veldhuis, M.-C. (2016). Fractal analysis of urban catchments and their representation in semi-distributed models: imperviousness and sewer system. *Hydrology and Earth System Sciences Discussions*, (October), 1–23. <https://doi.org/10.5194/hess-2016-527>
- Gironás, J., Niemann, J. D., Roesner, L. A., Rodriguez, F., & Andrieu, H. (2010). Evaluation of methods for representing urban terrain in stormwater modeling. *Journal of Hydrologic Engineering*, 15(January), 14. [https://doi.org/10.1061/\(ASCE\)HE.1943-5584.0000142](https://doi.org/10.1061/(ASCE)HE.1943-5584.0000142)
- Guinot, V., Sanders, B., Schubert, J., Guinot, V., Sanders, B., & Schubert, J. (2017). Dual integral porosity shallow water model for urban flood modelling To cite this version : HAL Id : hal-01465071 Dual integral porosity shallow water model for urban ood modelling Abstract 1 Introduction.
- Gupta, H. V., Clark, M. P., Vrugt, J. A., Abramowitz, G., & Ye, M. (2012). Towards a comprehensive assessment of model structural adequacy. *Water Resources Research*. <https://doi.org/10.1029/2011WR011044>
- Gupta, H. V., Kling, H., Yilmaz, K. K., & Martinez, G. F. (2009). Decomposition of the mean squared error and NSE performance criteria: Implications for improving hydrological modelling. *Journal of Hydrology*. <https://doi.org/10.1016/j.jhydrol.2009.08.003>
- Ha, S. J., Stenstrom, M. K., & Asce, F. (2008). Predictive Modeling of Storm-Water Runoff Quantity and Quality for a Large Urban Watershed. *Journal of Environmental Engineering*, 134(9), 703–711. [https://doi.org/10.1061/\(ASCE\)0733-9372\(2008\)134:9\(703\)](https://doi.org/10.1061/(ASCE)0733-9372(2008)134:9(703))

- Henonin, J., Russo, B., Mark, O., & Gourbesville, P. (2013). Real-time urban flood forecasting and modelling – a state of the art. *Journal of Hydroinformatics*, 15(3), 717. <https://doi.org/10.2166/hydro.2013.132>
- IDNR. (2010). *Report on Breach of Delhi Dam - IPE Review*.
- Jankowfsky, S., Branger, F., Braud, I., Gironás, J., & Rodriguez, F. (2013). Comparison of catchment and network delineation approaches in complex suburban environments: Application to the Chaudanne catchment, France. *Hydrological Processes*, 27(25), 3747–3761. <https://doi.org/10.1002/hyp.9506>
- Jankowfsky, S., Branger, F., Braud, I., Rodriguez, F., Debionne, S., & Viallet, P. (2014). Assessing anthropogenic influence on the hydrology of small peri-urban catchments: Development of the object-oriented PUMMA model by integrating urban and rural hydrological models. *Journal of Hydrology*, 517, 1056–1071. <https://doi.org/10.1016/j.jhydrol.2014.06.034>
- Janses, C., & SCE. (2016). Manning 's n Values for Various Land Covers To Use for Dam Breach Analyses by NRCS in Kansas, (December), 1–2. Retrieved from <https://www.wcc.nrcs.usda.gov/>
- Javier, J. R. N., Smith, J. A., Meierdiercks, K. L., Baeck, M. L., & Miller, A. J. (2007). Flash Flood Forecasting for Small Urban Watersheds in the Baltimore Metropolitan Region. *Weather and Forecasting*, 22(6), 1331–1344. <https://doi.org/10.1175/2007WAF2006036.1>
- Kidmose, J., Troldborg, L., Refsgaard, J. C., & Bischoff, N. (2015). Coupling of a distributed hydrological model with an urban storm water model for impact analysis of forced infiltration. *Journal of Hydrology*, 525, 506–520. <https://doi.org/10.1016/j.jhydrol.2015.04.007>
- Knighton, J., White, E., Lennon, E., & Rajan, R. (2014). Development of probability distributions for urban hydrologic model parameters and a Monte Carlo analysis of model sensitivity. *Hydrological Processes*, 28(19), 5131–5139. <https://doi.org/10.1002/hyp.10009>
- Krajewski, W. F., Ceynar, D., Demir, I., Goska, R., Kruger, A., Langel, C., ... Young, N. C. (2017). Real-time flood forecasting and information system for the state of Iowa. *Bulletin of the American Meteorological Society*, 98(3), 539–554. <https://doi.org/10.1175/BAMS-D-15-00243.1>
- Krajewski, W. F., Kruger, A., Singh, S., Seo, B.-C., & Smith, J. a. (2013). Hydro-NEXRAD-2: real-time access to customized radar-rainfall for hydrologic applications. *Journal of Hydroinformatics*, 15(2), 580. <https://doi.org/10.2166/hydro.2012.227>

- Krebs, G., Kokkonen, T., Valtanen, M., Setälä, H., & Koivusalo, H. (2014). Spatial resolution considerations for urban hydrological modelling. *Journal of Hydrology*, *512*, 482–497. <https://doi.org/10.1016/j.jhydrol.2014.03.013>
- Leandro, J., Schumann, A., & Pfister, A. (2016). A step towards considering the spatial heterogeneity of urban key features in urban hydrology flood modelling. *Journal of Hydrology*, *535*, 356–365. <https://doi.org/10.1016/j.jhydrol.2016.01.060>
- Legates, D. R., & McCabe Jr., G. J. (2005). Evaluating the Use of “Goodness of Fit” Measures in Hydrologic and Hydroclimatic Model Validation. *Water Resources Research*, *35*(1), 233–241. <https://doi.org/10.1029/1998WR900018>
- Leskens, J. G., Brugnach, M., Hoekstra, A. Y., & Schuurmans, W. (2014). Why are decisions in flood disaster management so poorly supported by information from flood models? *Environmental Modelling and Software*, *53*, 53–61. <https://doi.org/10.1016/j.envsoft.2013.11.003>
- Liu, L., Liu, Y., Wang, X., Yu, D., Liu, K., Huang, H., & Hu, G. (2015). Developing an effective 2-D urban flood inundation model for city emergency management based on cellular automata. *Natural Hazards and Earth System Sciences*, *15*(3). <https://doi.org/10.5194/nhess-15-381-2015>
- Mantilla, R., & Gupta, V. K. (2005). A GIS numerical framework to study the process basis of scaling statistics in river networks. *IEEE Geoscience and Remote Sensing Letters*, *2*(4), 404–408. <https://doi.org/10.1109/LGRS.2005.853571>
- Mark, O., Weesakul, S., Apirumanekul, C., Aroonnet, S. B., & Djordjević, S. (2004). Potential and limitations of 1D modelling of urban flooding. *Journal of Hydrology*. <https://doi.org/10.1016/j.jhydrol.2004.08.014>
- Meierdiercks, K. L., Smith, J. A., Baeck, M. L., & Miller, A. J. (2010). Heterogeneity of Hydrologic Response in Urban Watersheds. *Journal of the American Water Resources Association*, *46*(6), 1221–1237. <https://doi.org/10.1111/j.1752-1688.2010.00487.x>
- Mignot, E., Paquier, A., & Haider, S. (2006). Modeling floods in a dense urban area using 2D shallow water equations. *Journal of Hydrology*. <https://doi.org/10.1016/j.jhydrol.2005.11.026>
- Miller, J. D., Kim, H., Kjeldsen, T. R., Packman, J., Grebby, S., & Dearden, R. (2014). Assessing the impact of urbanization on storm runoff in a peri-urban catchment using historical change in impervious cover. *Journal of Hydrology*, *515*, 59–70. <https://doi.org/10.1016/j.jhydrol.2014.04.011>
- Neal, J., Schumann, G., & Bates, P. (2012). A subgrid channel model for simulating river hydraulics and floodplain inundation over large and data sparse areas. *Water Resources Research*, *48*(11), 1–16. <https://doi.org/10.1029/2012WR012514>

- Neelz, S., & Pender, G. (2013). Benchmarking the latest generation of 2D hydraulic modelling packages, 194. Retrieved from [http://evidence.environment-agency.gov.uk/FCERM/Libraries/FCERM\\_Project\\_Documents/SC120002\\_Benchmarking\\_2D\\_hydraulic\\_models\\_Report.sflb.ashx](http://evidence.environment-agency.gov.uk/FCERM/Libraries/FCERM_Project_Documents/SC120002_Benchmarking_2D_hydraulic_models_Report.sflb.ashx)
- NOAA. (1978). Probable Maximum Precipitation Estimates , United States East of the 105th Meridian. *Hydrometeorological Report*, (51).
- Nobre, A. D., Cuartas, L. A., Momo, M. R., Severo, D. L., Pinheiro, A., & Nobre, C. A. (2016). HAND contour: A new proxy predictor of inundation extent. *Hydrological Processes*, 30(2), 320–333. <https://doi.org/10.1002/hyp.10581>
- Obermayer, A., Guentert, F. W., Angermair, G., Tandler, R., Braunschmidt, S., & Milojevic, N. (2010). Different approaches for modelling of sewer caused urban flooding. *Water Science and Technology*, 62(9), 2175–2182. <https://doi.org/10.2166/wst.2010.439>
- Ochoa-Rodriguez, S., Wang, L. P., Gires, A., Pina, R. D., Reinoso-Rondinel, R., Bruni, G., ... Ten Veldhuis, M. C. (2015). Impact of spatial and temporal resolution of rainfall inputs on urban hydrodynamic modelling outputs: A multi-catchment investigation. *Journal of Hydrology*, 531, 389–407. <https://doi.org/10.1016/j.jhydrol.2015.05.035>
- Ogden, F. L., Raj Pradhan, N., Downer, C. W., & Zahner, J. A. (2011). Relative importance of impervious area, drainage density, width function, and subsurface storm drainage on flood runoff from an urbanized catchment. *Water Resources Research*, 47(12), 1–12. <https://doi.org/10.1029/2011WR010550>
- Peleg, N., Blumensaat, F., Molnar, P., Fatichi, S., & Burlando, P. (2016). Partitioning spatial and temporal rainfall variability in urban drainage modelling. *Hydrology and Earth System Sciences Discussions*, (October), 1–20. <https://doi.org/10.5194/hess-2016-530>
- Petrucci, G., & Bonhomme, C. (2014). The dilemma of spatial representation for urban hydrology semi-distributed modelling: Trade-offs among complexity, calibration and geographical data. *Journal of Hydrology*, 517, 997–1007. <https://doi.org/10.1016/j.jhydrol.2014.06.019>
- Quintero, F., Krajewski, W. F., Mantilla, R., Small, S., & Seo, B.-C. (2016). A Spatial–Dynamical Framework for Evaluation of Satellite Rainfall Products for Flood Prediction. *Journal of Hydrometeorology*, 17(8), 2137–2154. <https://doi.org/10.1175/JHM-D-15-0195.1>
- Rawls, W. J., Brakensiek, D. L., & Miller, N. (1983). Green-ampt Infiltration Parameters from Soils Data. *Journal of Hydraulic Engineering*, 109(1), 62–70. [https://doi.org/10.1061/\(ASCE\)0733-9429\(1983\)109:1\(62\)](https://doi.org/10.1061/(ASCE)0733-9429(1983)109:1(62))

- Renard, B., Kavetski, D., Kuczera, G., Thyer, M., & Franks, S. W. (2010). Understanding predictive uncertainty in hydrologic modeling: The challenge of identifying input and structural errors. *Water Resources Research*, *46*(5).  
<https://doi.org/10.1029/2009WR008328>
- Rodriguez, F., Bocher, E., & Chancibault, K. (2013). Terrain representation impact on periurban catchment morphological properties. *Journal of Hydrology*, *485*, 54–67.  
<https://doi.org/10.1016/j.jhydrol.2012.11.023>
- Rossel, F., Gironás, J., Mejía, A., Rinaldo, A., Rodriguez, F., Giron??s, J., ... Rodriguez, F. (2014). Spatial characterization of catchment dispersion mechanisms in an urban context. *Advances in Water Resources*, *74*(3), 290–301.  
<https://doi.org/10.1016/j.advwatres.2014.09.005>
- Russo, B., Sunyer, D., Velasco, M., & Djordjević, S. (2015). Analysis of extreme flooding events through a calibrated 1D/2D coupled model: the case of Barcelona (Spain). *Journal of Hydroinformatics*, *17*(3), 473.  
<https://doi.org/10.2166/hydro.2014.063>
- Salas, F. R., Somos-Valenzuela, M. A., Dugger, A., Maidment, D. R., Gochis, D. J., David, C. H., ... Noman, N. (2017). Towards Real-Time Continental Scale Streamflow Simulation in Continuous and Discrete Space. *Journal of the American Water Resources Association*, pp. 11111752–1688. <https://doi.org/10.1111/1752-1688.12586>
- Salvadore, E., Bronders, J., & Batelaan, O. (2015). Hydrological modelling of urbanized catchments: A review and future directions. *Journal of Hydrology*.  
<https://doi.org/10.1016/j.jhydrol.2015.06.028>
- Sanzana, P., Gironás, J., Braud, I., Branger, F., Rodriguez, F., Vargas, X., ... Jankowsky, S. (2017). A GIS-based urban and peri-urban landscape representation toolbox for hydrological distributed modeling. *Environmental Modelling and Software*, *91*, 168–185. <https://doi.org/10.1016/j.envsoft.2017.01.022>
- Schubert, J. E., & Sanders, B. F. (2012). Building treatments for urban flood inundation models and implications for predictive skill and modeling efficiency. *Advances in Water Resources*, *41*, 49–64. <https://doi.org/10.1016/j.advwatres.2012.02.012>
- Schubert, J. E., Sanders, B. F., Smith, M. J., & Wright, N. G. (2008). Unstructured mesh generation and landcover-based resistance for hydrodynamic modeling of urban flooding. *Advances in Water Resources*, *31*(12), 1603–1621.  
<https://doi.org/10.1016/j.advwatres.2008.07.012>
- Simões, N. E., Ochoa-Rodríguez, S., Wang, L. P., Pina, R. D., Marques, A. S., Onof, C., & Leitão, J. P. (2015). Stochastic urban pluvial flood hazard maps based upon a spatial-temporal rainfall generator. *Water (Switzerland)*, *7*(7), 3396–3406.  
<https://doi.org/10.3390/w7073396>



- Sitzenfrei, R. (2012). Stochastic Generation of Urban Water Systems for Case Study Analysis: Forum Umwelttechnik und Wasserbau - Band 11, 378. Retrieved from [http://www.amazon.de/Stochastic-Generation-Urban-Systems-Analysis/dp/3902811447/ref=sr\\_1\\_1?s=books-intl-de&ie=UTF8&qid=1353759872&sr=1-1](http://www.amazon.de/Stochastic-Generation-Urban-Systems-Analysis/dp/3902811447/ref=sr_1_1?s=books-intl-de&ie=UTF8&qid=1353759872&sr=1-1)
- Smith, B. K., Smith, J. A., Baeck, M. L., Villarini, G., & Wright, D. B. (2013). Spectrum of storm event hydrologic response in urban watersheds. *Water Resources Research*, 49(5), 2649–2663. <https://doi.org/10.1002/wrcr.20223>
- Smith, G. P., Wasko, C. D., & Miller, B. M. (2012). Modelling the influence of buildings on flood flow. *Floodplain Management National Conference*.
- Sto. Domingo, N. D., Refsgaard, A., Mark, O., & Paludan, B. (2010). Flood analysis in mixed-urban areas reflecting interactions with the complete water cycle through coupled hydrologic-hydraulic modelling. *Water Science and Technology*. <https://doi.org/10.2166/wst.2010.365>
- Sun, N., Hall, M., Hong, B., & Zhang, L. (2014). Impact of SWMM Catchment Discretization: Case Study in Syracuse, New York. *Journal of Hydrologic Engineering*, 19(1), 223–234. [https://doi.org/10.1061/\(ASCE\)HE.1943-5584.0000777](https://doi.org/10.1061/(ASCE)HE.1943-5584.0000777)
- Sun, N., Hong, B., & Hall, M. (2014). Assessment of the SWMM model uncertainties within the generalized likelihood uncertainty estimation (GLUE) framework for a high-resolution urban sewershed. *Hydrological Processes*, 28(6), 3018–3034. <https://doi.org/10.1002/hyp.9869>
- Syme, W. J. (1991). Dynamically Linked Two Dimensional / Hydrodynamic Modelling Program for Rivers , Estuaries and Coastal Waters, (Syme), 135.
- Syme, W. J. (2008). Flooding in Urban Areas-2D Modelling Approaches for Buildings and Fences. In *9th National Conference on Hydraulics in Water Engineering* (pp. 23–26).
- Teng, J., Jakeman, A. J., Vaze, J., Croke, B. F. W., Dutta, D., & Kim, S. (2017). Flood inundation modelling: A review of methods, recent advances and uncertainty analysis. *Environmental Modelling and Software*, 90(April), 201–216. <https://doi.org/10.1016/j.envsoft.2017.01.006>
- Thomas Steven Savage, J., Pianosi, F., Bates, P., Freer, J., & Wagener, T. (2016). Quantifying the importance of spatial resolution and other factors through global sensitivity analysis of a flood inundation model. *Water Resources Research*, 52(11), 9146–9163. <https://doi.org/10.1002/2015WR018198>

- Thorndahl, S., Einfalt, T., Willems, P., Ellerbæk Nielsen, J., Ten Veldhuis, M. C., Arnbjerg-Nielsen, K., ... Molnar, P. (2017). Weather radar rainfall data in urban hydrology. *Hydrology and Earth System Sciences*, *21*(3), 1359–1380. <https://doi.org/10.5194/hess-21-1359-2017>
- Wang, L. P., Ochoa-Rodríguez, S., Van Assel, J., Pina, R. D., Pessemier, M., Kroll, S., ... Onof, C. (2015). Enhancement of radar rainfall estimates for urban hydrology through optical flow temporal interpolation and Bayesian gauge-based adjustment. *Journal of Hydrology*, *531*, 408–426. <https://doi.org/10.1016/j.jhydrol.2015.05.049>
- Wright, D. B., Smith, J. A., Villarini, G., & Baeck, M. L. (2014). Long-term high-resolution radar rainfall fields for urban hydrology. *Journal of the American Water Resources Association*, *50*(3), 713–734. <https://doi.org/10.1111/jawr.12139>
- XPSolutions. (n.d.). xp2D Reference Manual. Retrieved from [https://www.innovyze.com/products/xp2d/xp2d\\_manual.pdf](https://www.innovyze.com/products/xp2d/xp2d_manual.pdf)
- Yang, L., Smith, J. A., Baeck, M. L., & Zhang, Y. (2016). Flash flooding in small urban watersheds: Storm event hydrologic response. *Water Resources Research*, *52*(6), 4571–4589. <https://doi.org/10.1002/2015WR018326>
- Zalenski, G., Krajewski, W. F., Quintero, F., Restrepo, P., & Buan, S. (2017). Analysis of national weather service stage forecast errors. *Weather and Forecasting*, *32*(4). <https://doi.org/10.1175/WAF-D-16-0219.1>